Aus der Medizinischen Fakultät Charité – Universitätsmedizin Berlin und
Max-Delbrück-Centrum für Molekulare Medizin in der Helmholtz-Gemeinschaft

DISSERTATION

The role of SORLA in islet amyloid polypeptide transport and islet amyloid deposition

Die Bedeutung von SORLA für den Transport von islet amyloid polypeptide und die Ablagerung von Amyloid in Langerhans-Inseln

zur Erlangung des akademischen Grades
Doctor of Philosophy (PhD)

vorgelegt der Medizinischen Fakultät
Charité – Universitätsmedizin Berlin

von

Alexis Zi Le Shih
aus Toronto, Kanada

Datum der Promotion: 23.03.2024

Table of Contents

List of Tables

List of Figures

List of Abbreviations

Aβ: Amyloid-beta

AD: Alzheimer disease

APP: Amyloid precursor protein

CPE: Carboxypeptidase E

CR: Complement-type repeats

GSIS: Glucose-stimulated insulin secretion

GTT: Glucose tolerance test

HFD: High-fat diet

hIAPP: Human islet amyloid polypeptide

IP: Intraperitoneal

KO: Knockout

ND: Normal diet

PAM: Peptidyl-glycine alpha-amidating monooxygenase

PC: Prohormone convertase

RT: Room temperature

SORLA: Sorting-related receptor with A-type repeats

T2D: Type 2 diabetes

TGN: *trans*-Golgi network

ThioS: Thioflavin S

TUNEL: Terminal deoxynucleotidyl transferase dUTP nick end labeling

VPS10P: Vacuolar protein sorting 10 protein

WT: Wildtype

Abstract

Sorting-related receptor with type A repeats (SORLA) is a sorting receptor encoded by *SORL1*, a major risk gene for Alzheimer disease (AD). SORLA is protective against AD by preventing the accumulation of amyloid-beta peptides into amyloid plaque deposits in the brain. Similar to AD, amyloid is a pathological hallmark found in the pancreas of type 2 diabetes patients. The main amyloidogenic component in pancreatic islet is a small peptide hormone produced by the beta cell, called islet amyloid polypeptide (IAPP). However, the underlying mechanisms of islet amyloid formation remain unclear. Recent advances in single-cell transcriptomic analyses have revealed that SORLA transcript is also expressed in beta cells. Yet, the role of SORLA in islets has not been studied previously. Based on the established understanding of SORLA in amyloid formation in the brain, we postulated that it may function similarly in islet beta cells. Specifically, we hypothesized that SORLA regulates islet amyloid formation through mediating IAPP transport and turnover.

To test this hypothesis, we first examined the effect of SORLA deficiency on islet amyloid formation, cell death and overall glucose homeostasis by comparing wildtype (WT) mice with animals carrying a targeted *Sorl1* disruption (KO). Since mouse IAPP is non-amyloidogenic, SORLA WT and KO lines that overexpress a human *IAPP* (hIAPP) transgene were generated. The loss of SORLA significantly increased both the prevalence and severity of islet amyloid deposition in hIAPP transgenic mice compared with WT controls. Aggravated amyloid deposition was also accompanied with increased islet cell death in hIAPP/KO mice. However, when analyzed at 7 months of age, the increased amyloid burden had not affected overall glucose homeostasis or beta cell function. Next, we performed *in vitro* studies to elucidate the mechanism by which SORLA regulates IAPP and islet amyloid formation. Results from microscale thermophoresis showed that SORLA interacted more strongly with the precursor (proIAPP) than the mature form of IAPP. Its preference towards partially processed IAPP was further corroborated in cell studies in which SORLA mediated endocytosis of proIAPP, but not mature IAPP, delivering it to the endolysosomal degradation pathway.

Altogether, studies in this dissertation have uncovered a novel role of SORLA in pancreatic islets, where SORLA protects against islet amyloid deposition and

associated cell death, likely through clearance of extracellular proIAPP secreted by beta cells.

Zusammenfassung

Der *Sorting Related Receptor with A-type Repeats* (SORLA) ist ein Sortierrezeptor, der von *SORL1* kodiert wird, einem der Hauptrisikogene für die sporadische Alzheimer-Krankheit (AD). SORLA schützt vor Alzheimer, indem es die Akkumulation von Amyloid-beta-Peptiden in Amyloid-Plaque-Ablagerungen im Gehirn verhindert. Ähnlich wie bei AD ist Amyloid ein pathologisches Merkmal des Pankreas bei Patienten mit Typ-2-Diabetes. Die wichtigste amyloidogene Komponente in den Langerhans-Inselzellen des Pankreas ist ein kleines Peptidhormon, das von den Betazellen produziert wird und als *islet amyloid polypeptide* (IAPP) bezeichnet wird. Die Mechanismen, die der Bildung von Insel-Amyloid zugrunde liegen, sind jedoch nach wie vor unklar. Jüngste Fortschritte bei Einzelzell-Transkriptomanalysen haben gezeigt, dass das SORLA-Transkript auch in Betazellen zu finden ist. Die Rolle von SORLA in Langerhans-Inseln wurde jedoch bisher nicht untersucht. Auf der Grundlage der etablierten Rolle von SORLA bei der Amyloidbildung im Gehirn stellten wir die Hypothese auf, dass es in den Betazellen der Langerhans-Inseln eine ähnliche Funktion haben könnte. Insbesondere postulieren wir, dass SORLA die Amyloidbildung in Inselzellen durch die Kontrolle von IAPP-Transport und -Umsatz reguliert.

Um unsere Hypothese zu testen, untersuchten wir zunächst die Auswirkungen eines SORLA-Defizits auf die Amyloidbildung in den Inselzellen, den Zelltod und die allgemeine Glukosehomöostase, indem wir Wildtyp-Mäuse (WT) mit Tieren verglichen, welche einen induzierten *Sorl1* Gendefekt trugen (KO) Tieren. Da das IAPP der Maus nicht amyloidogen ist, wurden SORLA WT- und KO Mausstämme erzeugt, die ein humanes IAPP (hIAPP) Transgen überexprimierten. Wir konnten zeigen, dass der Verlust von SORLA sowohl die Prävalenz als auch den Schweregrad der Insel-Amyloid-Ablagerungen in hIAPP-transgenen Mäusen im Vergleich zu WT-Kontrollen deutlich erhöht. Die verstärkte Amyloidablagerung ging bei hIAPP/KO-Mäusen auch mit einem erhöhten Absterben der Inselzellen einher. Bei 7 Monate alten Tiere führte die erhöhte Amyloidbelastung jedoch weder zu einer Beeinträchtigung der Glukosehomöostase noch der Betazellfunktion. Als Nächstes untersuchten wir in *in vitro* Studien, durch welchen Mechanismus SORLA die Bildung von IAPP und Insel-Amyloid regulieren könnte. Mittels der Methode der *microscale thermophoresis* wurde gezeigt, dass SORLA stärker mit der IAPP-Vorstufe (proIAPP) als mit reifem IAPP interagiert. Die Präferenz von SORLA für teilweise prozessiertes IAPP wurde in Zellstudien bestätigt, in

denen SORLA die Endozytose von proIAPP, aber nicht von reifem IAPP vermittelte und es so dem endolysosomalen Abbauweg zuführte.

Insgesamt haben die Studien in dieser Dissertation eine neuartige Rolle von SORLA in den Langerhans-Inselzellen aufgedeckt. Hier schützt SORLA vor Insel-Amyloid-Ablagerungen und dem damit verbundenen Zelltod, wahrscheinlich durch Beseitigung von extrazellulärem proIAPP, das von Betazellen sezerniert wird.

1. Introduction

1.1. Islet amyloid polypeptide

1.1.1. Physiological roles of islet amyloid polypeptide

Islet amyloid polypeptide (IAPP or amylin) is a small, 37-amino acid long hormone secreted from pancreatic islet beta cells that impacts various aspects of systemic glucose and energy homeostasis. However, the molecular pathways of IAPP-mediated effects on glucose and energy homeostasis remain largely elusive due to the structural complexity of its receptors. IAPP receptors are heterodimers of the calcitonin receptor and one of the three isoforms of receptor activity-modifying proteins (RAMPs), and they exist with varying ligand binding selectivity (Christopoulos et al. 1999; McLatchie et al. 1998; Muff, Bühlmann, Fischer, and Born 1999). IAPP receptors are highly expressed in the brain and have been shown to promote satiety, delay gastric emptying, control food intake, body weight and energy expenditure (R. Akter et al. 2016; Lutz 2010). In addition to central regulation, IAPP has been shown to maintain blood glucose homeostasis by modulating insulin secretion (Z. L. Wang et al. 1993; Samuel Gebre-Medhin et al. 1998; S. Gebre-Medhin, Olofsson, and Mulder 2000).

IAPP is first synthesized as a preprohormone (Figure 1), upon removal of its N-terminal signal peptide in the endoplasmic reticulum (ER), the C-terminal extended precursor undergoes further processing and modifications in the Golgi and secretory granules prior to production of mature IAPP. First, the C-terminally extended propeptide of proIAPP is cleaved by prohormone convertase (PC1/3) to produce a partially processed intermediate proIAPP. Then, the N-terminally extended propeptide of proIAPP is removed by PC2. Finally, mature IAPP is generated in the secretory granules by actions of carboxypeptidase E (CPE) and peptidyl-glycine α-amidating monooxygenase (PAM), which remove the basic residues lysine and arginine, and amidate its C-terminal, respectively. Mature IAPP is stored in densely packed mature secretory granules and secreted together with insulin in a molar ratio of 1 to 100 in response to glucose and other non-glucose secretagogues, such as leucine and glutamine (Kahn et al. 1990). By contrast, unprocessed IAPP is released constitutively (Marzban, Trigo-Gonzalez, and Verchere 2005).

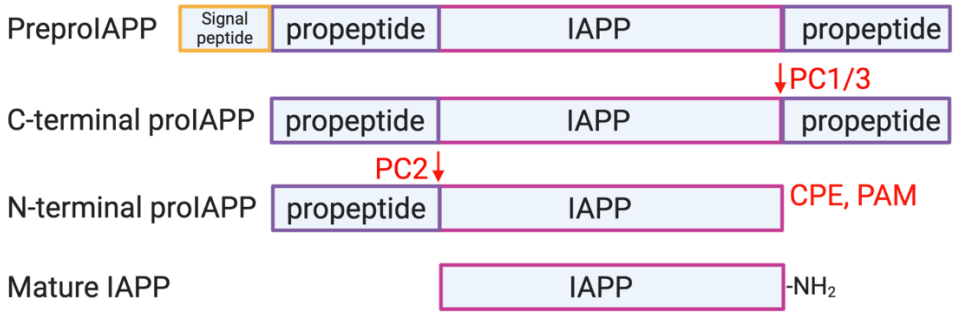

Figure 1: Processing of IAPP precursor
IAPP is first synthesized as a prepropeptide. Upon removal of its signal peptide, two propeptides flanking the C- and N-terminal ends of proIAPP are cleaved by prohormone convertases, PC1/3 and PC2 respectively. Mature IAPP is produced by final modifications at the C-terminal end when basic residues are removed by carboxypeptidase E (CPE) and its C-terminal end amidated by peptidyl-glycine α-amidating monooxygenase (PAM). Created with Biorender.com

1.1.2. IAPP and islet amyloid-mediated cytotoxicity in type 2 diabetes

IAPP is an intrinsically disordered soluble peptide. In humans, IAPP has the propensity to adopt a structured, beta-sheet conformation that is prone to aggregation into oligomers, fibrils, and eventually large insoluble amyloid deposits (Figure 2) (R. Akter et al. 2016). The formation of IAPP oligomers and islet amyloids in the pancreas promotes beta cell dysfunction, cell death, and type 2 diabetes (T2D). T2D is a metabolic disease characterized by hyperglycemia, insulin resistance, and reduced insulin release. Approximately 90% of T2D patients display islet amyloid plaques in their pancreata, with the amount of amyloid deposits positively correlating with the severity of the disease (Röcken, Linke, and Saeger 1992; Kahn, Andrikopoulos, and Verchere 1999). It is increasingly recognized that oligomeric forms or prefibrillar aggregates of human IAPP (hIAPP) are the more cytotoxic agent promoting beta cell apoptosis, while amyloid plaques develop secondarily (S. Zraika et al. 2010; Haataja, Gurlo, Huang, and Butler 2008). Toxic IAPP oligomers are likely to form both intracellularly along the secretory pathways but also extracellularly from secreted IAPP. They disrupt cellular membrane structures, such as the mitochondrial membrane and plasma membrane, activating beta cell death (Gurlo et al. 2010; Raleigh, Zhang, Hastoy, and Clark 2017). Other mechanisms of IAPP-mediated cytotoxicity include islet inflammation (Masters et al. 2010), ER stress (C. J. Huang et al. 2007), and oxidative stress (S. Zraika et al. 2009).

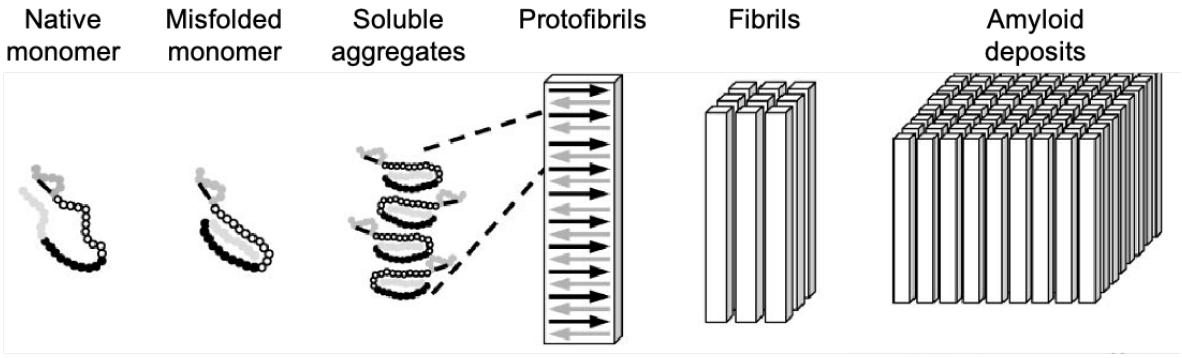

Figure 2: Model illustrating formation of islet amyloid
Native IAPP exist as an unstructured, monomeric peptide. Perturbations in the folding or trafficking of IAPP promote its misfolding into intramolecular beta-sheets. Accumulation of misfolded IAPP results in soluble aggregates and later larger protofibrils. The presence of protofibrils accelerate the assembly into insoluble amyloid fibrils and amyloid deposits. Adapted from Hull, Rebecca L., Gunilla T. Westermark, Per Westermark, and Steven E. Kahn. 2004. "Islet Amyloid: A Critical Entity in the Pathogenesis of Type 2 Diabetes." Journal of Clinical Endocrinology and Metabolism. https://doi.org/10.1210/jc.2004-0405. (Hull, Westermark, Westermark, and Kahn 2004).

1.1.3. Factors promoting islet amyloid formation

The causes of islet amyloid formation associated to T2D are complex and remain incompletely understood. One of the many contributing factors is the local concentration of the amyloidogenic peptide IAPP. Thus, maintaining IAPP homeostasis is essential to minimize its propensity to aggregate. In beta cells, an imbalance between IAPP synthesis, secretion, and clearance is therefore likely to promote the formation of oligomers and insoluble islet amyloid deposits. The following is a brief summary of cellular processes that promote islet amyloid formation. These include overproduction, impaired processing, and impaired clearance of IAPP.

Overproduction of IAPP

During the development of T2D, insulin resistance increases the demand of beta cells to produce and secrete insulin as a compensatory mechanism to maintain normoglycemia (Cerf 2013). Since IAPP is produced and co-secreted along with insulin from the secretory granules (Kahn et al. 1990), overproduction and hypersecretion of IAPP promote the accumulation of IAPP into amyloid. However, *in vivo* studies have shown that overexpression of the human IAPP transgene alone is insufficient to induce significant islet amyloid formation, arguing that other factors are involved as well (Fox et al. 1993; Höppener et al. 1993; D'Alessio et al. 1994; Janson et al. 1996).

Impaired proIAPP processing

In addition to the quantity of IAPP, the variety of IAPP produced, i.e. partially processed vs mature forms, also contributes to amyloidogenicity. It is established that the mature form of IAPP contains a segment of aggregation-prone amino acids at positions 20 – 29 (P. Westermark et al. 1990). In addition to mature IAPP, recent histological studies have shown that the partially processed proIAPP intermediates are also present in islet amyloid (J. F. Paulsson, Andersson, Westermark, and Westermark 2006). Moreover, proIAPP peptides have a strong binding affinity towards heparan sulfate proteoglycans, another component of islet amyloid deposits (Park and Verchere 2001). The interaction between proIAPP and heparin may therefore be important in initiating the early steps of the amyloid propagation cascade. As detailed in section 1.1.1., mature IAPP is produced by a series of processing events from its precursors proIAPP. Recent studies of the processing enzymes prohormone convertases in cell lines and hIAPP transgenic mice have shown that impaired processing of proIAPP results in increased islet amyloid formation and islet cell death (Abedini, Tracz, Cho, and Raleigh 2006; Johan F. Paulsson and Westermark 2005; Marzban et al. 2006). Thus, complete processing of proIAPP into its mature form is essential to prevent undesirable formation of islet amyloid.

Impaired clearance of IAPP

The regulation of protein clearance and turnover is important to maintain a healthy homeostasis in beta cells. Failure to remove excess, misfolded, or aggregation-prone IAPP can therefore promote islet amyloid formation and development of T2D (Mukherjee, Morales-Scheihing, Butler, and Soto 2015). Two major pathways have been shown to regulate IAPP clearance, namely the ubiquitin-proteosome system and the autophagy-lysosomal pathway.

The ubiquitin-proteosome system (UPS)

The majority of intracellular cytosolic proteins in pancreatic islet beta cells are degraded through the ubiquitin-proteosome system (UPS) (Hartley, Brumell, and Volchuk 2009). Proteins destined for degradation are marked by ubiquitination and degraded by the 26S proteosome. Patients with T2D have reduced proteasomal activity and increased

accumulation of polyubiquitinated proteins (Costes et al. 2011). Studies have shown that both the amyloidogenic human and non-amyloidogenic murine IAPP are degraded through UPS as pharmacological inhibition of the proteosome results in increased IAPP content and associated cell death (Casas et al. 2007; Singh, Trikha, Sarkar, and Jeremic 2016).

The autophagy-lysosomal pathway clears aggregated IAPP

Autophagy is responsible for the turnover of protein aggregates and other cellular components, including damaged organelles. It plays an integral part in beta cell function and T2D pathophysiology as islets from diabetic subjects contain significantly higher amounts of autophagosomes compared to non-diabetic subjects (Masini et al. 2009). Autophagy is required to package IAPP oligomers into autophagosomes for degradation and to protect against beta cell death and development of T2D as demonstrated in hIAPP-expressing mice lacking the autophagy initiator Autophagy Related 7 (ATG7) (Shigihara et al. 2014; Kim et al. 2014; Rivera et al. 2014). Furthermore, autophagic activity is enhanced under metabolic stress induced by high-fat diet, suggesting that autophagy is a compensatory mechanism to remove excessive IAPP produced under conditions of obesity and insulin resistance.

Taken together, it is likely that multiple degradation pathways, including the ubiquitin-proteosome and autophagy-lysosomal pathways, are involved in maintaining IAPP homeostasis under different (patho)physiological conditions. However, the molecular regulators involved in IAPP handling remain to be elucidated. For instance, it is unclear how secreted IAPP peptides or extracellular IAPP aggregates are directed to the proteosomes or lysosomes for degradation.

Zinc-metalloproteases

In addition to proteosomes and lysosomes, IAPP can be degraded by zinc-metalloproteases, including insulin-degrading enzyme (IDE) (Bennett, Duckworth, and Hamel 2000), neprilysin (Sakeneh Zraika et al. 2010), and matrix metalloproteinase-9 (MMP9) (Kathryn Aston-Mourney et al. 2013). However, conflicting results have been reported on their effects on IAPP homeostasis. For instance, inhibition of IDE has been shown to prevent IAPP degradation and to promote amyloid fibril formation in a beta cell

line (Bennett, Hamel, and Duckworth 2003), while inhibition of IDE failed to promote islet amyloid formation in primary islets of hIAPP-transgenic mice (Hogan et al. 2016). It is also important to note that most studies of IDE, neprilysin, and MMP9 in IAPP degradation and amyloid formation were performed using pharmacological inhibitors in cultured cell line or isolated islets, which may not fully recapitulate their physiological functions *in vivo*.

Additional factors

Other amyloid promoting factors include pH and calcium concentration in secretory granules (Charge, de Koning, and Clark 1995). Also, the molar ratio between IAPP and insulin appears to be important to prevent IAPP from adopting a beta sheet structure and to stabilize its monomer form (Per Westermark et al. 1996).

In summary, the mechanisms of islet amyloid formation are multifaceted and likely involve a combination of molecular changes that concertedly create pathological conditions that favor aggregation and propagation of IAPP into oligomers and insoluble amyloid plaques.

1.1.4. Human IAPP transgenic mouse models

Mouse models are commonly used to study systemic metabolism and disease pathogenesis, including the role of islet amyloid in T2D. However, unlike human IAPP, rodent forms of the peptide do not form islet amyloid as their amino acid sequence display several substitutions in the amyloidogenic region of hIAPP (position 20 to 29), where proline residues disrupt β-sheet structure and destabilizes oligomers (Figure 3) (P. Westermark et al. 1990; Chiu, Singh, and de Pablo 2013). Thus, transgenic lines with beta cell-specific expression of the hIAPP transgene driven by the rat insulin II gene promoter were generated to study islet amyloid formation and its role in T2D pathophysiology (Matveyenko and Butler 2006). Mice homozygous for hIAPP transgene develop islet amyloid deposits but this is accompanied by a rapid decline in beta cell function, increased cell death, and early development of T2D leading to death if left untreated (Janson et al. 1996). Therefore, studies are generally performed in hemizygous hIAPP mice, which do not develop spontaneous amyloid deposits or diabetes unless additional diabetogenic stressors through dietary, pharmacological, or

genetic interventions are introduced (Ahrén, Oosterwijk, Lips, and Höppener 1998; Höppener et al. 1993; Couce et al. 1996; Höppener et al. 1999). In addition to hemizygosity, biological sex is an important factor. Female hIAPP transgenic mice are more resilient to developing islet amyloid and diabetes due to the protective effects of estrogen on insulin resistance (Janson et al. 1996; Geisler et al. 2002). Therefore, male mice are commonly selected to study islet amyloid.

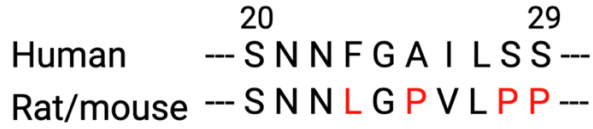

Figure 3: Amino acid sequences at position 20 to 29 of human and rodent IAPP
Unlike human IAPP, the rodent form is non-amyloidogenic due to substitutions of amino acids (red) in the amyloidogenic region (position 20 to 29) of human IAPP. In particular, the presence of proline residues in rodent IAPP disrupt and destabilizes β-sheet structures. Created with Biorender.com

1.2. Sorting-related receptor with type A repeats (SORLA)

1.2.1. Structure and biosynthesis of the receptor

The sorting-related receptor with A-type repeats (SORLA, LR11) is a 250 kDa type-1 transmembrane receptor of the vacuolar protein sorting 10 protein (VPS10P) domain receptor gene family (Jacobsen et al. 1996). Mammalian members of this gene family share a VPS10P domain in their extracellular region. The VPS10P domain is a large ligand binding region that assumes the shape of a funnel formed by a ten-bladed β-propeller fold. This ligand-binding domain was initially identified in the yeast vacuolar protein sorting 10 (Vps10) protein, a sorting receptor that transports carboxypeptidase Y (CPY) from late Golgi compartments to the vacuole (the yeast lysosome) (Marcusson et al. 1994). SORLA is also referred to as the lipoprotein receptor LR11 because it contains another ligand-binding region comprised of a cluster of 11 complement-type repeats (CR) that is found in low-density lipoprotein (LDL) receptor-related proteins. In addition to ligand binding, the ectodomain of SORLA contains a β-propeller region for pH-dependent release of ligands, an epidermal growth factor (EGF) type repeat domain, and a fibronectin type III (FNIII) domain (Figure 4). The short cytoplasmic tail of SORLA consists 54 amino acid residues and interacts with various adaptor proteins, such as the retromer, to direct the receptor to specific intracellular trafficking routes (Nielsen et al. 2007).

SORLA is first synthesized as a pro-receptor in the ER. Upon enzymatic removal of its N-terminal propeptide by furin in the *trans*-Golgi network (TGN), mature SORLA is released through the constitutive secretory pathway to the cell surface. From there, it undergoes endocytosis to shuttle through various intracellular compartments and to carry out its function as a sorting receptor for cargo along the endocytic and secretory routes of the cell. Since the aim of my dissertation is to examine the function of SORLA as a sorting receptor in pancreatic islet beta cells, I will focus on the known physiological roles and trafficking routes of the membrane-bound SORLA in the next sections.

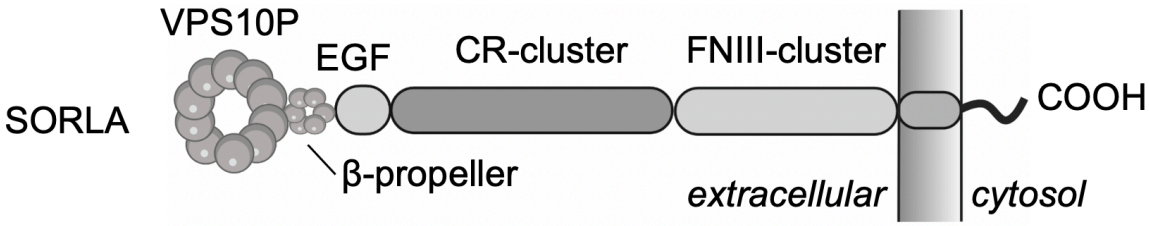

Figure 4: Structural organization of SORLA
SORLA is a type 1 transmembrane receptor. Its extracellular domain contains two established ligand binding regions, the VPS10P domain and the CR-cluster. It has a short cytoplasmic tail which binds to adaptor proteins or retromers for directed trafficking pathways. Abbreviations: vacuolar protein sorting 10 protein (VSP10P); epidermal growth factor (EGF); complement-type repeats (CR); fibronectin type III (FNIII). This figure is created with Biorender.com and published in Shih *et al*. 2022.

1.2.2. Trafficking routes of SORLA

SORLA is a multi-ligand receptor that follows multiple intracellular trafficking routes, including bi-directional sorting between the TGN and endosomal compartments, as well as transport to and from the cell surface (Monti and Andersen 2018). Over twenty ligands have been identified so far to interact with SORLA. Their trafficking routes can be broadly summarized into three main pathways: (1) bi-directional sorting between the TGN and endosomes, (2) anterograde sorting to endolysosomal compartment, and (3) endocytosis. The following is a brief description of each of these three SORLA-mediated trafficking routes.

(1) Bi-directional sorting between the TGN and endosomes

SORLA reduces amyloidogenic production of amyloid-beta (Aβ) peptides by sorting its precursor amyloid precursor protein (APP) from early endosomes to the TGN. This transport is mediated by interaction between the cytoplasmic tail of SORLA and the adaptor proteins PACS1 and retromer (Fjorback et al. 2012; Burgert et al. 2013; Schmidt et al. 2007). In addition to retrograde sorting, SORLA needs to return from the TGN to endosomes to replenish receptor levels required for maintaining APP transport. Anterograde transport of SORLA is mediated by the Golgi-localized adaptor proteins GGA1 and GGA2 (Dumanis et al. 2015), which also facilitate the sorting of newly synthesized Aβ from endosomes for lysosomal degradation. Another example of SORLA-dependent ligand sorting from the TGN to endosomes is lipoprotein lipase in the brain, which binds to the CR cluster of the receptor (Klinger et al. 2011). By sorting to the late endosomes, SORLA facilitate onward transport of lipoprotein lipase to lysosomes for degradation.

(2) Sorting from endosome to cell surface

In addition to endosomes-TGN sorting, SORLA also mediates transport from endosomes to other cellular compartments, including cell surface and lysosomes. For instance in neurons, SORLA interacts with sorting nexin 27 (SNX27) to divert APP from early endosomes to the cell surface, thereby reduces amyloidogenic processing into Aβ (T. Y. Huang et al. 2016). Alternatively, SORLA also directs newly synthesized Aβ in early endosomes to lysosomes for catabolism (Caglayan et al. 2014). In addition to neurons, SORLA has been shown to transport the human epidermal growth factor receptor 2 (HER2) from intracellular vesicles to the cell surface, thereby promoting its oncogenic signaling in cancer cells (Pietilä et al. 2019). Loss of SORLA results in impaired recycling of HER2, accumulation in lysosomes and suppression of tumor growth.

(3) Endocytosis

Although the majority of SORLA is localized in the Golgi, a substantial proportion of the receptor is found at the cell surface where it functions as an endocytic receptor (Jacobsen et al. 2001). A number of extracellular factors, including apolipoproteins and cytokines (e.g. interleukin-6) have been identified as ligands endocytosed by SORLA

(Nilsson et al. 2008; Larsen and Petersen 2017). In most cases, SORLA-bound ligands were directed to the late endosomes, en route to the lysosomal degradation pathway.

1.2.3. Relevance of SORLA in Alzheimer disease

SORLA is highly expressed in neurons and its encoding gene *SORL1* is a risk factor associated with both late-onset (Rogaeva et al. 2007; Lambert et al. 2013) and early-onset forms (Pottier et al. 2012) of Alzheimer disease (AD). Thus, extensive studies have been carried out to elucidate its neuronal functions. One of the most established roles of SORLA is its protection against amyloid plaques formation in the brain, a pathological hallmark of AD (Malik and Willnow 2020). The main amyloidogenic agent of amyloid plaques in AD are Aβ peptides, processing products of APP. The amyloidogenic process begins with the internalization of APP from the cell surface into endosomes, where it is proteolytically processed by β- and γ-secretases to generate amyloidogenic Aβ peptide (Willnow and Andersen 2013; Andersen et al. 2005) (Figure 5). The majority of Aβ is secreted and accumulated in the extracellular space, thereby promoting the aggregation and formation of insoluble amyloid plaques. SORLA reduces the overall amyloid burden in the brain by regulating the trafficking pathways of APP and Aβ. Firstly, SORLA binds to internalized APP via its CR repeats (Andersen et al. 2006; Mehmedbasic et al. 2015) and direct its transport from early endosomes to the TGN through actions of retromer and monomeric adaptor proteins such as Golgi-localized, γ-ear-containing, Arf-binding proteins (GGA1) and phosphofurin acidic cluster sorting protein 1 (PACS1), preventing the generation of Aβ (Schmidt et al. 2007; Burgert et al. 2013) (Figure 5 ,(1)). Secondly, SORLA binds to newly synthesized Aβ via its VPS10P domain and directs nascent Aβ from endosomes to lysosomes for degradation, further reducing accumulation of Aβ in the brain (Caglayan et al. 2014; Dumanis et al. 2015) (Figure 5, (2)). Furthermore, it has been shown that SORLA interacts with SNX27, which promotes recycling of APP from endosomes to the cell surface and also reduces amyloidogenic processing into Aβ (T. Y. Huang et al. 2016) (Figure 5,(3)).

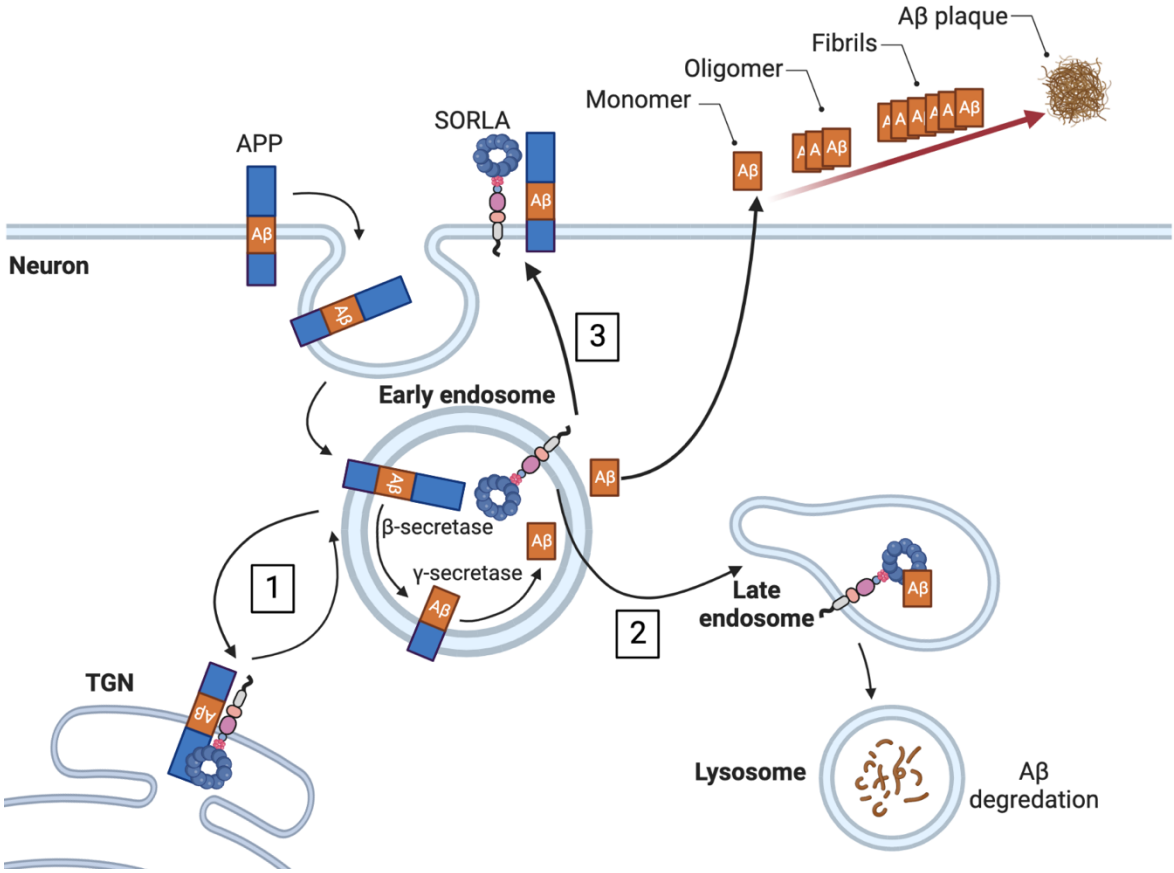

Figure 5: Sorting pathways whereby SORLA reduces amyloid burden in the brain
Extracellular amyloid plaques in the brain are formed by aggregation of Aβ peptides released during APP processing. Internalized APP from the cell surface is processed into Aβ by secretases in early endosomes. SORLA reduces overall Aβ production through [1] transport of APP from endosomes to the TGN via adaptor proteins AP1 and PACS1. SORLA is then recycled back from the TGN to early endosomes via adaptor protein GGA; [2] transport of newly released Aβ to late endosomes for lysosomal degradation; and [3] diversion of APP from endosomes to the cell surface through interaction with adaptor protein SNX27. Abbreviations: phosphofurin acidic cluster sorting protein 1 (PACS1), Golgi-localized, γ-ear-containing Arf-binding proteins (GGA1), sorting nexin 27 (SNX27). Created with Biorender.com

1.2.4. Emerging roles for SORLA in metabolism

SORLA is classically referred as a neuronal receptor and implicated in neurodegenerative diseases. However, it is also expressed in peripheral tissues, such as the liver, kidney, adipose tissues, and endocrine tissues as documented in the Human Protein Atlas. Recent human and mouse genome-wide association studies have identified multiple single-nucleotide polymorphisms in *SORL1* associated with metabolic traits, namely obesity and waist circumference (Smith et al. 2010; Parks et al. 2013). Further *in vivo* studies in SORLA-deficient or SORLA overexpressing mice have shown that SORLA promotes obesity and glucose intolerance through inhibition of lipolytic activity (Schmidt et al. 2016) and thermogenesis (Whittle et al. 2015) in white adipose tissues. SORLA inhibits lipolytic activity in adipocytes through increasing expression of

insulin receptor at the cell surface and enhancing downstream insulin signaling. It sorts internalized insulin receptors from the endosomes towards the TGN to be recycled and incorporated into vesicles destined to the cell surface (Schmidt et al. 2016). By transporting insulin receptor to the TGN, SORLA also prevents endolysosomal degradation of insulin receptor and maintain levels of surface expression.

Another major organ system that plays a central role in metabolism is the endocrine pancreas, which secretes hormones from islets to maintain glucose homeostasis. Recent single-cell RNA sequencing (scRNAseq) analyses in human pancreatic tissues have revealed the presence of SORLA transcripts in islet endocrine cells but not exocrine cells (Segerstolpe et al. 2016) (Figure 6), suggesting a role for SORLA in regulating islet hormones. In addition to the study by Segerstolpe *et al.*, additional transcriptomic studies have also provided evidence for SORLA transcripts in both human and murine islets (Muraro et al. 2016; Neelankal John, Ram, and Jiang 2018). Together, multiple transcriptomic studies suggested SORLA as an emerging candidate in the control of energy homeostasis and metabolism. However, the underlying cell biology of how SORLA functions in islet endocrine cells, and its roles in metabolic diseases, such as diabetes, remains to be elucidated in detail.

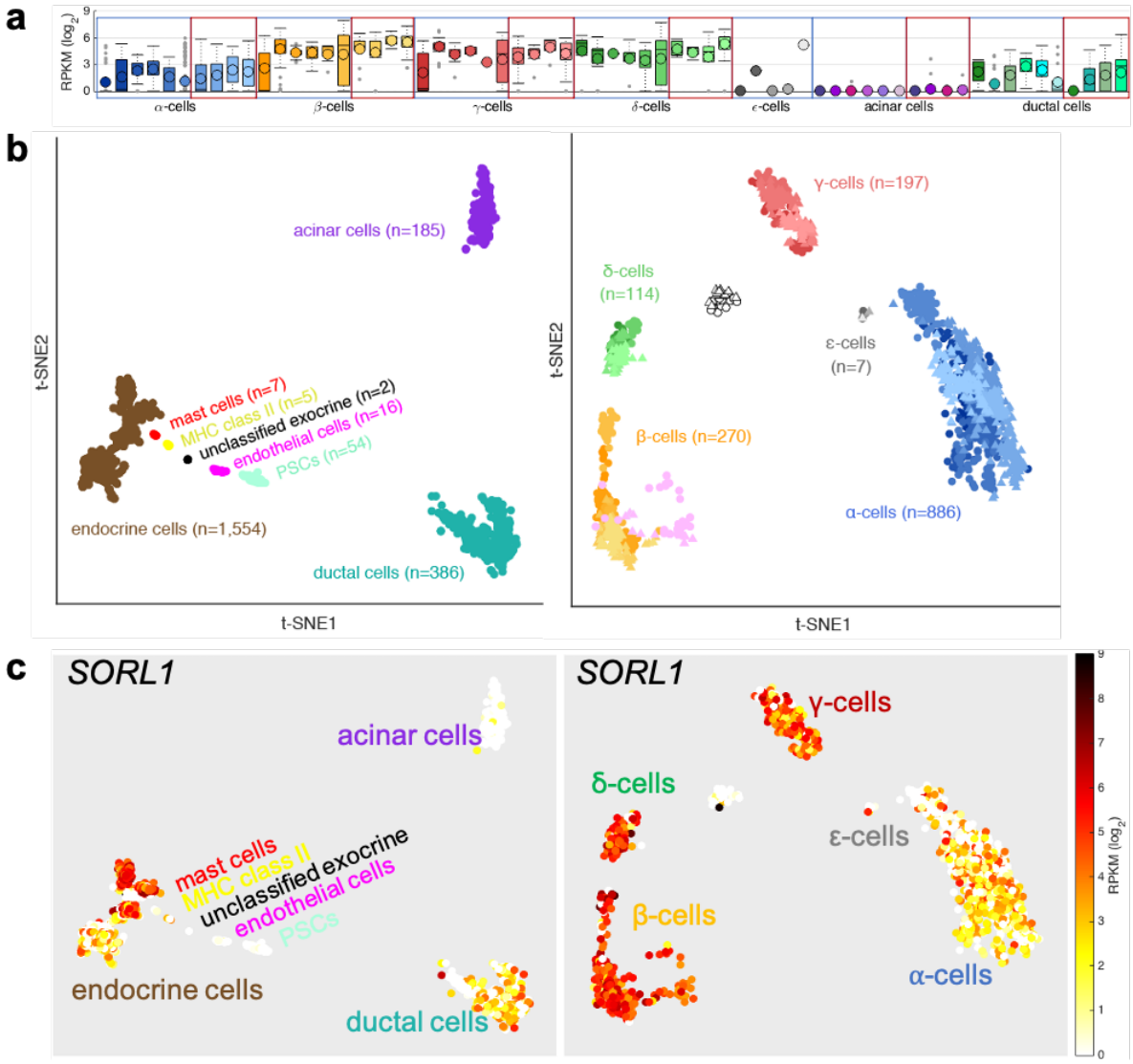

Figure 6 Expression of *SORL1* across human pancreatic tissues of healthy and T2D subjects
(**a**) Box plots of *SORL1* expression levels in seven major pancreatic cell types. Each bar represents an individual donor, with the bars in blue boxes corresponding to healthy subjects and the bars in red boxes corresponding to T2D subjects. (**b**) Two-dimensional projections of all sequenced cells into related biological clusters including endocrine, ductal and acinar cells (left panel) or endocrine only cell types (right panel) based on t-distributed stochastic neighbor embedding (t-SNE) plots. (**c**). Expression of *SORL1* (log_2RPKM) in all sequenced cells corresponding to their clusters shown in (b). *Sorl1* expression is absent in acinar cells but lowly expressed in ductal cells and more highly expressed in endocrine cells. Among endocrine cell types, *SORL1* expression is higher in beta cells compared to alpha cells. This figure is adapted from Segerstolpe, Åsa, Athanasia Palasantza, Pernilla Eliasson, Eva Marie Andersson, Anne Christine Andréasson, Xiaoyan Sun, Simone Picelli, Alan Sabirsh, Maryam Clausen, Magnus K. Bjursell, David M. Smith, Maria Kasper, Carina Ämmälä and Rickard Sandberg. 2016. "Single-Cell Transcriptome Profiling of Human Pancreatic Islets in Health and Type 2 Diabetes." Cell Metabolism 24 (4): 593–607. https://doi.org/10.1016/j.cmet.2016.08.020. (Segerstolpe et al. 2016) and generated with https://sandberglab.se/tool/pancreas/

1.3. Aim of this study

Recent transcriptomic studies of human and murine islets revealed that SORLA transcripts (*SORL1*) are also found in islet endocrine cells and with highest abundance in the insulin-producing beta cells (Muraro et al. 2016; Segerstolpe et al. 2016; Neelankal John, Ram, and Jiang 2018). Given the fundamental role of SORLA in regulating amyloidogenic processes in neurons through control of APP and Aβ trafficking, I hypothesized that SORLA may also play a role in control of IAPP transport and islet amyloid formation in pancreatic islet beta cells. To query this hypothesis in my thesis project, I examined the effects of SORLA deficiency on islet amyloid deposition, beta cell function, and overall glucose homeostasis comparing wildtype and SORLA-knockout mice that express hIAPP in islet beta cells, an animal model of islet amyloid. Furthermore, using primary islet cells and an established cell line, I determined the expression and subcellular localization of SORLA, its interaction with pro- and mature forms of IAPP, and the underlying molecular mechanisms of its impact on islet amyloid formation.

2. Materials and methods

2.1. Mouse models

Global SORLA knockout mice on a C57Bl/6J background (KO BL/6) were previously generated in house and described in (Andersen et al. 2005). To study the role of SORLA in islet amyloid deposition, SORLA KO mice were crossed with human IAPP transgenic mice (FVB/N-Tg(Ins2-IAPP)RHFSoel/J) purchased from The Jackson Laboratory (#08232) according to the breeding scheme in Figure 7. In the latter mouse line, beta cell-specific expression of the *hIAPP* transgene is under the regulatory control of the rat insulin II promoter. All in all, four genotypes were generated in this study, namely SORLA WT and KO mice with hemizygous expression of *hIAPP* (hIAPP:SORLA WT or KO), as well as SORLA WT and KO without *hIAPP* transgene expression (SORLA WT or KO). Genotypes were confirmed by PCR.

All animal experiments were approved by the Berlin State Office for Health and Social Affairs (LAGESO, Berlin, Germany). Animals were housed in the animal facility of the Max Delbrück Center, in a 12 h light/ 12 h dark cycle. Animals were fed a standard chow diet (4.5% crude fat, 39% carbohydrates) or a HFD (60% crude fat, 21% carbohydrates, 19% protein; #E15741-34; ssniff, Soest, Germany). For HFD studies, mice began HFD feeding at 4 weeks of age upon weaning. Previous study has shown that islet amyloid formation is rarely found in female mice (Verchere et al. 1996). Thus, only male mice were used in this study.

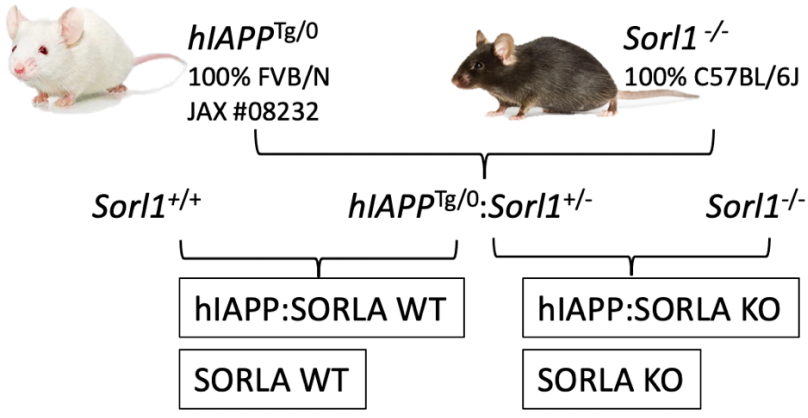

Figure 7: Breeding scheme to generate hIAPP-expressing SORLA KO and WT mice
Transgenic mice hemizygous for beta cell-specific *hIAPP* transgene expression were purchased from Jackson Laboratory and crossed with global SORLA KO mice that were generated in-house. In the second generation, hIAPP$^{Tg/0}$:Sorl1$^{+/-}$ were bred with SORLA WT (Sorl1$^{+/+}$) or KO (Sorl1$^{-/-}$) animals to generate experimental mice of the four final genotypes shown here. Created with PowerPoint.

2.2. Measurements for body weight and fasting glucose

Body weight and fasting blood glucose levels were measured every 2 weeks in mice aged between 4 and 30 weeks of age. After body weight was measured, mice were fasted for 6 h during the light-cycle (starting between 8:00 and 9:00) prior to blood glucose measurement using a glucometer (Contour® NEXT ONE).

2.3. Collection of fasting blood plasma for hormones measurement

For measurement of fasting circulating blood insulin and IAPP levels, mice were fasted for 6 h prior to blood collection. Blood was collected by bleeding the submandibular vein into EDTA-treated MiniCollect® tube. Blood plasma was separated by centrifugation at 1500 g for 10 min at 4°C. Plasma was stored at -80°C until further measurement by ELISA as described in section 2.11.

2.4. Glucose tolerance test (GTT)

Mice were fasted for 16 h during the dark-cycle, starting at 17:00. On the day of GTT, mice were weighed and fasting blood glucose were measured. A glucose solution in PBS was given intraperitoneally at a dose of 2 g/ kg body weight for ND-fed mice and 0.75 g/ kg body weight for HFD-fed mice. A lower glucose dose was administered to HFD mice to ensure that glucose measurements did not exceed the maximum detection range of the glucometer. Blood glucose levels were measured at regular intervals (20, 40, 60, 90, 120 min) by bleeding at the tail tip.

2.5. Glucose-stimulated insulin secretion (GSIS) *in vivo*

Mice were fasted for 16 h during the dark-cycle, starting at 17:00. On the day of GSIS, mice were weighed and a glucose solution in PBS was given by intraperitoneal injection at a dose of 2 g / kg body weight for both ND- and HFD-fed mice. Blood samples were collected at time 0, 2, and 30 min and plasma were separated as described in section 2.3. Insulin was measured by ELISA as described in section 2.11.

2.6. Preparation of pancreas for histology

For murine tissues, immediately after cervical dislocation, pancreata were excised from 33- to 35-week-old mice, fixed in 4% paraformaldehyde overnight at 4°C, followed by step-wise dehydration in 15% sucrose in PBS for 6 h, then 30% sucrose in PBS overnight at 4°C. Pancreas tissues were cryopreserved in Tissue-Tek® O.C.T. and kept at -80°C until sectioning (10 µm) on a cryostat. Human pancreas biopsies from 3 healthy and anonymized subjects were provided by Assoc. Prof. Esben Søndergaard (Steno Diabetes Center Aarhus) in the form of paraffin-embedded sections.

2.7. Islet isolation

Pancreata were perfused with 1 – 2 ml of 900 U/ml collagenase (Sigma C9407) solution in HBSS (ThermoFisher 14175,). Perfused pancreata were excised and digested with 2 ml of collagenase solution at 37°C for 13 min, followed by manual shaking for 60 – 90 s. Digested tissue suspension was washed with ice-cold HBSS with 1 mM $CaCl_2$ and filtered through a 70 µm nylon filter. Islets were hand-picked and cultured in 11 mM glucose RPMI 1640 (PAN biotech P04-16516), supplemented with 2 mM L-Glutamine (Gibco 25030-024), 100 U/mL penicillin (Gibco 15140-122), 100 mg/mL streptomycin, and 10% FBS (Gibco 10270-106). Islets were recovered overnight and maintained in a 37°C incubator at 5% CO_2.

2.8. Static insulin and hIAPP secretion from isolated islets

After an overnight recovery from islet isolation, islets were subjected to a series of secretion buffers for the assay. For each sample, a total of 30 similar sized islets were collected into low-binding Eppendorf tubes and preincubated in 250 µl of Krebs-ringer buffer with HEPES (KRBH) (129 mM NaCl, 4.8 mM KCl, 1.2 mM $MgSO_4$, 1.2 mM KH_2PO_4, 5 mM $NaHCO_3$, 2.5 mM $CaCl_2$, 10 mM HEPES and 0.25% BSA, at pH 7.4) supplemented with the specified concentration of glucose for 1 h, followed by an additional 1 h at the indicated conditions. Islet secretions were collected after each incubation period and islets were harvested at the end of the assay to measure total protein and hormone content. Islet secretions and lysates were kept at -80°C prior to measurement by ELISA as described in section 2.11. Levels of secreted hormones

were normalized to total islet protein content as quantified by bicinchoninic acid assay (BCA).

2.9. Dynamic insulin secretion from isolated islets

Similar to static islet secretion described in section 2.8, groups of 30 islets per sample were used to test dynamic islet secretion. Dynamic islet secretion was performed together with Dr. Thilo Speckmann in the laboratory of Prof. Annette Schürmann (German Institute of Human Nutrition Potsdam-Rehbruecke) using the PERI 4.2 machine (Biorep Technologies, USA). In detail, islets were continuously perifused with KRBH buffer with the specified glucose concentration at a flow rate of 100 µl/ min. Islets were equilibrated in 11 mM glucose KRBH for 60 min prior to stimulation in the following sequence: 11 mM glucose (18 min), 1.67 mmol/l glucose (60 min), 16.7 mM glucose (34 min), 1.67 mM glucose (30 min), and 30 mM KCl in 1.67 mM glucose KRBH (10 min). Islets were collected at the end of the assay and lysed in TE buffer (10 mM Tris-HCl, 1 mM EDTA and 1% Triton) to determine total islet DNA content (Quant-iT Picogreen DNA kit, Thermo Fisher Scientific, USA). Levels of secreted insulin were measured by ELISA as described in section 2.11. and data were normalized to total DNA content.

2.10. Insulin extraction by acid ethanol in islets and pancreases

Whole pancreas was removed, weighed and submerged in 5 ml of ice-cold acid ethanol solution (70% ethanol, 0.18M HCl). Pancreata were homogenized mechanically and incubated in acid ethanol overnight at 4^{o}C. For islets, groups of 30 islets per sample were combined in 30 µl of ice-cold acid ethanol and vortexed at maximum speed for 1 min. Islet homogenate was incubated on ice for 3 h with intermittent vortex every 30 min. Both pancreatic and islet homogenates were centrifuged at 2000 rpm for 15 min at 4^{o}C and supernatants were collected and stored at -80^{o}C until determination of insulin content by ELISA as described in section 2.11.

2.11. ELISA measurements of insulin, human (pro)IAPP

Insulin immunoreactivity was measured using the ultra sensitive mouse insulin ELISA kit (Crystal Chem, 90080) according to manufacturer’s protocol.

Human proIAPP$_{1-48}$ and mature IAPP immunoreactivities were measured by Dr. Yi-Chun Chen in the laboratory of Prof. Bruce Verchere (University of British Columbia) using an in-house ELISA (Courtade et al. 2017).

2.12. Cell line and culture

SH-SY5Y neuroblastoma cells (ATCC CRL-2266) were cultured in Dulbecco's Modified Eagle Medium/Nutrient Mixture F-12 (DMEM/F-12) media (Gibco, USA), supplemented with 10% FBS, 1% Non Essential Amino Acid, 100 U/mL penicillin and 100 mg/mL streptomycin. Stable SORLA-overexpressing SH-SY5Ycell line was generated previously (Dumanis et al. 2015) and cultured in the presence of 90 µg/ml zeocin (Invitrogen, USA). Cultured cells were tested regularly for mycoplasma infection.

2.13. Staining for confocal microscopy

2.13.1. Immunostaining

Prior to immunostaining, 10 µm of cryo-preserved tissue sections were rehydrated in 0.3% Triton X-100/PBS for 15 min. Rehydrated slides were then heated in antigen retrieval solution (10 mM citrate buffer with 0.05% Tween-20, pH 6.0) at 95°C for 10 min and allowed to cool to room temperature.

All samples including cells and tissue sections were permeabilized in 0.3% Triton X-100, 0.1% BSA in Tris-buffered saline (TBS) for 10 min at RT and blocked in 3% BSA in TBS for overnight at 4°C. Sections were incubated with primary antibodies (Table 1) for 2 h at RT, followed by 3 times washes in TBS-Tween and incubation with fluorophore-conjugated secondary antibodies (Table 2) for 1 h at RT. Following 3 washes, nuclei were stained with DAPI (tissue sections 1:4000 or cells 1:8000). Images were acquired as a single plane image using a Zeiss confocal microscope (LSM700).

2.13.2. Proximity ligation assay (PLA)

Proximity ligation assay (PLA) is a microscopy-based tool to detect closely interacting proteins with single molecule resolution. PLA was performed according to manufacturer’s protocol (Sigma, Duolink™). Briefly, fixed dispersed islet cells were blocked overnight at 4°C, followed by standard incubation with primary antibodies

raised in different species for 2 h. Then, samples were incubated with PLA reagents which are secondary antibodies conjugated with oligonucleotides. If the two proteins of interests are in close proximity, the pair of oligonucleotides are able to hybridize and ligate to form a closed, circular DNA template for further amplification by DNA polymerase. The amplified signals from oligos are coupled with fluorochromes for visualization by fluorescence microscopy. To determine subcellular localization of PLA signal, cells were additionally immunolabeled with primary and secondary antibodies for the indicated compartment marker protein. Finally, cell nuclei were stained with DAPI (Roche).

2.13.3. Thioflavin S staining

Thioflavin S (ThioS) is a fluorescent dye routinely used in histology to identify amyloid as it readily binds to beta-sheet rich structures. In this study, ThioS was used to assess the presence of amyloid in pancreatic islets. Pancreatic tissue sections were first immunostained for insulin to identify islet beta cells, followed by staining with 0.5% (wt/vol) ThioS (Sigma T1892) for 2 min, washing in 70% ethanol twice, and a final wash in water.

The prevalence of islet amyloid formation was quantified as the percentage of islets containing amyloid, while the severity of islet amyloid was assessed based on the percentage of islet area with ThioS positive staining. The mean value for each animal was taken from the analysis of 22 – 30 islets. Confocal images of islet amyloid staining were analyzed using CellProfiler (Cambridge, MA, USA).

2.13.4. TUNEL staining

Terminal deoxynucleotidyl transferase dUTP nick end labeling (TUNEL) is a method to identify cells undergoing apoptotic cell death based on DNA fragmentation. The technique utilizes the enzyme terminal deoxynucleotidyl transferase which attaches fluorescently-labeled deoxynucleotides the 3’-hydroxyl termini of DNA breaks. In this study, islet cell deaths from pancreatic tissue sections were identified by TUNEL staining according to manufacturer’s protocol. Tissue sections were additionally immunostained for insulin and glucagon to quantify proportions of beta and alpha cells per islet, respectively. All nuclei were counterstained with DAPI. The mean value for

each animal was taken from analysis of 22 – 30 islets. Confocal images of TUNEL staining were analyzed using CellProfiler (Cambridge, MA, USA).

2.14. Preparation of peptides

Synthetic peptides of mouse proIAPP$_{1-70}$, proIAPP$_{1-51}$ and mature amidated IAPP with disulfide bond between Cys-2 and Cys7 (Figure 15b) (NCBI Reference Sequence: NP_034621.1) were commercially synthesized by Biosyntan (Berlin, Germany). Synthetic human Aβ$_{1-40}$ peptides were purchased from Bachem, Germany (#4095737). Peptides were dissolved in PBS and stored at -80°C prior to experimentation. His-tag ectodomain of human SORLA was previously generated and purified in-house (Andersen et al. 2005).

2.15. Microscale thermophoresis (MST)

Microscale thermophoresis (MST) is a fluorescence-based method to characterize binding interactions and affinities of molecules, such as DNA and proteins, in solutions. This technique is based on a physical phenomenon known as thermophoresis, i.e. the movements of molecules in a temperature gradient. Movement is influenced by a number of factors, such as the size, charge, and conformation of molecules. During the assay, the test sample containing two different purified proteins (e.g. receptor and target ligand) is heated by an infrared laser and the movements of the molecules during the temperature gradient is recorded and analyzed to determine if there is binding between the two proteins and their associated binding affinity (K_d). In this study, the ectodomain of SORLA was fluorescently labeled using the Protein Labeling Kit RED-NHS (NanoTemper Technologies) according to the manufacturer's instructions. The concentration of labeled SORLA was kept constant (3 nmol/l) in PBS with 0.05 % Tween 20, while non-labeled ligand (i.e., mouse pro or mature IAPP peptides) was serially titrated between 7.6 nmol/l and 250 µmol/l. Labeled SORLA and ligands were loaded into Monolith NT.115 Premium Capillaries (NanoTemper Technologies) and the measurement was performed using the Monolith NT.115 (NanoTemper Technologies) at 100 % LED power and medium MST power. An MST on-time of 2.5 s was used for analysis, and a K_d was derived for this interaction using MO.Affinity Analysis software version 2.3 (NanoTemper Technologies).

2.16. Peptide uptake assay

SH-SY5Y cells stably overexpressing SORLA and parental cells were seeded on glass coverslip one day before peptide uptake. Cells were incubated for 30 min in serum-free medium before treatment with 20 μM (pro)IAPP for 30 min. To examine the involvement of clathrin-mediated endocytosis, cells were treated with 100 μM dynasore (Cayman Chemical, 14062-10). Cells were immediately fixed in 4% paraformaldehyde and immunofluorescence staining was performed to examine the presence of internalized peptide, SORLA and subcellular organelles. Lysosomes were stained by incubating cells with 500 nM LysoTracker Deep Red (Thermo Fisher Scientific, L12492) in normal growth media for 1 h before uptake assay.

2.17. Statistical analysis

Statistical analyses of quantitative data were performed using Prism 7.0 (GraphPad software) and presented as mean ± standard error of mean (SEM) with the indicated number of replicates, as shown in figure legends. Normality of data was analyzed with the D'Agostino-Pearson normality test. Statistical differences between two groups and those with low number of sample size ($n < 8$) were analyzed unpaired Student’s t-test. Comparisons between three or more groups were analyzed by one-way or two-way ANOVA. Additional Bonferroni's multiple comparisons post-hoc test was applied to determine the interaction of two independent variables (i.e. genotypes and diet groups for this study). A p-value of less than 0.05 was considered statistically significant, where * $p<0.05$, ** $p<0.01$, *** $p<0.001$, and **** $p<0.0001$.

Table 1: List of primary antibodies

This table is derived from the supplementary data of Shih, Alexis Z.L., Yi-Chun Chen, Thilo Speckmann, Esben Søndergaard, Annette Schürmann, C. Bruce Verchere, and Thomas E. Willnow. 2022. “SORLA Mediates Endocytic Uptake of ProIAPP and Protects against Islet Amyloid Deposition.” (Shih et al. 2022).

Antibody	**Manufacturer/ provider**	**Catalog #**	**Host Species**	**Dilution**
SORLA	J. Gliemann (University of Aarhus, Denmark)		Goat	1:200 (IF), 1:400 (PLA)
Insulin	Agilent, USA	IR002	Guinea pig	1:3
Mouse IAPP	Peninsula Laboratories, USA	T-4145	Rabbit	1:400
Human IAPP	Peninsula Laboratories, USA	T-4149	Rabbit	1:400
Glucagon	Abcam, USA	Ab10988	Mouse	1:500
Somatostatin (SST)	Abcam, USA	Ab111912	Rabbit	1:250
Pancreatic polypeptide (PPY)	Sigma-Aldrich, USA	AB939-I	Rabbit	1:500
Syntaxin6 (STX6)	BD bioscience, USA	BD610636	Mouse	1:200
EEA1	BD bioscience, USA	BD610457	Mouse	1:100
Rab4	Abcam, USA	Ab13252	Rabbit	1:100
Rab4	BD bioscience	BD610889	Mouse	1:100
Rab9	Invitrogen, USA	MA3-067	Mouse	1:100
Rab11	BD bioscience, USA	BD610657	Mouse	1:100
TGN38	BD bioscience, USA	BD610899	Mouse	1:50

Ki67	Abcam, USA	Ab16667	Rabbit	1:100

Table 2: List of secondary antibodies

This table is derived from the supplementary data of Shih, Alexis Z.L., Yi-Chun Chen, Thilo Speckmann, Esben Søndergaard, Annette Schürmann, C. Bruce Verchere, and Thomas E. Willnow. 2022. “SORLA Mediates Endocytic Uptake of ProIAPP and Protects against Islet Amyloid Deposition.” (Shih et al. 2022).

Antibody	**Manufacturer**	**Catalog number**	**Host Species**	**Dilution**
Anti-goat AlexaFluor488	Abcam, USA	ab150129	Donkey	1:1000
Anti-mouse AlexaFluor555	Abcam, USA	Ab150106	Donkey	1:1000
Anti-mouse AlexaFluor647	Invitrogen, USA	A31571	Donkey	1:1000
Anti-guinea pig Cy3	Jackson ImmunoResearch, UK	706-165-148	Donkey	1:1000
Anti-guinea pig AlexaFluor647	Merck Milipore	AP193SA6	Donkey	1:1000
Anti-rabbit AlexaFluor555	Invitrogen , USA	A31572	Donkey	1:1000
Anti-rabbit AlexaFluor647	Abcam, USA	Ab150075	Donkey	1:1000

3. Results

3.1. SORLA expression is enriched in islet beta cells

Expression of SORLA in pancreatic islets have been demonstrated at the transcript level by RNA sequencing (Muraro et al. 2016; Neelankal John, Ram, and Jiang 2018). However, its expression at the protein level in islets remined to be validated. Therefore, my first goal in this study was to examine whether, and in which islet cell type SORLA protein is expressed. I performed immunofluorescence staining on mouse pancreatic tissue sections and demonstrated that SORLA was enriched in islets of WT mice (Fig. 8). Additional staining with specific markers of islet cell type revealed that SORLA was largely expressed in the beta cells (insulin positive) but it was also present in alpha cells (glucagon positive), delta cells (somatostatin positive) and PP cells (pancreatic polypeptide positive) (Figure 8a). Next, I confirmed the loss of SORLA immunoreactivity in islets of SORLA knockout wildtype BL/6 mice (KO, BL/6) (Figure 8b). In addition to mouse models, I further assessed the relevance of SORLA expression in humans. I found that SORLA was predominately expressed in islet beta cells but not alpha cells of human pancreatic tissue (Figure 8c). Together, the results from mouse and human pancreata staining confirmed that SORLA is expressed at the protein level in islet beta cells.

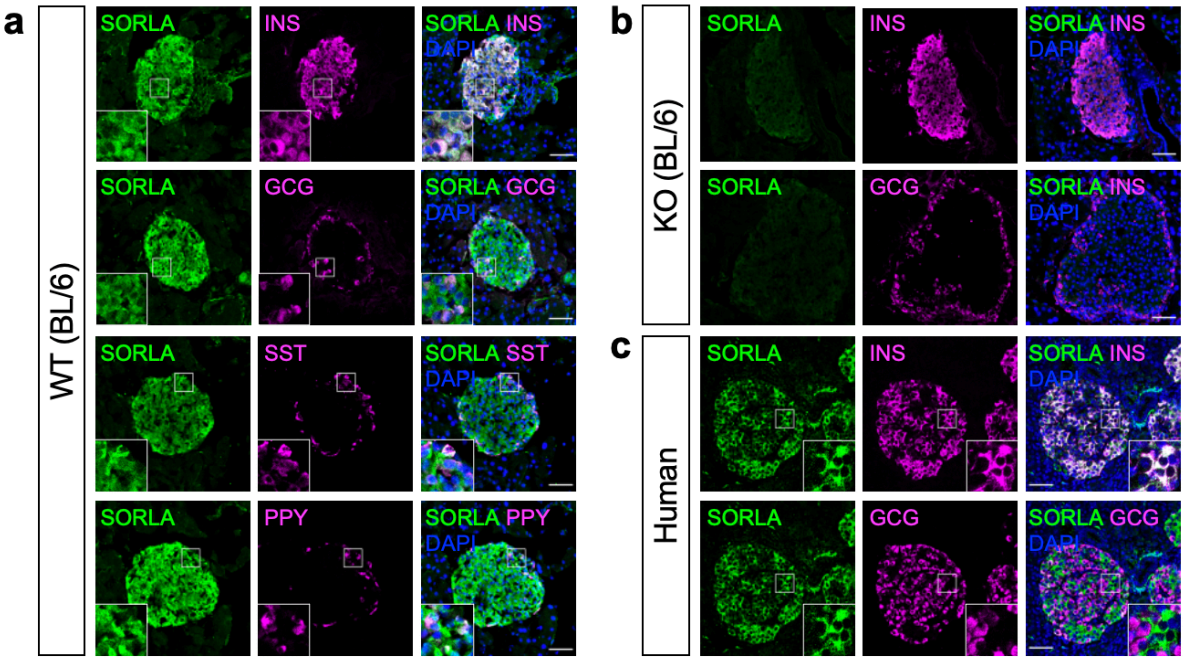

Figure 8: SORLA is expressed in mouse and human pancreatic islet beta cells.

(**a, b**) Pancreatic tissue sections from (a) WT (BL/6) and (b) SORLA KO (BL/6) mice were immunostained for SORLA (green) and islet cell markers (magenta) including insulin (INS), glucagon (GCG), somatostatin (SST), and pancreatic polypeptide (PPY). Nuclei were counterstained with DAPI (blue). SORLA expression is successfully depleted in SORLA KO islets. (**c**) Human pancreatic biopsies tissue sections from non-diabetic patients were immunostained for of SORLA (green) and insulin or glucagon (magenta). Single and merged channel configurations of representative images are displayed. The insets represent zoomed-in areas as indicated by white boxes in the overview images. Scale bars, 50 μm. This figure is adapted from Shih et al. 2022.

3.2. Loss of SORLA increases islet amyloid deposition and islet cell death

Unlike human, rodent IAPP is non-amyloidogenic. To examine the effects of SORLA deficiency on islet amyloid deposition, I therefore crossed SORLA KO mice with a transgenic line that expresses *hIAPP* under regulatory control of the rat insulin II promoter. In this study, I performed comparative analyses in male hIAPP-expressing mice deficient for *Sorl1* (hIAPP:SORLA KO) and hIAPP-expressing wildtype control (hIAPP:SORLA WT) animals. Since metabolic stress imposed by high-fat diet (HFD) feeding promotes islet amyloid formation (Höppener et al. 2008), I performed the studies in mice fed a normal chow diet (ND) or a HFD (60% crude fat) for 6 months. I assessed the amount of amyloid deposited by histological staining of pancreas tissue sections with thioflavin S (ThioS), a dye which binds to the characteristic beta-sheet structures in amyloid (Rajamohamedsait and Sigurdsson 2012). Additionally, I immunostained for insulin to identify islets in the pancreas. I then analyzed two parameters of islet amyloid deposition, prevalence and severity. The prevalence of islet amyloid was assessed based on the percentage of amyloid-containing islets, while the severity of islet amyloid was quantified based on the percentage of amyloid area per total islet area.

In these studies, hIAPP:SORLA KO mice developed increased amyloid prevalence as compared to hIAPP:SORLA WT mice in both ND and HFD conditions (Figure 9b). Interestingly, HFD further increased amyloid prevalence in hIAPP:SORLA WT mice compared to those fed with ND, but such effect was not observed in SORLA-deficient mice (Figure 9b). Similarly, hIAPP:SORLA KO mice developed worsened amyloid severity compared to hIAPP:SORLA WT mice when fed with ND (0.56±0.16% vs 6.9±1.8% ThioS positive islet area) (Figure 9c). However, the protective effect of SORLA on amyloid severity was blunted after HFD feeding.

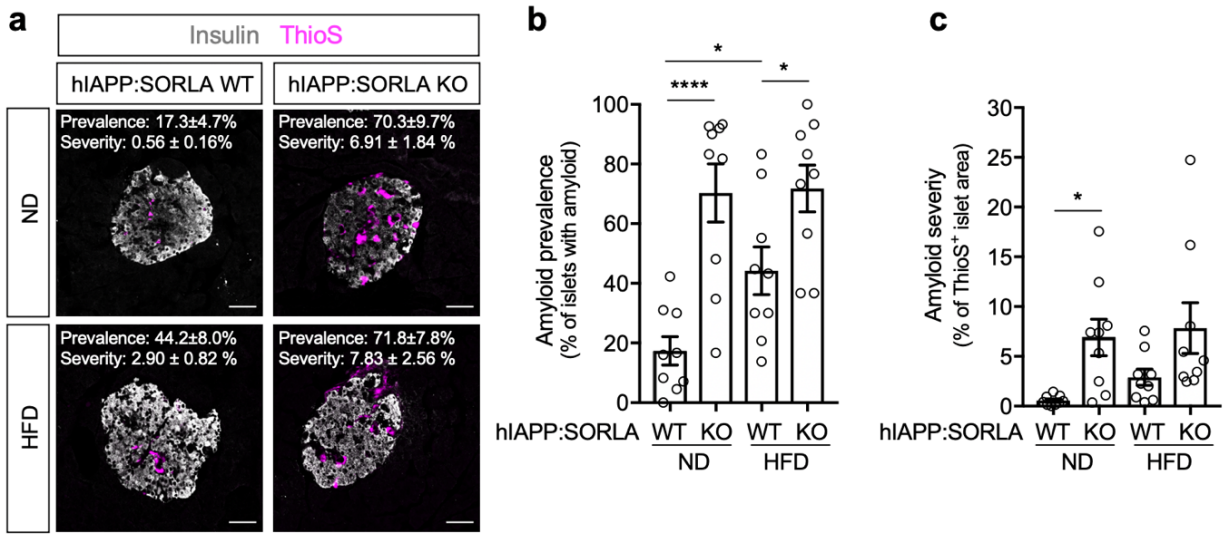

Figure 9: Loss of SORLA in hIAPP-expressing mice increases islet amyloid.
(**a**) Islet amyloid was identified by histological staining with thioflavin S (ThioS, magenta) and islets were identified by immunostaining for insulin (white) on pancreatic sections from ND- or HFD-fed hIAPP:SORLA WT or KO mice at 33- to 35-weeks of age. Scale bars, 50 µm. (**b**) Islet amyloid prevalence was assessed based on the percentage of amyloid-containing islets, while (**c**) islet amyloid severity was quantified based on the percentage ThioS$^+$ area per total islet area (n = 9 mice per genotype, 20 – 30 islets per mouse). Data are expressed as mean ± SEM. Statistical significance of differences was determined by two-way ANOVA with post hoc test. * $p < 0.05$, **** $p < 0.0001$. This figure is adapted from Shih et al. 2022.

Islet amyloid is a pathological hallmark of T2D and is associated with beta cell dysfunction and cell death (MacArthur et al. 1999; Jurgens et al. 2011). I therefore examined whether the increased islet amyloid found in hIAPP:SORLA KO mice correlated with increased islet cell death by performing TUNEL staining. Consistent with increased amyloid, ND-fed hIAPP:SORLA KO mice exhibited a small but significantly higher amounts of islet cell death (3.3±1.4%) when compared to hIAPP:SORLA WT (1.4±0.6%). In HFD-fed animals, similar effects to the blunted islet amyloid burden was observed in SORLA KO mice, as there was no longer statistically significant difference in cell death between SORLA genotypes (hIAPP:SORLA WT 3.3±0.9%, KO 4.8±2.8%) (Figure 10a, b). Since islet amyloid is probable cause of cell death, I performed linear regression analysis to validate the correlation between islet amyloid severity and islet cell death, which demonstrated a positive relationship (Figure 10c). In addition to cell death, I examined the effects of SORLA deficiency on overall islet area and cell composition. Despite increased cell death found in ND-fed hIAPP:SORLA WT animals, there were no significant reduction in their islet area (Figure 10d), as well as the proportions of beta cell (Figure 10e) and alpha cell (Figure 10f) area per islet. It has been shown that beta cell proliferation is induced under conditions of insulin resistance, such as obesity and pregnancy, in order to maintain overall cell mass and the increased

demand for insulin (Rieck and Kaestner 2010; Dhawan, Georgia, and Bhushan 2007). I therefore examined if increased cell proliferation may explain for the lack of beta cell loss in ND-fed hIAPP:SORLA KO mice by performing ki67 staining (Figure 10g). Overall, percentage of proliferative cells in islets is low and comparable between SORLA genotypes (Figure 10h). Together, the results suggest that the increased islet amyloid and associated cell death observed in hIAPP:SORLA KO mice at 7 months-old likely represent an early event in the worsening of islet pathology.

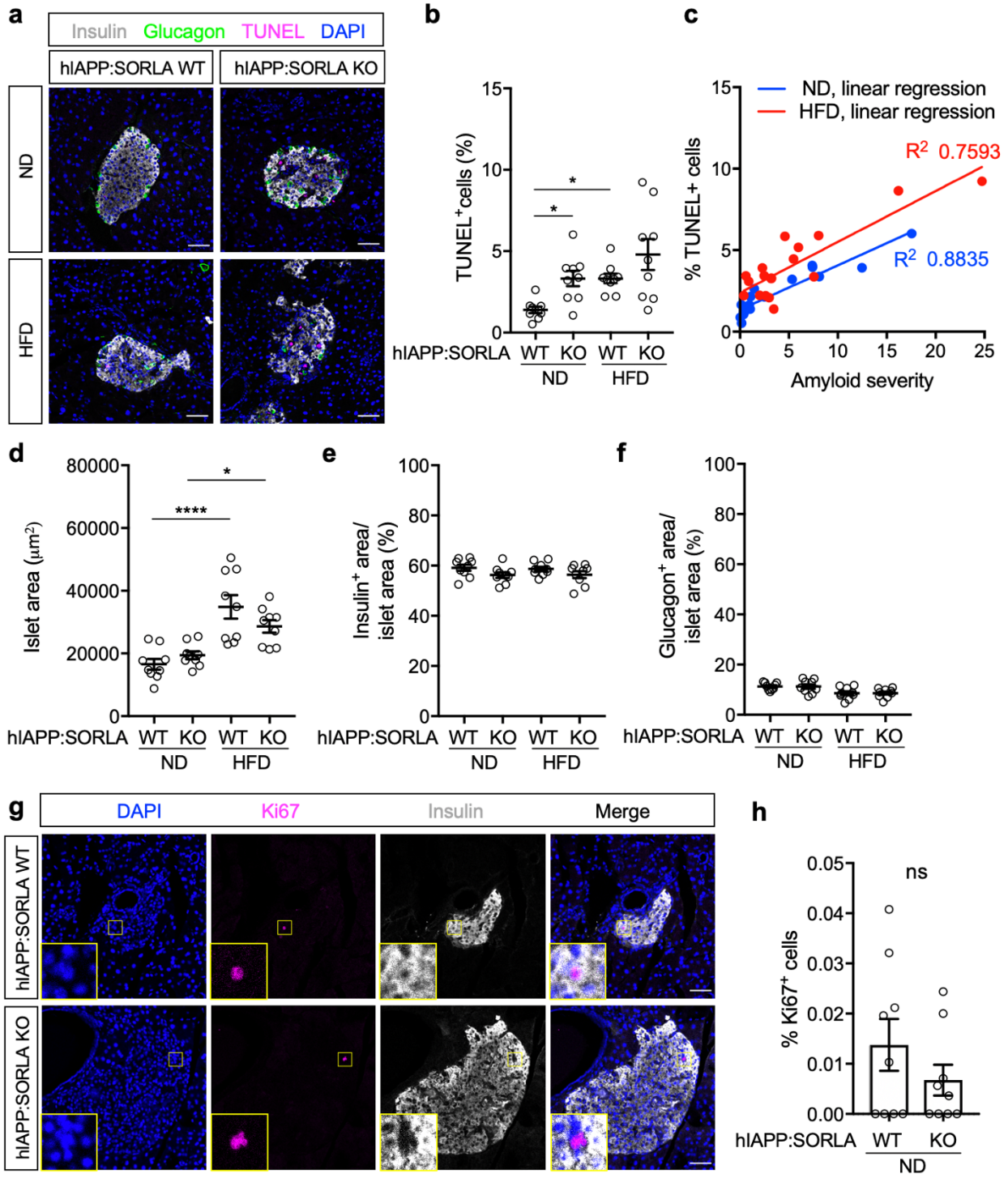

Figure 10: Increased islet amyloid in hIAPP:SORLA KO mice is associated to increased cell death. (**a**) Apoptotic islet cells were identified by TUNEL staining (magenta) on pancreas sections from ND- or HFD-fed mice of the indicated genotype at 33- to 35-weeks of age. Beta and alpha cells were identified by immunostaining for insulin (white) and glucagon (green), respectively. Nuclei were counterstained by DAPI (blue). Scale bars, 50 µm. (**b, d-e**) Quantifications of (b) the percentage of TUNEL$^+$ cells, (d) islet area, percentages of (e) insulin$^+$ (beta cell) area, and (f) glucagon$^+$ (alpha cell) area per islet on sections as exemplified in panel a (n = 9 mice per genotype). (**c**) The correlation between islet amyloid severity and cell death in hIAPP transgenic mice was tested using linear regression. (**g**) Proliferative cells were identified by Ki67 staining (magenta) on pancreatic sections from ND-fed, 33- to 35-weeks old mice. Islets were identified by insulin staining (grey) and nuclei were counterstained with DAPI (blue). Higher magnifications of the areas indicated by yellow boxes were depicted in the insets. Scale bars, 50 µm. (**h**) Quantifications of the percentage of proliferative islet cells. (n = 9 mice per genotype). Data are

expressed as mean ± SEM. Statistical significance of differences was determined by two-way ANOVA with post hoc test. * $p < 0.05$, **** $p < 0.0001$, ns = non-significant. This figure is adapted from Shih et al. 2022.

3.3. Glucose homeostasis and beta cell function are maintained in SORLA-deficient hIAPP mice

In addition to assessing islet amyloid deposition and morphological features at the end of the animal study, I followed the metabolic consequences of SORLA deficiency during the course of the treatment regime. In order to determine whether the SORLA-mediated effects were dependent on hIAPP expression, non-hIAPP mice were included in these metabolic studies.

Starting at approximately 26 weeks of age, SORLA-deficient mice fed with ND began to gain more body weight compared to WT mice (Figure 11a). However, the loss of SORLA did not affect fasting blood glucose levels in both hIAPP-expressing and non-transgenic mice (Figure 11b). To determine the ability of mice to metabolize glucose and maintain stable blood glucose levels after glucose spike, I performed glucose tolerance tests (GTT), where I monitored the changes in blood glucose upon intraperitoneal glucose administration. The results showed that hIAPP-expressing mice developed significantly worsened glucose tolerance as compared to their non-hIAPP transgenic littermate controls, while the loss of SORLA did not affect glucose tolerance (Figure 11c). Although there was no observable impairment in glucose tolerance in SORLA KO mice, there may still be a defect in beta cell function as glucose homeostasis is regulated by both the actions of insulin secretion by beta cells and by glucose uptake in peripheral tissues, such as muscles and adipose tissues. I therefore examined more specifically the ability of beta cells to secrete insulin in response to glucose in mice (Figure 11d) and isolated islets (Figure 11e). After intraperitoneal glucose injection, the fold change in insulin secretion was comparable between SORLA WT and KO mice, independent of hIAPP expression (Figure 11d). Similarly, loss of SORLA did not affect insulin secretions from isolated islets under normal culture condition (11 mmol/l glucose), low glucose (1.67 mmol/l), high glucose (16.7 mmol/l) conditions, nor following membrane depolarization by KCl (30 mmol/l) (Figure 11e).

To determine if loss of SORLA contributes to the pathogenesis of T2D, I metabolically challenged mice with HFD for 6 months starting at the age of 4 weeks. Towards the end of HFD feeding, mice deficient for SORLA in both hIAPP-expressing

and non-transgenic lines grew heavier as compared to WT (Figure 12a). Although fasting blood glucose levels trended to increase over time (from 4 to 31 weeks), particularly in hIAPP-expressing mice, there were no significant differences between SORLA genotypes (Figure 12b). Next, I performed glucose tolerance tests in HFD-fed mice to assess their response to glucose and ability to maintain glucose homeostasis. Similar to ND-fed mice, the expression of hIAPP transgene significantly worsened glucose tolerance in both SORLA WT and KO mice under HFD (Figure 12b). Although currently statistically insignificant, HFD-fed hIAPP:SORLA KO mice displayed a trend towards worsening glucose tolerance compared to hIAPP:SORLA WT mice. This may be attributed to a buildup of insulin resistance associated to the increased body weight in hIAPP:SORLA KO mice compared to WT (Figure 12a).

In summary, the *in vivo* results showed that loss of SORLA increases islet amyloid deposition and islet cell death without apparent impairment of islet morphology, beta cell function or overall glucose homeostasis. Increased amyloid pathology and cell death was seen in normal chow fed mice, suggesting a protective role of SORLA in the pancreas under physiological conditions.

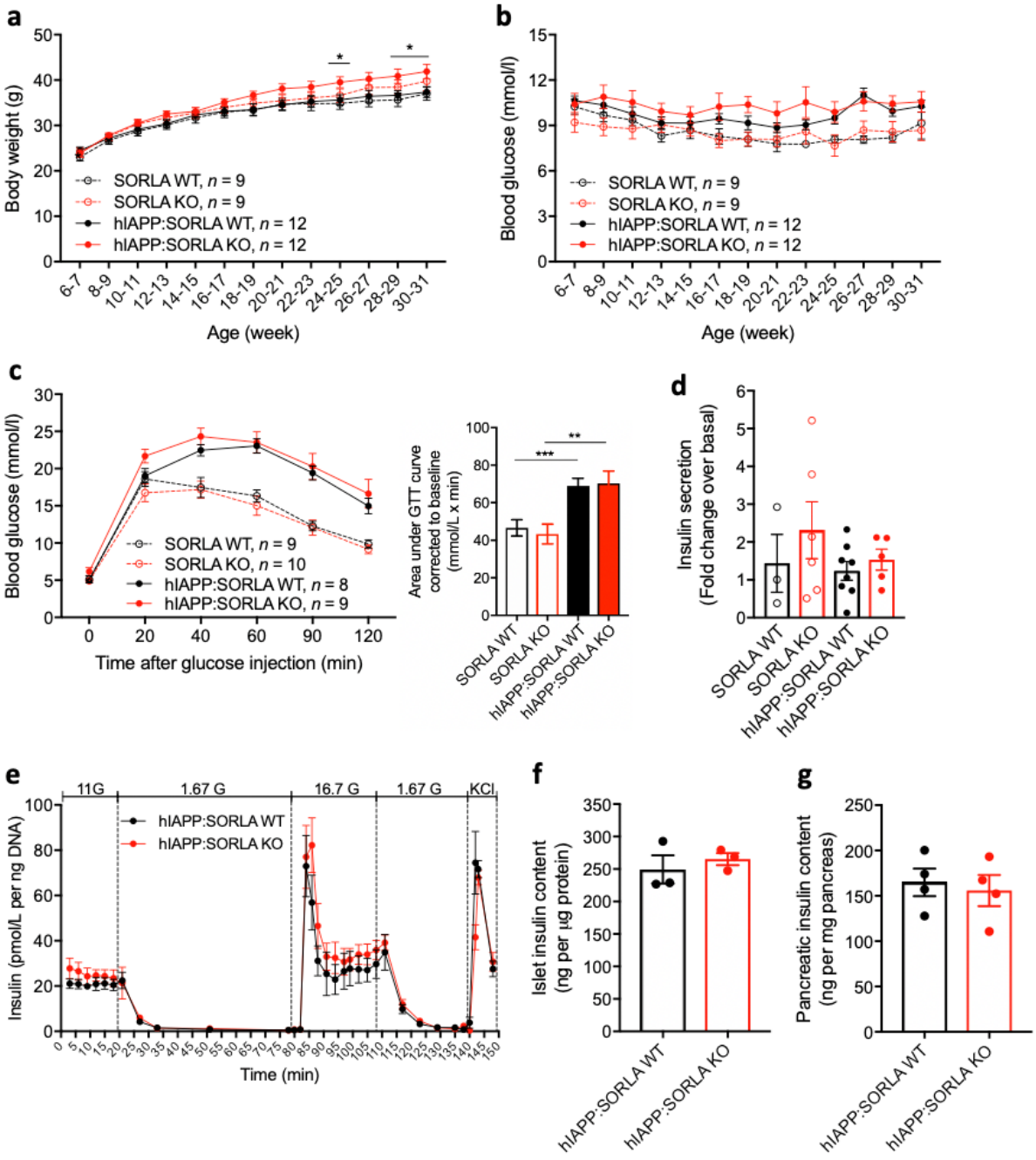

Figure 11: **Characterization of the effect of SORLA deficiency on metabolism and beta cell function in mice fed with a normal chow diet.**
(a-b) (a) Body weight and (b) fasting blood glucose levels of mice of the indicated genotype were monitored every 2 weeks. **(c)** Glucose tolerance tests (GTT) were performed by intraperitoneally glucose administration at a dose of 2 g/kg body weight after a 16 h fast in 30- to 32-weeks old mice. Glucose clearance was quantified based on the area under the GTT curves corrected to baseline. **(d)** Glucose-stimulated insulin secretion (GSIS) was performed in 31- to 33-weeks old mice of the indicated genotypes (SORLA WT, *n* = 3; SORLA KO, *n* = 6; hIAPP:SORLA WT, *n* = 8; hIAPP:SORLA KO, *n* = 5). A glucose dose of 2 g/kg body was administered intraperitoneally after a 16 h fast. Insulin secretions are represented as the fold change at 30 min post-glucose injection over fasting. **(e)** Dynamic GSIS was performed on perifused islets from 31- to 33-weeks old hIAPP:SORLA WT or KO mice (*n* =3 mice per genotype, with technical duplicates). (**f-g**) Quantifications of insulin content in (f) isolated islets and (g) whole pancreas. Data are expressed as mean ± SEM. Statistical significance of differences between hIAPP:SORLA WT and hIAPP:SORLA KO in (a), and between non-hIAPP and hIAPP mice (c) is determined by unpaired Student t-test. * $p < 0.05$, ** $p < 0.01$, *** $p < 0.001$. This figure is adapted from Shih et al. 2022.

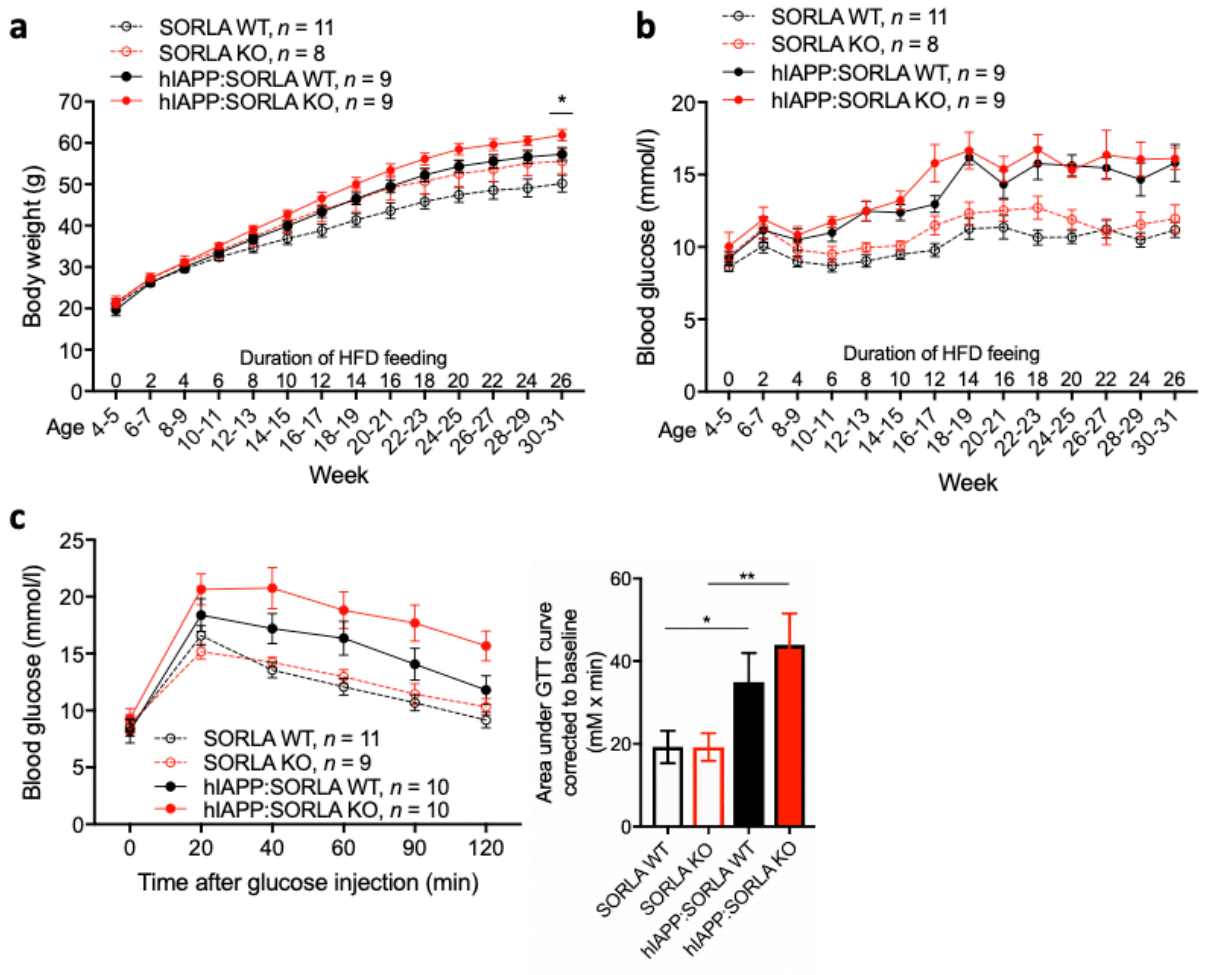

Figure 12: Characterization of the effect of SORLA on glucose homeostasis in HFD-fed mice (a-b) (a) Body weight and (b) fasting blood glucose levels of mice of the indicated genotype were monitored every 2 weeks during HFD feeding. **(c)** Glucose tolerance tests (GTT) were performed by glucose administration at a dose of 0.75 g/kg body weight intraperitoneally after a 16 h fast in 30- to 32-weeks old mice. Glucose clearance was quantified based on the area under the GTT curves corrected to baseline. Data are expressed as mean ± SEM. Statistical significance of differences between hIAPP:SORLA WT and hIAPP:SORLA KO in (a), and between non-hIAPP and hIAPP mice (c) were determined by unpaired Student's t-test, * $p < 0.05$, ** $p < 0.01$. This figure is adapted from Shih et al. 2022.

3.4. SORLA does not regulate the production and processing of IAPP

Following the *in vivo* studies, I aimed to elucidate the molecular mechanisms by which SORLA may regulate islet amyloid formation. Studies have shown that both pro- and mature forms of IAPP were found in islet amyloid (J. F. Paulsson, Andersson, Westermark, and Westermark 2006), and that impaired proIAPP processing has been proposed to contribute to islet amyloid formation (Johan F. Paulsson and Westermark 2005; Chen, Taylor, and Verchere 2018). I therefore first tested if SORLA functions as a sorting receptor to transport proIAPP along its biosynthetic pathway that is necessary for complete processing and maturation. Such a function would recapitulate the

established role of this receptor in neuronal APP sorting (Andersen et al. 2005; Dumanis et al. 2015; Burgert et al. 2013; Schmidt et al. 2007). ELISA measurements on human IAPP performed by Yi-Chun Chen showed that ND-fed hIAPP:SORLA WT and KO mice had similar fasting plasma levels of mature hIAPP (Figure 13a) and prohIAPP (Figure 13b) at both young (6-7 week) and advanced (33-36 week) age. To more specifically determine the processing efficiency of prohIAPP into mature hIAPP, I calculated their ratio which was also comparable between hIAPP:SORLA WT and KO mice (Figure 13c). Similar results were obtained in mice fed a HFD (Figure 13d-f).

Since the levels of circulating plasma (pro)IAPP are influenced by both the amount of islet secretion and peripheral uptake, I further validated these results by measuring the hormone secreted directly from isolated islets of 31-33 weeks old mice. In addition, I tested the amount of prohIAPP, mature hIAPP, and their ratios under three different glucose (G) doses representative of metabolic states, they are standard culture condition (11 mmol/l G), low G (1.67 mmol/l); and high G (16.7 mmol/l) (Figure 13g). There were no significant differences in the levels of secreted mature hIAPP, prohIAPP nor their ratio (Figure 13h-j) between SORLA genotypes. There were also no differences in total islet content of mature hIAPP nor prohIAPP (Figure 13 k,l), documenting that SORLA does not impact the overall production or proteolytic processing of IAPP.

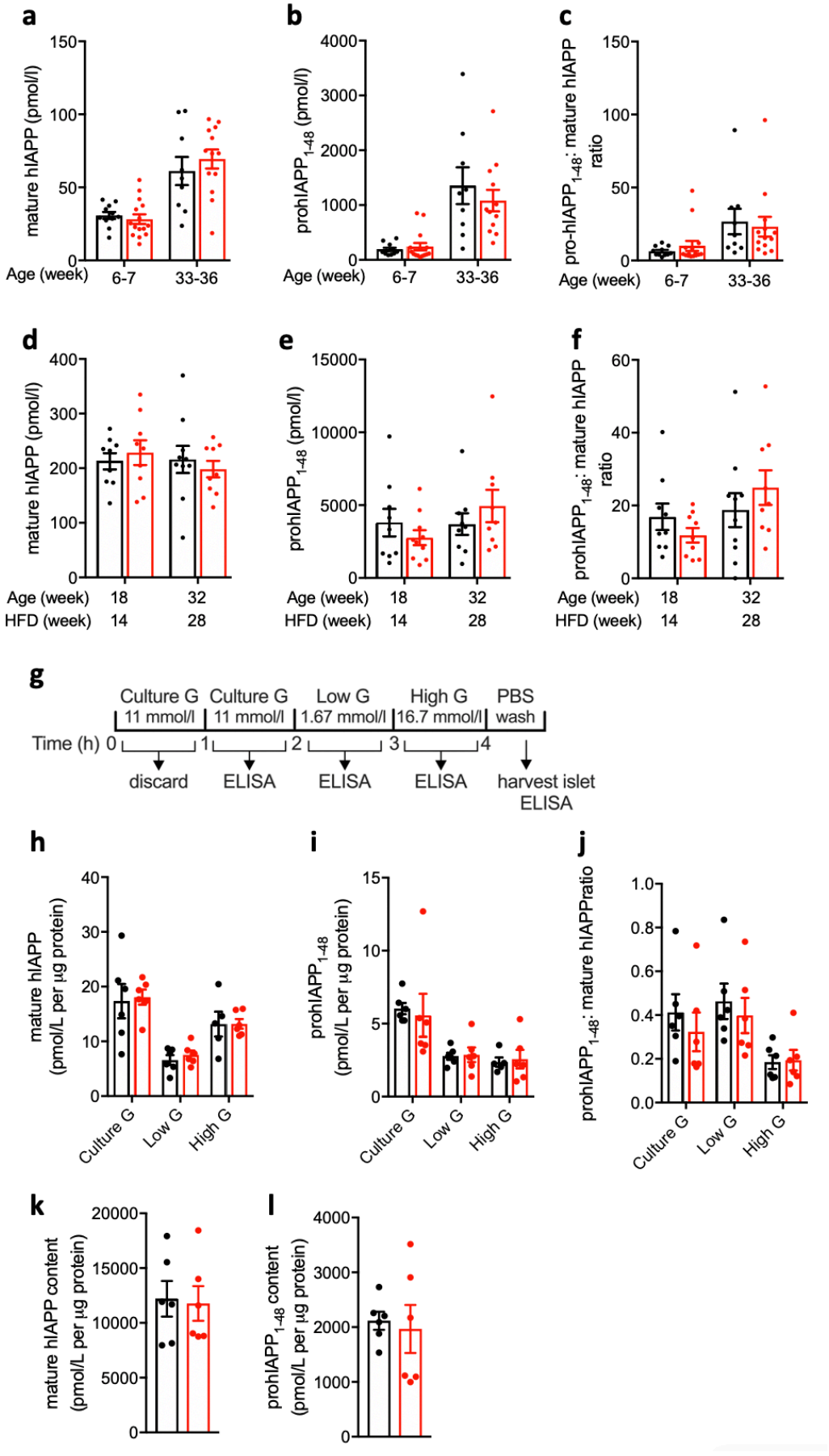

Figure 13: Loss of SORLA does not impact hIAPP processing.

(a-f) Fasting levels of plasma (a, d) mature hIAPP, (b, e) prohIAPP$_{1-48}$, and (c, f) pro- to mature-hIAPP ratio were measured in hIAPP:SORLA WT (black bars) and hIAPP:SORLA KO (red bars) mice at the indicated age. Animals were fed a (a-c) ND or a (d-f) HFD. No statistically significant differences in data were seen comparing genotypes using unpaired Student t-test (n = 6-15). (**g**) Schematic workflow of *in vitro* islet secretion assay. Islets were incubated to a series of secretion buffers containing the indicated glucose (G) concentrations. After 1 h of incubation, the buffer was collected for ELISA measurements. (**h-l**) Secreted levels of (h) mature hIAPP, (i) prohIAPP$_{1-48}$, (j) their ratio as well as their islet content of (**k-l**) in isolated islets of ND-fed hIAPP:SORLA WT (black bars) and hIAPP:SORLA KO (red bars) mice. Data are expressed as mean ± SEM. No statistically significant differences in data were seen comparing genotypes by unpaired Student t-test (n = 6). This figure is adapted from the supplementary data in Shih et al. 2022.

3.5. SORLA is localized in beta cell secretory granules and endosomes

As a sorting receptor, SORLA shuttles between the Golgi, endosomal compartments, and plasma membrane as documented in neurons and other cell types (Schmidt et al. 2007), I therefore tested if SORLA is localized to these cellular compartments in primary islet beta cells from WT (BL/6) mice by immunostaining (Figure 14a). The degree of colocalization between SORLA and each compartment marker was quantified based on Mander's colocalization coefficients (Figure 14b), which showed that SORLA was predominately colocalized with secretory granules (insulin, IAPP), moderately with early (Rab4), late (Rab9), and recycling endosomes (Rab11), and at low levels with the TGN (STX6). Additionally, I performed proximity ligation assays (PLA) to validate close spatial protein-protein interactions between SORLA and IAPP. Again, using dispersed primary islet cells from WT (BL/6) mice, I observed that PLA signals from interacting SORLA and IAPP were localized around the cell periphery and in the vicinity of Rab4 positive early endosomes (Figure 14c, top). I repeated PLA on islets from hIAPP-transgenic animals to validate that SORLA interacts in a similar fashion with human IAPP (Figure 14c, middle). The results showed the same PLA patterns as with mouse IAPP. Finally, PLA signals for interaction of SORLA and IAPP were absent in SORLA KO cells, which served as a negative control (Figure 14c, bottom).

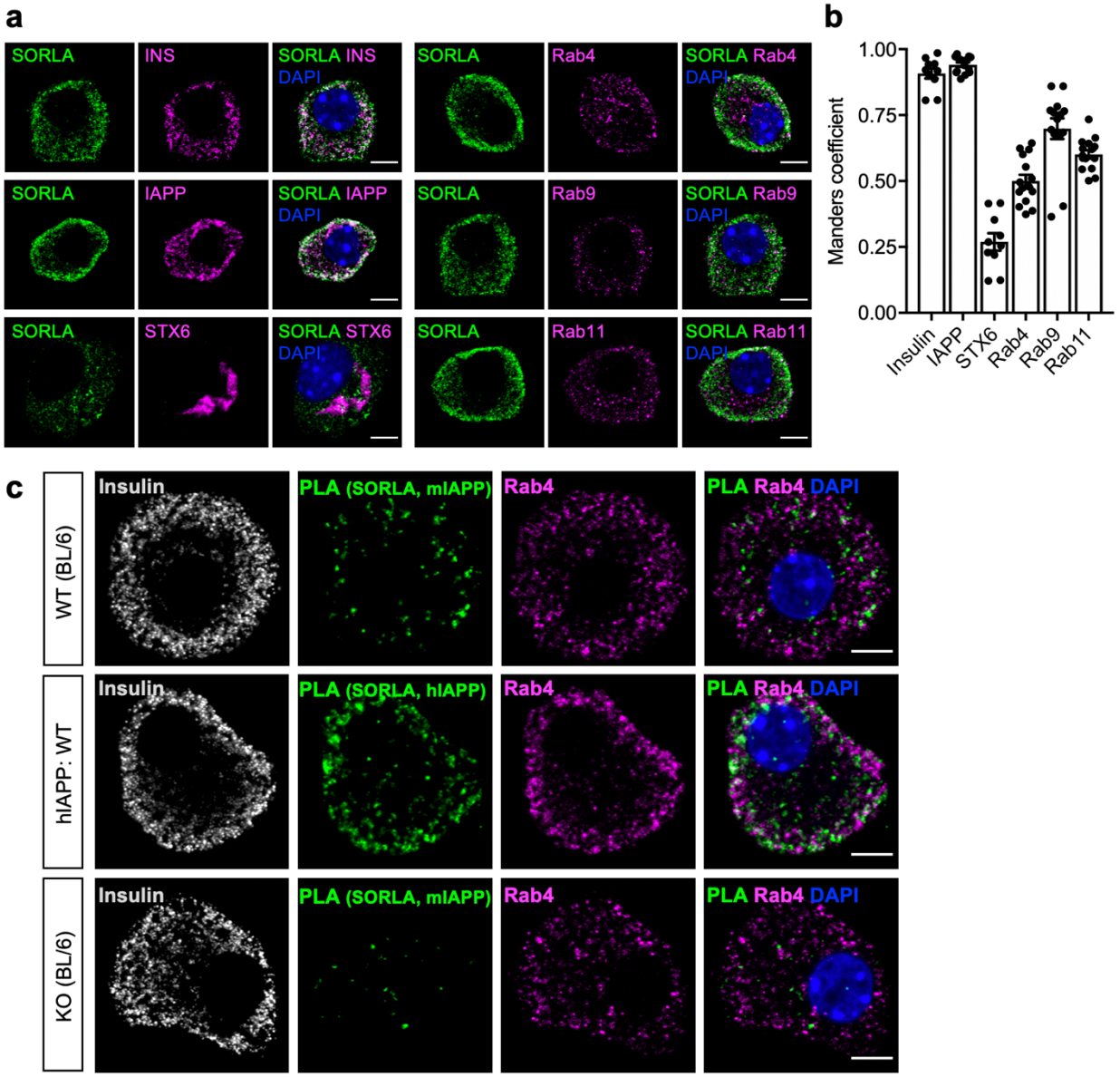

Figure 14: Subcellular localization of SORLA and its interaction with IAPP in beta cells. (**a**) Islets from WT(BL/6) mice were dispersed into single cells and immunostained for SORLA (green) and compartment markers (magenta): insulin or IAPP (secretory vesicles), syntaxin-6, STX6 (TGN), Rab4 (early endosomes), Rab9 (late endosomes), or Rab11 (recycling endosomes). Nuclei were counterstained with DAPI. (**b**) Quantification of colocalization between SORLA and each compartment marker using Manders' colocalization coefficient (n =10-15 cells). Data are expressed as mean ± SEM. (**c**) Proximity ligation assay (PLA) to identify closely interacting SORLA and IAPP was performed on dispersed islet cells from WT(BL/6) (test for mouse IAPP) or hIAPP:SORLA WT (test for human IAPP), or SORLA KO (negative control) mice. Cells were immunostained for insulin (white) to identify beta cells, Rab4 (magenta) for early endosome and nuclei were counterstained with DAPI (blue). (a, c) Single and merged channel configurations are shown. Scale bars, 5 µm. This figure is adapted from Shih et al. 2022.

3.6. SORLA binds more strongly to proIAPP than mature IAPP

Next, I determined if SORLA functions as a receptor for IAPP, more specifically whether it binds to the pro- or mature form of the peptide. I did so by testing their binding interactions using microscale thermophoresis (MST). In this experiment, I first

fluorescently-labeled a His-tagged ectodomain of human SORLA, which was expressed and purified as previously described (Andersen et al. 2005) (Figure 15a). Then, I tested the binding interactions between the fluorescently-labeled SORLA ectodomain and unlabeled forms of the mouse N-terminally extended proIAPP ($proIAPP_{1-70}$), C-terminally extended proIAPP ($proIAPP_{1-51}$) or mature IAPP (Figure 15b). Mouse (pro)IAPP peptides were used as they are more soluble and stable as monomers *in vitro* than the amyloidogenic human species (Wu and Shea 2013). MST analysis and their binding curves demonstrated that there was a gradual change in the thermophoretic movement of the fluorescently-labeled SORLA upon binding with the serially titrated non-labeled IAPP ligands, and that applied to all forms of IAPP (Figure 15c). Binding constants derived from the K_d model of fit further revealed that SORLA ectodomain bound more strongly to the two proforms ($proIAPP_{1-70}$ K_d ~ 268±43 nM and $proIAPP_{1-51}$ K_d ~ 329±29 nM) as compared to a weaker binding to mature IAPP (K_d ~ 921±177 nM).

In addition to intracellular sorting, SORLA can also function as an endocytic receptor, which typically releases its ligands in acidic milieu such as endosomes and lysosomes. I therefore repeated the above MST analyses under different pH conditions (7.4, 5.5 and 4.5). The results showed that binding interactions between SORLA and each (pro)IAPP peptide were the strongest at pH 7.4, weaker at pH 5.5, and absent at pH 4.5 (Figure 15d-f), supporting the hypothesis that SORLA acts as an endocytic receptor for IAPP.

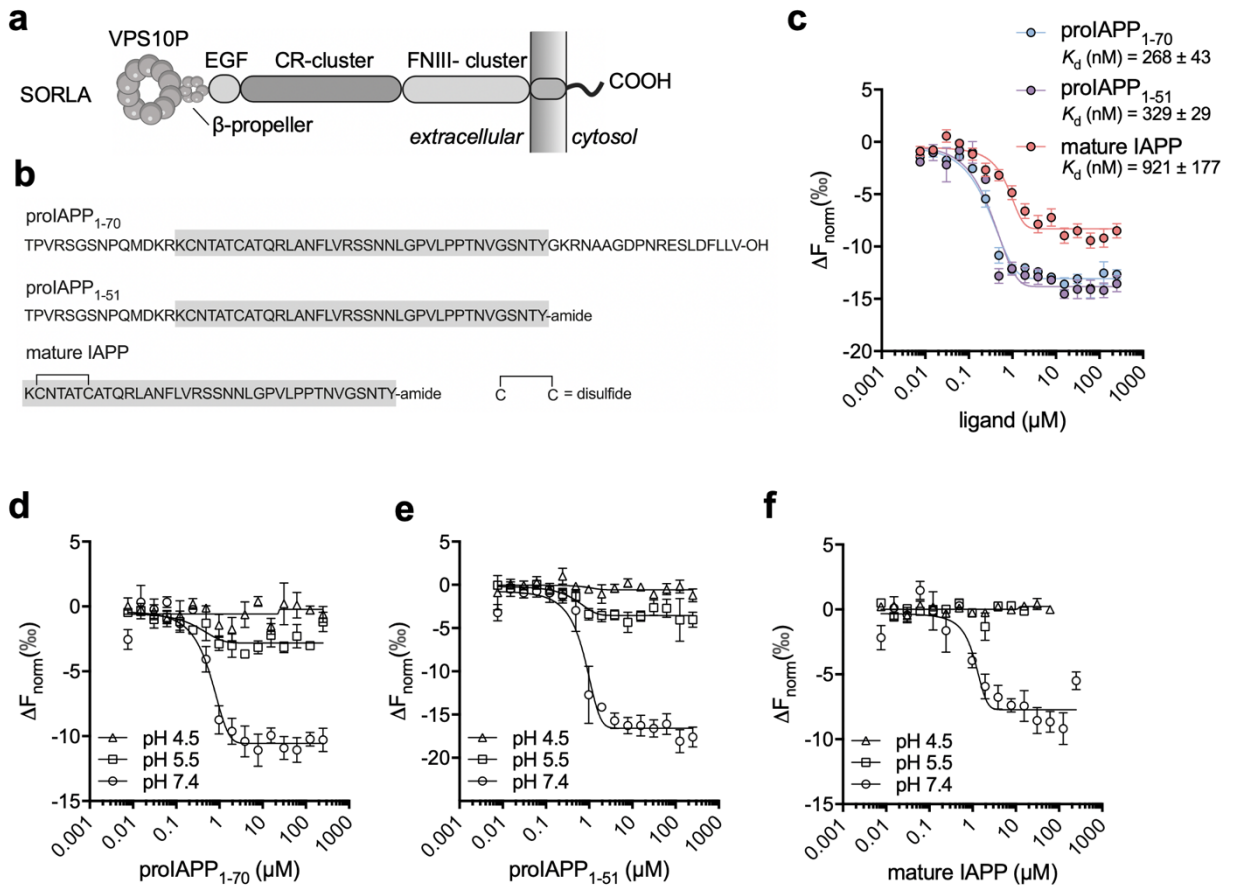

Figure 15: SORLA preferentially binds to the IAPP precursors (proIAPP) at pH 7.4.
(**a**) Structural domains of SORLA, containing the vacuolar protein sorting 10 protein (VPS10P) domain, 10CC-domain (not depicted), β-propeller, epidermal growth factor (EGF) repeats, clusters of complement-type repeats (CR), and fibronectin type III (FNIII). (drawn not to scale) (**b**) Amino acid sequences of the mouse proIAPP$_{1-70}$, proIAPP$_{1-51}$, and mature IAPP peptides. (**c**) Direct binding interactions between SORLA ectodomain and different forms of mouse IAPP peptides were determined by microscale thermophoresis (MST) at pH 7.4. His-tagged human SORLA ectodomain was previously produced in HEK293-EBNA cells and purified using Ni^{2+} affinity chromatography as described in (Andersen et al. 2005). Constant amount of the fluorescently-labeled SORLA ectodomain (3 nmol/l) was incubated with serially titrated non-labeled IAPP (7.6 nmol/l – 250 μmol/l). Average K_d was derived from at least 3 independent experiments. Data are expressed as mean ± SEM. (d-f) Binding interactions between SORLA ectodomain and (d) proIAPP$_{1-70}$, (e) proIAPP$_{1-51}$, and (f) mature IAPP was analyzed by MST at pH 7.4, 5,5 and 4,5 as described in (c). This figure is adapted from Shih et al. 2022.

3.7. SORLA mediates endocytosis of proIAPP to the endolysosomal pathway

The results so far indicated that SORLA was likely to be an endocytic receptor for IAPP. I tested this hypothesis by assessing the ability of SORLA to mediate endocytic uptake of IAPP in SH-SY5Y cells that stably overexpress SORLA. The neuroblastoma SH-SY5Y cell line was chosen as it is routinely used to study SORLA-mediated protein trafficking (Andersen et al. 2005; Dumanis et al. 2015). Moreover, SH-SY5Y cells do not express IAPP endogenously (Figure 16, DMSO), allowing me to detect uptake of unlabeled IAPP peptides from the media.

In this experiment, I incubated SORLA-expressing SY5Y and parental SY5Y WT cells with serum-free medium containing proIAPP$_{1-70}$, proIAPP$_{1-51}$, or mature IAPP peptides. I then evaluated cellular uptake of IAPP peptides by immunostaining. Interestingly, intracellular uptake was observed for the two pro-forms, but not for mature IAPP (Figure 16a, top panel). Further quantifications showed that proIAPP$_{1-70}$ was the most readily internalized variant, followed by moderate uptake of proIAPP$_{1-51}$ (Figure 16b). To test if peptide uptake was mediated by endocytosis, I treated cells with the dynamin inhibitor dynasore, which effectively inhibited the internalization proIAPP peptides from the media (Figure 16a, middle panel). Finally, no IAPP peptides were internalized in parental SY5Y WT cells that lack SORLA expression (Figure 16a, bottom panel).

Since SORLA binds to small peptides such as Aβ through its VPS10P domain (Kitago et al. 2015), I next tested if proIAPP is also bound to the same ligand binding domain. I performed a competitive binding assay where I co-incubated SY5Y-SORLA cells with proIAPP$_{1-70}$ and 5-fold molar excess of Aβ. Indeed, the ability of SORLA to internalize proIAPP$_{1-70}$ was diminished in the presence of excess Aβ (Figure 16c), suggesting that the VPS10P domain is likely the binding region responsible for proIAPP uptake.

Lastly, to identify if the internalized proIAPP peptides were directed to the TGN for recycling to the biosynthetic pathway or to lysosomes for degradation, I performed immunostaining for early endosome (EEA1), TGN (TGN38) and labeled lysosomes with lysotracker (Figure 16d). Quantification of double-immunostainings showed that proIAPP peptides were predominately directed to early endosomes (EEA1, 89.9%). Moderate amounts of the peptide were found in lysosomes (lysotracker, 51.6%) and a small percentage in the TGN (TGN38, 25.2%) (Figure 16e). These results suggested that SORLA mediates endocytosis of proIAPP towards the endolysosomal pathway for catabolism.

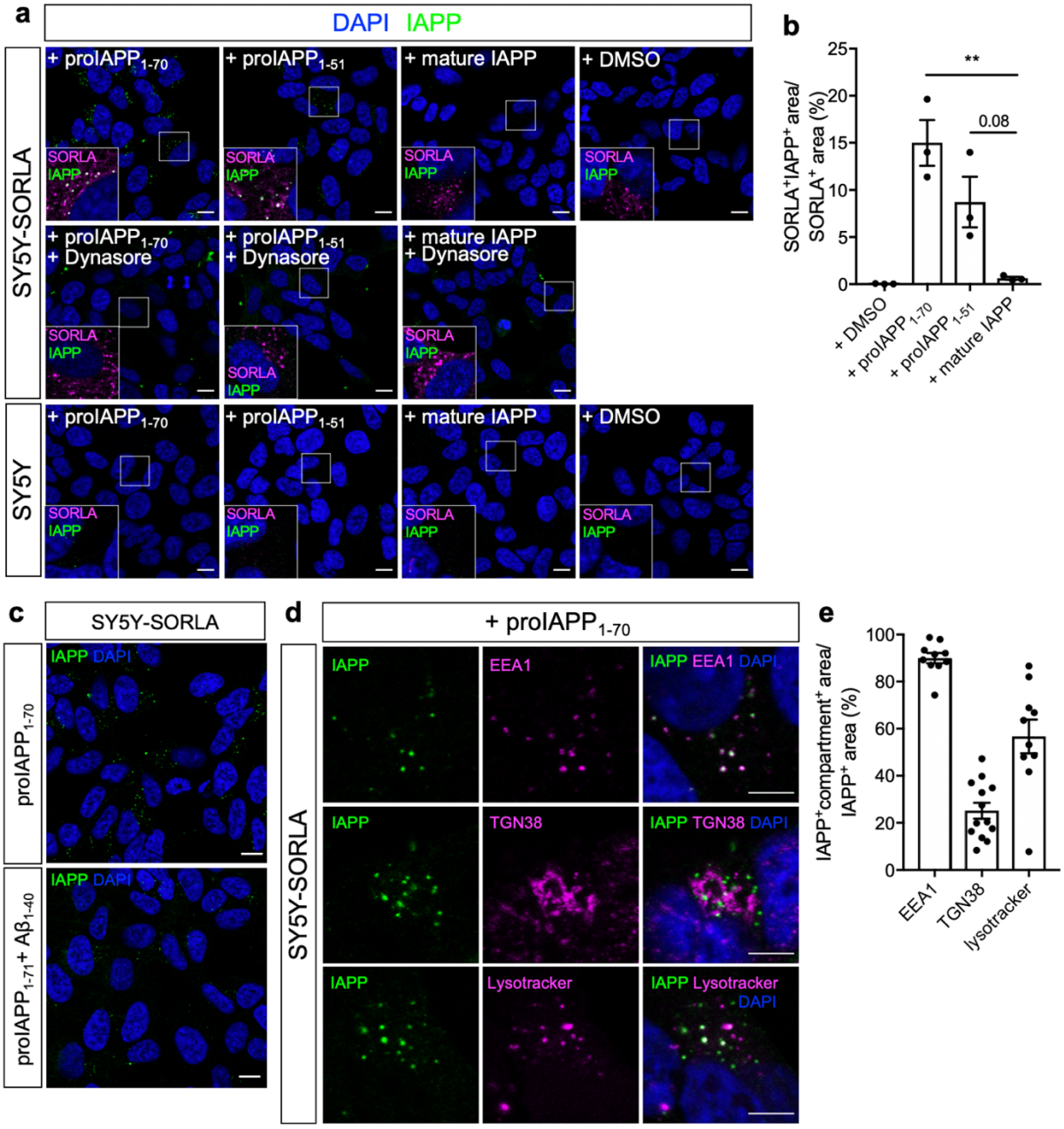

Figure 16: SORLA acts as an endocytic receptor of proIAPP towards the endolysosomal pathway. **(a)** SY5Y cells that stably express SORLA (top and middle panels) and parental SY5Y cells (bottom panel) were incubated with 20 µmol/l of proIAPP$_{1-70}$, proIAPP$_{1-51}$, or mature IAPP peptides, or with 0.1% DMSO for 30 min. To examine clathrin-mediated endocytosis, cells were additionally treated with 100 µmol/l dynasore (middle panel). Cells were immunostained for SORLA (magenta) and IAPP (green), and nuclei were counterstained with DAPI. Higher magnifications of the areas indicated by white boxes were depicted in the insets. Scale bars, 10 µm. **(b)** Quantifications of the amount of each IAPP peptide being internalized in SORLA-expressing SY5Y cells (n =3 independent experiments, each with 3 – 4 images per condition). **(c)** Uptake of proIAPP$_{1-70}$ in SORLA-expressing SY5Y cells was inhibited by 100 µmol/l Aβ$_{1-40}$ for 30 min. Internalized proIAPP$_{1-70}$ in cells were then immunolabeled by for IAPP (green) and nuclei were counterstained with DAPI (blue). Representative images from three independent experiments. Scale bars, 10 µm. **(d)** proIAPP$_{1-70}$ treated SORLA-expressing SY5Y cells were additionally immunostained for IAPP (green) and compartment markers (magenta) EEA1 or TGN38. Lysosomes were labeled by preincubating cells with Lysotracker Deep Red for 1 hour prior to uptake assay. Scale bars, 5 µm. **(e)** Quantifications of the degree of colocalization between internalized IAPP$_{1-70}$ and each compartment marker (n = 10-13 images per marker). Data are expressed as mean ± SEM. Statistical significance of differences in (b) was determined by one-way ANOVA with post hoc test. ** $p < 0.01$. This figure is adapted from Shih et al. 2022.

4. Discussion

4.1. SORLA is a novel receptor for IAPP and a regulator of islet amyloid deposition

Islet amyloid is a pathological feature of T2D that compromises the ability of beta cells to secrete sufficient insulin for maintaining blood glucose homeostasis. The main component of islet amyloid was first identified as IAPP in 1986 (Per Westermark, Wernstedt, Wilander, and Sletten 1986). However, progress to elucidate the regulatory pathways of IAPP aggregation and amyloid fibril formation has been slow and limited. Using transgenic mouse models, we have identified SORLA as a novel protective regulator counteracting islet amyloid formation and associated islet cell death. Complementary results from molecular studies in established cells lines further revealed the underlying cellular pathways whereby SORLA controls the initial stages of IAPP aggregation. Here, we propose a model where SORLA functions as a clearance receptor specific for soluble secreted proIAPP (Figure 17). SORLA-mediated endocytosis of proIAPP directs it towards the endolysosomal compartments for catabolism, thereby reducing the accumulation of extracellular proIAPP and limiting its propensity to aggregate into amyloid fibrils.

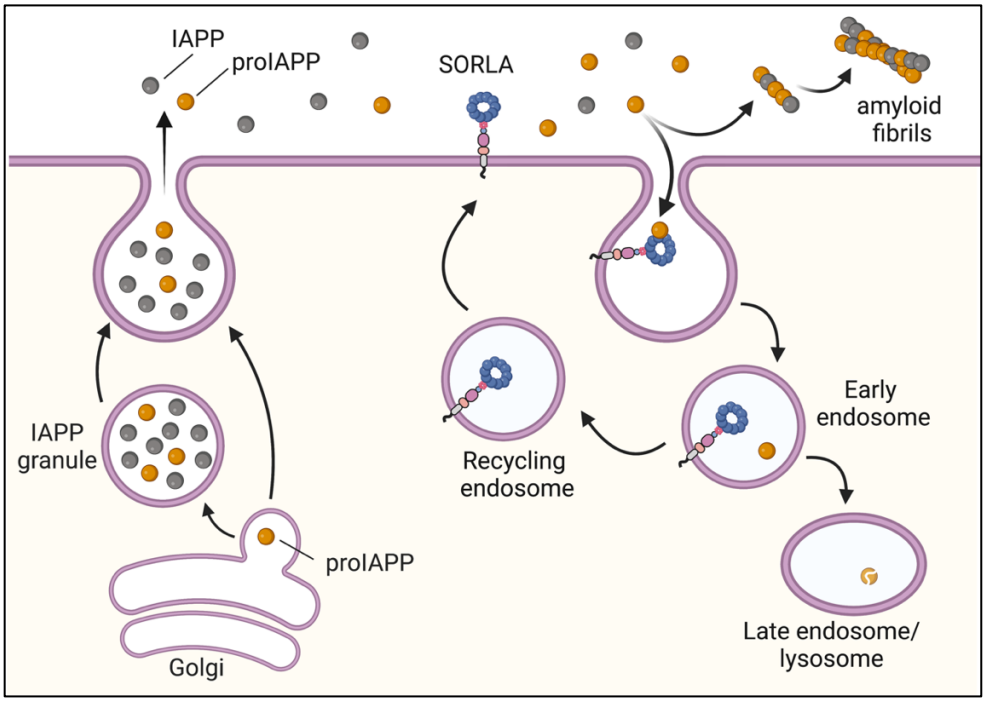

Figure 17: Proposed model of SORLA action on proIAPP clearance in pancreatic islet beta cells
Mature IAPP and the partially processed proIAPP are secreted from islet beta cells. Results from this study have demonstrated that SORLA is protective against islet amyloid. We proposed that SORLA reduces the propensity of aggregation and islet amyloid formation by mediating endocytic uptake of the

secreted, extracellular proIAPP towards the endolysosomal pathway for degradation. This figure is created with Biorender.com and published in Shih et al. 2022.

4.1.1. The significance of SORLA in islet amyloid, beta cell function and type 2 diabetes

In this study, hemizygous hIAPP transgenic mice either wildtype or deficient for SORLA were examined under two dietary conditions, namely normal chow diet and 6-months of high fat diet beginning at 4-5 weeks of age. In the normal diet group, a significant amount of islet amyloid deposits already developed in 7-months old hIAPP:SORLA KO mice but not in WT controls (Figure 9). This observation was astounding as previous studies on hIAPP transgenic mice models have demonstrated that islet amyloids do not develop spontaneously unless a state of insulin resistance or obesity was introduced genetically (e.g. leptin deficient mice), pharmacologically (e.g. dexamethasone treatment), or through dietary interventions (Couce et al. 1996; Höppener et al. 1999; Hull et al. 2003). Observations from the normal diet group thus suggest that SORLA plays an integral role in regulating IAPP homeostasis under normal physiological conditions. In the HFD group, the protective effect of SORLA against islet amyloid observed under normal diet was no longer obvious (Figure 9). It is likely that the protective effects of SORLA are masked by hypersecretions of hIAPP in response to HFD, which results in a 5-fold increase in the levels of plasma mature IAPP (Figure 13 a, d) and proIAPP (Figure 13 b, e) in 32- to 36-weeks-old HFD-fed animals compared to the normal diet group. One weakness of using transgenic mouse models is the supraphysiological levels of hIAPP expression. Accordingly, an alternative approach is the use of knock-in mouse models which express physiological levels of the hIAPP transgene. In 2012, such hIAPP knock-in mice were generated, where the non-amyloidogenic mouse IAPP gene was replaced with the human sequence to drive its expression under the control of the endogenous mIAPP promoter (Hiddinga et al. 2012). Due to a more moderate, physiological expression of hIAPP transgene, hIAPP knock-in mice remain healthy when fed a normal diet and require introduction of HFD feeding to induce hIAPP cytotoxicity (Shigihara et al. 2014). Therefore, I would expect to observe no significant differences in islet amyloid burden in SORLA-deficient mice when fed with a normal diet, unless HFD or other inventions that induce insulin resistance were introduced.

Islet amyloid is associated with a decline in beta cell function and beta cell death as well as the development of T2D (Verchere et al. 1996; MacArthur et al. 1999; Jurgens et al. 2011). In the normal diet group, hIAPP-expressing mice deficient in SORLA exhibited increased islet cell death when compared to WT controls, a finding consistent with the increased islet amyloid observed in these animals. However, insulin secretion, fasting glucose levels, and glucose tolerance were comparable between SORLA genotypes. These findings of a normal beta cell function may be explained by the age of the mice at which metabolic studies were performed. In this study, islet histology and glucose homeostasis were examined in 7-months-old mice. Development of diabetes is a slow and gradual process, which began with the build-up of insulin resistance and associated beta cell compensation prior to a dramatic decline in beta cell mass and hyperglycaemia. Thus, it is plausible that the findings in this study represent the early stages of diabetes development preceding full blown pathology (also referred to as prediabetes). One may speculate that the observed increase in islet amyloid and cell death in SORLA-deficient mice will likely result in beta cell failure and hyperglycaemia in mice at an older age as previous study has shown that hyperglycemia was developed in hIAPP transgenic mice > 13 months of age (Verchere et al. 1996).

4.1.2. The mechanistic role of SORLA in IAPP handling

Following the observation that SORLA protects against islet amyloid formation, we aimed to elucidate the underlying mode of receptor action. Although SORLA has not been studied in pancreatic islets previously, substantial work has been performed to understand its role in amyloid formation in the brain. In neurons, SORLA reduces amyloid load by regulating the transport and amyloidogenic processing of APP into Aβ (Andersen et al. 2005; Schmidt et al. 2007; Offe et al. 2006). Similarly in islet beta cells, impaired processing of proIAPP into mature IAPP in its biosynthetic pathway has been shown to promote islet amyloid deposition (Johan F. Paulsson and Westermark 2005; Marzban et al. 2006). The biosynthesis of mature IAPP involves movement of nascent proIAPP from the ER to the Golgi and further to secretory granules for processing and other post-translational modifications. Prior studies have identified various enzymes as key players of IAPP processing and maturation, including PC1/3, PC2, PAM and CPE (J. Wang et al. 2001; Marzban, Trigo-Gonzalez, and Verchere 2005; Marzban,

Soukhatcheva, and Verchere 2005). However, the identity of a facilitator that mediates transport of proIAPP to the Golgi and/or secretory granule for processing remains elusive. Accordingly, the initial hypothesis was that SORLA regulates the processing of IAPP precursors in beta cells by sorting newly synthesized proIAPP to secretory vesicles. To proof such a function of SORLA in proIAPP processing, we measured the ratio of pro- and mature IAPP levels, which reflects the processing efficiency of proIAPP, in circulating blood plasma as well as secretions from isolated islets of hIAPP-expressing transgenic mice. Contrary to the initial hypothesis, the results documented that SORLA does not regulate proIAPP processing as the ratios between pro- and mature IAPP were comparable between SORLA genotypes (Figure 13). This conclusion subsequently directed the investigation to another balancing arm of IAPP homeostasis, i.e. clearance and degradation of the peptide.

During the development of T2D, conditions of insulin resistance and obesity increase the demand for insulin (hyperinsulinemia) to maintain glucose homeostasis. Since IAPP is stored and secreted together with insulin in beta cells, there is also increased production and release of the amyloidogenic peptide during early T2D which promotes its aggregation and amyloid fibril formation. Conceptually, it is clear that overproduction of IAPP will result in increased islet amyloid. However, studies have indicated that overproduction of the peptide alone is insufficient for islet amyloid formation. For instance, islet amyloid was not found in non-diabetic individuals with hyperinsulinemia (Clark et al. 1990). Similarly, transgenic mice expressing supraphysiological levels of hIAPP failed to spontaneously develop significant amount of islet amyloid (G. Westermark et al. 1995). Therefore, it is clear that other mechanisms controlling IAPP homeostasis play an equally important role in the regulation of islet amyloid formation, including its clearance and degradation. In this study, colocalization analysis and PLA of SORLA and IAPP provided the first indications that SORLA interacts with IAPP in early endosomes, which are the early cellular hubs for protein recycling and degradation (Figure 14). Further biophysical studies with MST identified that IAPP bound to SORLA most strongly at pH 7.4, while the interaction was lost a low pH (Figure 15). Such pH-dependent release of ligands is a hallmark of endocytosis. Finally, (pro)IAPP uptake experiment in cell lines demonstrated that proIAPP was internalized and directed towards the early endosome and lysosomal compartment in a process dependent on SORLA (Figure 16). This SORLA-mediated

transport of proIAPP was abolished in the presence of the dynamin inhibitor dynasore, indicating clathrin-mediated endocytosis.

The finding that SORLA mediates clearance of extracellular proIAPP is of particular significance as it addresses an open question in the field of islet amyloid biology. Whether the initial site of IAPP aggregation originates intracellularly or extracellularly remains controversial. Cryo-immunogold labelling for oligomeric IAPP in beta cells of T2D patients and hIAPP transgenic mice demonstrated the presence of IAPP oligomers in the secretory pathway, supporting an intracellular origin (Gurlo et al. 2010). On the other hand, studies on cultured islets of hIAPP transgenic mice have shown that islet amyloid formation is elevated with increased IAPP secretions but reduced when secretion was inhibited, suggesting an extracellular origin of amyloid formation (K. Aston-Mourney et al. 2011). Results from this study supports the extracellular origin of IAPP oligomerization, which may also explain the underlying mechanism of their cytotoxicity on neighbouring cells and islet vasculature (Castillo et al. 2022). Understanding where islet amyloid forms is therefore important for effective and targeted therapeutic design for diabetes.

4.2. SORLA is a dual-regulator of neurodegeneration and metabolism

SORLA has a well-documented role in reducing amyloid plaques in the brain, as AD patients display reduced level of SORLA expression (Scherzer et al. 2004) and SORLA-deficient mouse models of AD have increased extracellular Aβ deposits and worsened AD pathology (Andersen et al. 2005; Dodson et al. 2008). Work from this dissertation has uncovered that SORLA also regulates amyloid formation in pancreatic islets through interaction with IAPP. While AD is a neurodegenerative disorder and T2D a metabolic disease, both diseases share much similarities in their pathophysiology, such as the presence of insulin resistance and amyloid deposits in the affected tissues (K. Akter et al. 2011). Epidemiological studies have also shown that patients with T2D have an increased risk in developing dementia and AD (Cheng et al. 2011; Barbagallo 2014; Biessels et al. 2006). IAPP can readily cross the blood-brain barrier to modulate satiety. Accumulating data have also shown that IAPP interacts and deposits together with Aβ in the brains of AD patients, highlighting the relevance of IAPP as a common etiological agent in both T2D and AD (Jackson et al. 2013; Wijesekara et al. 2017). Results from

this study have shown that proIAPP competes with Aβ for SORLA-mediated endocytosis (Figure 16c), suggesting that they are likely to interact to the same binding region in SORLA, i.e. that VPS10P domain. In this experiment, proIAPP was incubated with 5-molar excess of Aβ to ensure sufficient competitor was present in the assay. Further detail studies are needed to establish if SORLA has a higher binding preference towards proIAPP or Aβ. A previous study using an alternative binding analysis, called fluorescence polarization, has shown that the binding affinity between the SORLA's VPS10P region and Aβ to be 235 nM (Kitago et al. 2015). However, direct comparisons of the binding affinities to IAPP and Aβ should not be made as the method of detection and that the regions of SORLA (ectodomain vs VPS10P domain) included in the assays were different.

4.3. Targeted clearance of proIAPP as therapeutic strategy in diabetes treatment and islet transplantation

According to the World Health Organization, diabetes is currently affecting over 400 million people worldwide and is estimated to cost 3.4 million lives each year. Type 1 diabetes (T1D) is an autoimmune disease where pancreatic beta cells are attacked by the patient's immune system. It accounts for 5 – 10 % of all diabetes cases. By contrast, T2D is a metabolic disease caused by obesity and metabolic dysfunction and accounts for 80 – 90% of all cases of diabetes. Despite major advances in research and drug development, diabetes remains an incurable disease.

Current treatment options for T1D patients are restricted to insulin therapy, which requires life-long daily injections of insulin. In recent years, islet transplantation is becoming a promising alternative. However, it remains challenging to maintain the quality and viability of islets after transplantation long-term. Most patients are required to resume insulin therapy within five years of islet transplantation. Aside from immune rejection, islet graft loss is worsened by the rapid formation of islet amyloid (Potter et al. 2010).

For T2D, current treatments require intense lifestyle management, pharmacotherapies, and sometimes bariatric surgery for obese patient. Unlike T1D, the natural history of T2D development is slow and progress over many years. The first stage towards T2D is known as prediabetes, where blood glucose levels are higher

than normal but have not reached the clinical level to be diagnosed as diabetic. During this period, which spans over 5 to 10 years, insulin resistance in peripheral tissues continues to buildup. As a compensatory mechanism, islets beta cells increase their production of insulin to maintain blood glucose. Associated with increase insulin production is the elevated production and release of IAPP, which increases the propensity to form toxic oligomers and insoluble amyloid deposits.

Therefore, prevention of amyloid formation could be an effective strategy to improve islet transplantation success for T1D patients as well as maintaining beta cell function and survival in T2D patients. In this study, the finding that SORLA preferentially mediates extracellular clearance of proIAPP but not mature IAPP may prove to be particular advantageous. Its selective clearance of proIAPP allows the biologically active mature IAPP to be secreted and regulate energy homeostasis, while the partially processed forms with no known physiological functions to be degraded.

4.4. Conclusion and outlook

In summary, this study has uncovered a novel, non-neuronal role of SORLA in pancreatic islet beta cells. In detail, SORLA functions as an endocytic receptor for the soluble, partially processed form of IAPP and is protective against islet amyloid formation. These findings provided valuable insights into the molecular mechanism whereby SORLA may play a dual role in the pathophysiology of neurodegenerative and metabolic diseases.

Results from this study raise new and important questions that compel further experimentations to refine the current proposed model and to address the dual role of SORLA in neurodegenerative and metabolic diseases. For example, there are considerable differences in the amino acid sequences between the human and murine IAPP peptides, which contributes to their differences in amyloidogenicity (P. Westermark et al. 1990). Thus, it remains unclear if SORLA binds to and mediates endocytic uptake of the human IAPP and if so, whether it interacts with the monomeric, oligomeric, and/ or fibrillar forms. Based on established literature, I would speculate that SORLA is likely to interact similarly with both murine and human IAPP as structural studies have demonstrated the VPS10P domain of SORLA recognizes its ligand peptides without strict dependence on specific amino acid sequences, but rather based on their tertiary confirmation that is compatible with the funnel-shaped opening of the

domain (Kitago et al. 2015). This study tested the non-aggregating forms of murine IAPP peptides which remain soluble and monomeric in solution. Further optimization of the preparation and handling of synthetic human IAPP peptides will be required to allow quantitative measurements specifically for monomers or oligomers. Furthermore, in addition to SORLA, it will be interesting to determine if other members of the VPS10P domain receptors also interact with IAPP and/ or have functional roles in islet beta cell biology. For instance, the VPS10P domain receptor SorCS1 has been shown to maintain insulin biogenesis in secretory granules of beta cells, where obese mice deficient in SorCS1 are severely depleted of insulin-containing secretory granules and develop diabetes (Kebede et al. 2014). Finally, results from this study have laid the foundation for our recognition of a physiological role for SORLA in islet beta cells, especially in the regulation of islet amyloid. However further studies are needed to elucidate if the amyloid-reducing properties of SORLA in the pancreas translates to downstream protection against the development of type 2 diabetes.

References

Abedini, Andisheh, Sylvia M. Tracz, Jae-Hyun Cho, and Daniel P. Raleigh. 2006. "Characterization of the Heparin Binding Site in the N-Terminus of Human Pro-Islet Amyloid Polypeptide: Implications for Amyloid Formation." *Biochemistry* 45 (30): 9228–37. https://doi.org/10.1021/bi0510936.

Ahrén, B., C. Oosterwijk, C. J.M. Lips, and J. W.M. Höppener. 1998. "Transgenic Overexpression of Human Islet Amyloid Polypeptide Inhibits Insulin Secretion and Glucose Elimination after Gastric Glucose Gavage in Mice." *Diabetologia* 41 (11): 1374–80. https://doi.org/10.1007/s001250051079.

Akter, Kawser, Emily A. Lanza, Stephen A. Martin, Natalie Myronyuk, Melanie Rua, and Robert B. Raffa. 2011. "Diabetes Mellitus and Alzheimer's Disease: Shared Pathology and Treatment?" *British Journal of Clinical Pharmacology* 71 (3): 365–76. https://doi.org/10.1111/j.1365-2125.2010.03830.x.

Akter, Rehana, Ping Cao, Harris Noor, Zachary Ridgway, Ling Hsien Tu, Hui Wang, Amy G. Wong, Xiaoxue Zhang, Andisheh Abedini, Ann Marie Schmidt, and Daniel P. Raleigh. 2016. "Islet Amyloid Polypeptide: Structure, Function, and Pathophysiology." *Journal of Diabetes Research* 2016. https://doi.org/10.1155/2016/2798269.

Andersen, O. M., J. Reiche, V. Schmidt, M. Gotthardt, R. Spoelgen, J. Behlke, C. A. F. von Arnim, T. Breiderhoff, P. Jansen, X. Wu, K. R. Bales, R. Cappai, C. L. Masters, J. Gliemann, E. J. Mufson, B. T. Hyman, S. M. Paul, A. Nykjaer, and T. E. Willnow. 2005. "Neuronal Sorting Protein-Related Receptor SorLA/LR11 Regulates Processing of the Amyloid Precursor Protein." *Proceedings of the National Academy of Sciences* 102 (38): 13461–66. https://doi.org/10.1073/pnas.0503689102.

Andersen, Olav M., Vanessa Schmidt, Robert Spoelgen, Jørgen Gliemann, Joachim Behlke, Denise Galatis, William J. McKinstry, Michael W. Parker, Colin L. Masters, Bradley T. Hyman, Roberta Cappai, and Thomas E. Willnow. 2006. "Molecular Dissection of the Interaction between Amyloid Precursor Protein and Its Neuronal Trafficking Receptor SorLA/LR11." *Biochemistry*. https://doi.org/10.1021/bi052120v.

Aston-Mourney, K., R. L. Hull, S. Zraika, J. Udayasankar, S. L. Subramanian, and S. E. Kahn. 2011. "Exendin-4 Increases Islet Amyloid Deposition but Offsets the Resultant Beta Cell Toxicity in Human Islet Amyloid Polypeptide Transgenic Mouse Islets." *Diabetologia* 54 (7): 1756–65. https://doi.org/10.1007/s00125-011-2143-3.

Aston-Mourney, Kathryn, Sakeneh Zraika, Jayalakshmi Udayasankar, Shoba L. Subramanian, Pattie S. Green, Steven E. Kahn, and Rebecca L. Hull. 2013. "Matrix Metalloproteinase-9 Reduces Islet Amyloid Formation by Degrading Islet Amyloid Polypeptide." *Journal of Biological Chemistry* 288 (5): 3553–59. https://doi.org/10.1074/jbc.M112.438457.

Barbagallo, Mario. 2014. "Type 2 Diabetes Mellitus and Alzheimer's Disease." *World Journal of Diabetes* 5 (6): 889. https://doi.org/10.4239/wjd.v5.i6.889.

Bennett, Robert G., William C. Duckworth, and Frederick G. Hamel. 2000. "Degradation of Amylin by Insulin-Degrading Enzyme." *Journal of Biological Chemistry* 275 (47): 36621–25. https://doi.org/10.1074/jbc.M006170200.

Bennett, Robert G., Frederick G. Hamel, and William C. Duckworth. 2003. “An Insulin-Degrading Enzyme Inhibitor Decreases Amylin Degradation, Increases Amylin-Induced Cytotoxicity, and Increases Amyloid Formation in Insulinoma Cell Cultures.” *Diabetes* 52 (9): 2315–20. https://doi.org/10.2337/diabetes.52.9.2315.

Biessels, Geert Jan, Salka Staekenborg, Eric Brunner, Carol Brayne, and Philip Scheltens. 2006. “Risk of Dementia in Diabetes Mellitus: A Systematic Review.” *The Lancet Neurology* 5 (1): 64–74. https://doi.org/10.1016/S1474-4422(05)70284-2.

Burgert, Tilman, Vanessa Schmidt, Safak Caglayan, Fuyu Lin, Annette Füchtbauer, Ernst-Martin Füchtbauer, Anders Nykjaer, Anne-Sophie Carlo, and Thomas E. Willnow. 2013. “SORLA-Dependent and -Independent Functions for PACS1 in Control of Amyloidogenic Processes.” *Molecular and Cellular Biology* 33 (21): 4308–20. https://doi.org/10.1128/mcb.00628-13.

Caglayan, Safak, Shizuka Takagi-Niidome, Fan Liao, Anne Sophie Carlo, Vanessa Schmidt, Tilman Burgert, Yu Kitago, Ernst Martin Fuchtbauer, Annette Fuchtbauer, David M. Holtzman, Junichi Takagi, and Thomas E. Willnow. 2014. “Lysosomal Sorting of Amyloid-β by the SORLA Receptor Is Impaired by a Familial Alzheimer’s Disease Mutation.” *Science Translational Medicine* 6 (223). https://doi.org/10.1126/scitranslmed.3007747.

Casas, Sílvia, Ramon Gomis, Fiona M. Gribble, Jordi Altirriba, Sakari Knuutila, and Anna Novials. 2007. “Impairment of the Ubiquitin-Proteasome Pathway Is a Downstream Endoplasmic Reticulum Stress Response Induced by Extracellular Human Islet Amyloid Polypeptide and Contributes to Pancreatic β-Cell Apoptosis.” *Diabetes* 56 (9): 2284–94. https://doi.org/10.2337/db07-0178.

Castillo, Joseph J, Alfred C Aplin, Daryl J Hackney, Meghan F Hogan, Nathalie Esser, Andrew T Templin, Rehana Akter, Steven E Kahn, Daniel P Raleigh, Sakeneh Zraika, and Rebecca L Hull. 2022. “Islet Amyloid Polypeptide Aggregation Exerts Cytotoxic and Proinflammatory Effects on the Islet Vasculature in Mice.” *Diabetologia*, July. https://doi.org/10.1007/s00125-022-05756-9.

Cerf, Marlon E. 2013. “Beta Cell Dysfunction and Insulin Resistance.” *Frontiers in Endocrinology* 4 (MAR): 1–12. https://doi.org/10.3389/fendo.2013.00037.

Charge, Sophie B. P., Eelco J. P. de Koning, and Anne Clark. 1995. “Effect of PH and Insulin on Fibrillogenesis of Islet Amyloid Polypeptide in Vitro.” *Biochemistry* 34 (44): 14588–93. https://doi.org/10.1021/bi00044a038.

Chen, Yi-Chun, Austin J. Taylor, and C. Bruce Verchere. 2018. “Islet Prohormone Processing in Health and Disease.” *Diabetes, Obesity and Metabolism* 20 (September): 64–76. https://doi.org/10.1111/dom.13401.

Cheng, D., J. Noble, M.X. Tang, N. Schupf, R. Mayeux, and J.A. Luchsinger. 2011. “Type 2 Diabetes and Late-Onset Alzheimer’s Disease.” *Dementia and Geriatric Cognitive Disorders* 31 (6): 424–30. https://doi.org/10.1159/000324134.

Chiu, Chi-cheng, Sadanand Singh, and Juan J. de Pablo. 2013. “Effect of Proline Mutations on the Monomer Conformations of Amylin.” *Biophysical Journal* 105 (5): 1227–35. https://doi.org/10.1016/j.bpj.2013.07.029.

Christopoulos, George, Katie J. Perry, Maria Morfis, Nanda Tilakaratne, Yongyi Gao, Neil J. Fraser, Martin J. Main, Steven M. Foord, and Patrick M. Sexton. 1999.

"Multiple Amylin Receptors Arise from Receptor Activity-Modifying Protein Interaction with the Calcitonin Receptor Gene Product." *Molecular Pharmacology* 56 (1): 235–42. https://doi.org/10.1124/mol.56.1.235.

Clark, A., M. F. Saad, T. Nezzer, C. Uren, W. C. Knowler, P. H. Bennett, and R. C. Turner. 1990. "Islet Amyloid Polypeptide in Diabetic and Non-Diabetic Pima Indians." *Diabetologia* 33 (5): 285–89. https://doi.org/10.1007/BF00403322.

Costes, Safia, Chang Jiang Huang, Tatyana Gurlo, Marie Daval, Aleksey V. Matveyenko, Robert A. Rizza, Alexandra E. Butler, and Peter C. Butler. 2011. "β-Cell Dysfunctional ERAD/Ubiquitin/Proteasome System in Type 2 Diabetes Mediated by Islet Amyloid Polypeptide-Induced UCH-L1 Deficiency." *Diabetes* 60 (1): 227–38. https://doi.org/10.2337/db10-0522.

Couce, Marta, Laurie A. Kane, Timothy D. O'Brien, Jon Charlesworth, Walter Soeller, John McNeish, David Kreutter, Patrick Roche, and Peter C. Butler. 1996. "Treatment with Growth Hormone and Dexamethasone in Mice Transgenic for Human Islet Amyloid Polypeptide Causes Islet Amyloidosis and β-Cell Dysfunction." *Diabetes*. https://doi.org/10.2337/diab.45.8.1094.

Courtade, Jaques A., Agnieszka M. Klimek-Abercrombie, Yi Chun Chen, Nirja Patel, Phoebe Y.T. Lu, Cate Speake, Paul C. Orban, Behzad Najafian, Graydon Meneilly, Carla J. Greenbaum, Garth L. Warnock, Constadina Panagiotopoulos, and C. Bruce Verchere. 2017. "Measurementof Pro-Islet Amyloid Polypeptide (1-48) in Diabetes and Islet Transplants." *Journal of Clinical Endocrinology and Metabolism*. https://doi.org/10.1210/jc.2016-2773.

D'Alessio, David A., C Bruce Verchere, Steven E. Kahn, Vicki Hoagland, Denis G. Baskin, Richard D. Palmiter, and John W. Ensinck. 1994. "Pancreatic Expression and Secretion of Human Islet Amyloid Polypeptide in a Transgenic Mouse." *Diabetes* 43 (12): 1457–61. https://doi.org/10.2337/diab.43.12.1457.

Dhawan, Sangeeta, Senta Georgia, and Anil Bhushan. 2007. "Formation and Regeneration of the Endocrine Pancreas." *Current Opinion in Cell Biology* 19 (6): 634–45. https://doi.org/10.1016/j.ceb.2007.09.015.

Dodson, Sara E., Olav M. Andersen, Vinit Karmali, Jason J. Fritz, Dongmei Cheng, Junmin Peng, Allan I. Levey, Thomas E. Willnow, and James J. Lah. 2008. "Loss of LR11/SORLA Enhances Early Pathology in a Mouse Model of Amyloidosis: Evidence for a Proximal Role in Alzheimer's Disease." *Journal of Neuroscience* 28 (48): 12877–86. https://doi.org/10.1523/JNEUROSCI.4582-08.2008.

Dumanis, Sonya B., Tilman Burgert, Safak Caglayan, Annette Füchtbauer, Ernst Martin Füchtbauer, Vanessa Schmidt, and Thomas E. Willnow. 2015. "Distinct Functions for Anterograde and Retrograde Sorting of SORLA in Amyloidogenic Processes in the Brain." *Journal of Neuroscience* 35 (37): 12703–13. https://doi.org/10.1523/JNEUROSCI.0427-15.2015.

Fjorback, Anja W., Matthew Seaman, Camilla Gustafsen, Arnela Mehmedbasic, Suzanne Gokool, Chengbiao Wu, Daniel Militz, Vanessa Schmidt, Peder Madsen, Jens R. Nyengaard, Thomas E. Willnow, Erik Ilsø Christensen, William B. Mobley, Anders Nykjær, and Olav M. Andersen. 2012. "Retromer Binds the FANSHY Sorting Motif in SorLA to Regulate Amyloid Precursor Protein Sorting and Processing." *Journal of Neuroscience* 32 (4): 1467–80. https://doi.org/10.1523/JNEUROSCI.2272-11.2012.

Fox, Niles, James Schrementi, Masahiro Nishi, Shinyo Ohagi, Shu Jin Chan, Judith A. Heisserman, Gunilla T. Westermark, Arnold Leckström, Per Westermark, and Donald F. Steiner. 1993. “Human Islet Amyloid Polypeptide Transgenic Mice as a Model of Non-Insulin-Dependent Diabetes Mellitus (NIDDM).” *FEBS Letters* 323 (1–2): 40–44. https://doi.org/10.1016/0014-5793(93)81444-5.

Gebre-Medhin, S., C. Olofsson, and H. Mulder. 2000. “Islet Amyloid Polypeptide in the Islets of Langerhans: Friend or Foe?” *Diabetologia* 43 (6): 687–95. https://doi.org/10.1007/s001250051364.

Gebre-Medhin, Samuel, Hindrik Mulder, Milos Pekny, Gunilla Westermark, Jan Törnell, Per Westermark, Frank Sundler, Bo Ahrén, and Christer Betsholtz. 1998. “Increased Insulin Secretion and Glucose Tolerance in Mice Lacking Islet Amyloid Polypeptide (Amylin).” *Biochemical and Biophysical Research Communications* 250 (2): 271–77. https://doi.org/10.1006/bbrc.1998.9308.

Geisler, John G., Walter Zawalich, Kathleen Zawalich, Jonathan R.T. Lakey, Hans Stukenbrok, Anthony J. Milici, and Walter C. Soeller. 2002. “Estrogen Can Prevent or Reverse Obesity and Diabetes in Mice Expressing Human Islet Amyloid Polypeptide.” *Diabetes* 51 (7): 2158–69. https://doi.org/10.2337/diabetes.51.7.2158.

Gurlo, Tatyana, Sergey Ryazantsev, Chang Jiang Huang, Michael W. Yeh, Howard A. Reber, O. Joe Hines, Timothy D. O’Brien, Charles G. Glabe, and Peter C. Butler. 2010. “Evidence for Proteotoxicity in β Cells in Type 2 Diabetes: Toxic Islet Amyloid Polypeptide Oligomers Form Intracellularly in the Secretory Pathway.” *American Journal of Pathology* 176 (2): 861–69. https://doi.org/10.2353/ajpath.2010.090532.

Haataja, Leena, Tatyana Gurlo, Chang J. Huang, and Peter C. Butler. 2008. “Islet Amyloid in Type 2 Diabetes, and the Toxic Oligomer Hypothesis.” *Endocrine Reviews* 29 (3): 303–16. https://doi.org/10.1210/er.2007-0037.

Hartley, Taila, John Brumell, and Allen Volchuk. 2009. “Emerging Roles for the Ubiquitin-Proteasome System and Autophagy in Pancreatic β-Cells.” *American Journal of Physiology - Endocrinology and Metabolism* 296 (1). https://doi.org/10.1152/ajpendo.90538.2008.

Hiddinga, Henry J., Setsuya Sakagashira, Masayuki Ishigame, Pranathi Madde, Tokio Sanke, Kishio Nanjo, Yogish C. Kudva, James J. Lee, Jan van Deursen, and Norman L. Eberhardt. 2012. “Expression of Wild-Type and Mutant S20G HIAPP in Physiologic Knock-in Mouse Models Fails to Induce Islet Amyloid Formation, but Induces Mild Glucose Intolerance.” *Journal of Diabetes Investigation* 3 (2): 138–47. https://doi.org/10.1111/j.2040-1124.2011.00166.x.

Hogan, Meghan F., Daniel T. Meier, Sakeneh Zraika, Andrew T. Templin, Mahnaz Mellati, Rebecca L. Hull, Malcolm A. Leissring, and Steven E. Kahn. 2016. “Inhibition of Insulin-Degrading Enzyme Does Not Increase Islet Amyloid Deposition in Vitro.” *Endocrinology* 157 (9): 3462–68. https://doi.org/10.1210/en.2016-1410.

Höppener, J. W. M., H. M. Jacobs, N. Wierup, G. Sotthewes, M. Sprong, P. de Vos, R. Berger, F. Sundler, and B. Ahrén. 2008. “Human Islet Amyloid Polypeptide Transgenic Mice: In Vivo and Ex Vivo Models for the Role of HIAPP in Type 2 Diabetes Mellitus.” *Experimental Diabetes Research* 2008: 697035. https://doi.org/10.1155/2008/697035.

Höppener, J. W.M., C. Oosterwijk, M. G. Nieuwenhuis, G. Posthuma, J. H.H. Thijssen, Th M. Vroom, B. Ahrén, and C. J.M. Lips. 1999. “Extensive Islet Amyloid Formation Is Induced by Development of Type II Diabetes Mellitus and Contributes to Its Progression: Pathogenesis of Diabetes in a Mouse Model.” *Diabetologia* 42 (4): 427–34. https://doi.org/10.1007/s001250051175.

Höppener, J. W.M., J. S. Verbeek, E. J.P. de Koning, C. Oosterwijk, K. L. van Hulst, H. J. Visser-Vernooy, F. M.A. Hofhuis, S. van Gaalen, M. J.H. Berends, W. H.L. Hackeng, H. S. Jansz, J. F. Morris, A. Clark, P. J.A. Capel, and C. J.M. Lips. 1993. “Chronic Overproduction of Islet Amyloid Polypeptide/Amylin in Transgenic Mice: Lysosomal Localization of Human Islet Amyloid Polypeptide and Lack of Marked Hyperglycaemia or Hyperinsulinaemia.” *Diabetologia* 36 (12): 1258–65. https://doi.org/10.1007/BF00400803.

Huang, Chang Jiang, Chia Yu Lin, Leena Haataja, Tatyana Gurlo, Alexandra E. Butler, Robert A. Rizza, and Peter C. Butler. 2007. “High Expression Rates of Human Islet Amyloid Polypeptide Induce Endoplasmic Reticulum Stress-Mediated β-Cell Apoptosis, a Characteristic of Humans with Type 2 but Not Type 1 Diabetes.” *Diabetes* 56 (8): 2016–27. https://doi.org/10.2337/db07-0197.

Huang, Timothy Y., Yingjun Zhao, Xiaoguang Li, Xin Wang, I. Chu Tseng, Robert Thompson, Shichun Tu, Thomas E. Willnow, Yun Wu Zhang, and Huaxi Xu. 2016. “SNX27 and SORLA Interact to Reduce Amyloidogenic Subcellular Distribution and Processing of Amyloid Precursor Protein.” *Journal of Neuroscience* 36 (30): 7996–8011. https://doi.org/10.1523/JNEUROSCI.0206-16.2016.

Hull, Rebecca L., Sofianos Andrikopoulos, C. Bruce Verchere, Josep Vidal, Feng Wang, Miriam Cnop, Ronald L. Prigeon, and Steven E. Kahn. 2003. “Increased Dietary Fat Promotes Islet Amyloid Formation and β-Cell Secretory Dysfunction in a Transgenic Mouse Model of Islet Amyloid.” *Diabetes* 52 (2): 372–79. https://doi.org/10.2337/diabetes.52.2.372.

Hull, Rebecca L., Gunilla T. Westermark, Per Westermark, and Steven E. Kahn. 2004. “Islet Amyloid: A Critical Entity in the Pathogenesis of Type 2 Diabetes.” *Journal of Clinical Endocrinology and Metabolism*. https://doi.org/10.1210/jc.2004-0405.

Jackson, Kaleena, Gustavo A. Barisone, Elva Diaz, Lee Way Jin, Charles DeCarli, and Florin Despa. 2013. “Amylin Deposition in the Brain: A Second Amyloid in Alzheimer Disease?” *Annals of Neurology* 74 (4): 517–26. https://doi.org/10.1002/ana.23956.

Jacobsen, Linda, Peder Madsen, Christian Jacobsen, Morten S. Nielsen, Jørgen Gliemann, and Claus M. Petersen. 2001. “Activation and Functional Characterization of the Mosaic Receptor SorLA/LR11.” *Journal of Biological Chemistry* 276 (25): 22788–96. https://doi.org/10.1074/jbc.M100857200.

Jacobsen, Linda, Peder Madsen, Søren K. Moestrup, Anders H. Lund, Niels Tommerup, Anders Nykjær, Lars Sottrup-Jensen, Jørgen Gliemann, and Claus M. Petersen. 1996. “Molecular Characterization of a Novel Human Hybrid-Type Receptor That Binds the A2-Macroglobulin Receptor-Associated Protein.” *Journal of Biological Chemistry* 271 (49): 31379–83. https://doi.org/10.1074/jbc.271.49.31379.

Janson, J., W C Soeller, P C Roche, R T Nelson, A J Torchia, D K Kreutter, and P C Butler. 1996. “Spontaneous Diabetes Mellitus in Transgenic Mice Expressing

Human Islet Amyloid Polypeptide." *Proceedings of the National Academy of Sciences*. https://doi.org/10.1073/pnas.93.14.7283.

Jurgens, Catherine A., Mirna N. Toukatly, Corinne L. Fligner, Jayalakshmi Udayasankar, Shoba L. Subramanian, Sakeneh Zraika, Kathryn Aston-Mourney, Darcy B. Carr, Per Westermark, Gunilla T. Westermark, Steven E. Kahn, and Rebecca L. Hull. 2011. "β-Cell Loss and β-Cell Apoptosis in Human Type 2 Diabetes Are Related to Islet Amyloid Deposition." *American Journal of Pathology*. https://doi.org/10.1016/j.ajpath.2011.02.036.

Kahn, S. E., D. A. D'Alessio, M. W. Schwartz, W. Y. Fujimoto, J. W. Ensinck, G. J. Taborsky, and D. Porte. 1990. "Evidence of Cosecretion of Islet Amyloid Polypeptide and Insulin by β-Cells." *Diabetes* 39 (5): 634–38. https://doi.org/10.2337/diabetes.39.5.634.

Kahn, S E, S Andrikopoulos, and C B Verchere. 1999. "Islet Amyloid: A Long-Recognized but Underappreciated Pathological Feature of Type 2 Diabetes." *Diabetes* 48 (2): 241–53. https://doi.org/10.2337/diabetes.48.2.241.

Kebede, Melkam A., Angie T. Oler, Trillian Gregg, Allison J. Balloon, Adam Johnson, Kelly Mitok, Mary Rabaglia, Kathryn Schueler, Donald Stapleton, Candice Thorstenson, Lindsay Wrighton, Brendan J. Floyd, Oliver Richards, Summer Raines, Kevin Eliceiri, Nabil G. Seidah, Christopher Rhodes, Mark P. Keller, Joshua L. Coon, et al. 2014. "SORCS1 Is Necessary for Normal Insulin Secretory Granule Biogenesis in Metabolically Stressed β Cells." *Journal of Clinical Investigation* 124 (10): 4240–56. https://doi.org/10.1172/JCI74072.

Kim, Jinyoung, Hwanju Cheon, Yeon Taek Jeong, Wenying Quan, Kook Hwan Kim, Jae Min Cho, Yu Mi Lim, Seung Hoon Oh, Sang Man Jin, Jae Hyeon Kim, Moon Kyu Lee, Sunshin Kim, Masaaki Komatsu, Sang Wook Kang, and Myung Shik Lee. 2014. "Amyloidogenic Peptide Oligomer Accumulation in Autophagy-Deficient β Cells Induces Diabetes." *Journal of Clinical Investigation* 124 (8): 3311–24. https://doi.org/10.1172/JCI69625.

Kitago, Yu, Masamichi Nagae, Zenzaburo Nakata, Maho Yagi-Utsumi, Shizuka Takagi-Niidome, Emiko Mihara, Terukazu Nogi, Koichi Kato, and Junichi Takagi. 2015. "Structural Basis for Amyloidogenic Peptide Recognition by SorLA." *Nature Structural and Molecular Biology* 22 (3): 199–206. https://doi.org/10.1038/nsmb.2954.

Klinger, Stine C., Simon Glerup, Merete K. Raarup, Muriel C. Mari, Mette Nyegaard, Gerbrand Koster, Thaneas Prabakaran, Stefan K. Nilsson, Maj M. Kjaergaard, Oddmund Bakke, Anders Nykjær, Gunilla Olivecrona, Claus Munck Petersen, and Morten S. Nielsen. 2011. "SorLA Regulates the Activity of Lipoprotein Lipase by Intracellular Trafficking." *Journal of Cell Science* 124 (7): 1095–1105. https://doi.org/10.1242/jcs.072538.

Lambert, J C, Carla A Ibrahim-Verbaas, Denise Harold, Adam C Naj, Rebecca Sims, Céline Bellenguez, A L DeStafano, Joshua C Bis, Gary W Beecham, Benjamin Grenier-Boley, Giancarlo Russo, T A Thorton-Wells, N Jones, Albert V Smith, Vincent Chouraki, Charlene Thomas, M Arfan Ikram, Diana Zelenika, Badri N Vardarajan, et al. 2013. "Meta-Analysis of 74,046 Individuals Identifies 11 New Susceptibility Loci for Alzheimer's Disease." *Nature Genetics* 45 (12): 1452–58. https://doi.org/10.1038/ng.2802.

Larsen, Jakob Vejby, and Claus Munck Petersen. 2017. “SorLA in Interleukin-6 Signaling and Turnover.” *Molecular and Cellular Biology* 37 (11): 1–18. https://doi.org/10.1128/MCB.00641-16.

Lutz, Thomas A. 2010. “The Role of Amylin in the Control of Energy Homeostasis.” *American Journal of Physiology - Regulatory Integrative and Comparative Physiology* 298 (6). https://doi.org/10.1152/ajpregu.00703.2009.

MacArthur, D. L.A., E. J.P. De Koning, J. S. Verbeek, J. F. Morris, and A. Clark. 1999. “Amyloid Fibril Formation Is Progressive and Correlates with Beta-Cell Secretion in Transgenic Mouse Isolated Islets.” *Diabetologia* 42 (10): 1219–27. https://doi.org/10.1007/s001250051295.

Malik, Anna R., and Thomas E. Willnow. 2020. “VPS10P Domain Receptors: Sorting Out Brain Health and Disease.” *Trends in Neurosciences*, 1–16. https://doi.org/10.1016/j.tins.2020.08.003.

Marcusson, Eric G., Bruce F. Horazdovsky, Joan Lin Cereghino, Editte Gharakhanian, and Scott D. Emr. 1994. “The Sorting Receptor for Yeast Vacuolar Carboxypeptidase Y Is Encoded by the VPS10 Gene.” *Cell* 77 (4): 579–86. https://doi.org/10.1016/0092-8674(94)90219-4.

Marzban, Lucy, Christopher J. Rhodes, Donald F. Steiner, Leena Haataja, Philippe A. Halban, and C. Bruce Verchere. 2006. “Impaired NH2-Terminal Processing of Human Proislet Amyloid Polypeptide by the Prohormone Convertase PC2 Leads to Amyloid Formation and Cell Death.” *Diabetes*. https://doi.org/10.2337/db05-1566.

Marzban, Lucy, Galina Soukhatcheva, and C. Bruce Verchere. 2005. “Role of Carboxypeptidase E in Processing of Pro-Islet Amyloid Polypeptide in β-Cells.” *Endocrinology* 146 (4): 1808–17. https://doi.org/10.1210/en.2004-1175.

Marzban, Lucy, Genny Trigo-Gonzalez, and C. Bruce Verchere. 2005. “Processing of Pro-Islet Amyloid Polypeptide in the Constitutive and Regulated Secretory Pathways of β Cells.” *Molecular Endocrinology*. https://doi.org/10.1210/me.2004-0407.

Masini, M., M. Bugliani, R. Lupi, S. del Guerra, U. Boggi, F. Filipponi, L. Marselli, P. Masiello, and P. Marchetti. 2009. “Autophagy in Human Type 2 Diabetes Pancreatic Beta Cells.” *Diabetologia* 52 (6): 1083–86. https://doi.org/10.1007/s00125-009-1347-2.

Masters, Seth L, Aisling Dunne, Shoba L Subramanian, Rebecca L Hull, Gillian M Tannahill, Fiona A Sharp, Christine Becker, Luigi Franchi, Eiji Yoshihara, Zhe Chen, Niamh Mullooly, Lisa A Mielke, James Harris, Rebecca C Coll, Kingston H G Mills, K Hun Mok, Philip Newsholme, Gabriel Nuñez, Junji Yodoi, et al. 2010. “Activation of the NLRP3 Inflammasome by Islet Amyloid Polypeptide Provides a Mechanism for Enhanced IL-1β in Type 2 Diabetes.” *Nature Immunology* 11 (10): 897–904. https://doi.org/10.1038/ni.1935.

Matveyenko, Aleksey V., and Peter C. Butler. 2006. “Islet Amyloid Polypeptide (IAPP) Transgenic Rodents as Models for Type 2 Diabetes.” *ILAR Journal* 47 (3): 225–33. https://doi.org/10.1093/ilar.47.3.225.

McLatchie, Linda M., Neil J. Fraser, Martin J. Main, Alan Wise, Jason Brown, Nicola Thompson, Roberto Solari, Melanie G. Lee, and Steven M. Foord. 1998. “RAMPs Regulate the Transport and Ligand Specificity of the Calcitonin-Receptor-like

Receptor.” *Nature* 393 (6683): 333–39. https://doi.org/10.1038/30666.

Mehmedbasic, Arnela, Sofie K. Christensen, Jonas Nilsson, Ulla Rüetschi, Camilla Gustafsen, Annemarie Svane Aavild Poulsen, Rikke W. Rasmussen, Anja N. Fjorback, Göran Larson, and Olav M. Andersen. 2015. “SorLA Complement-Type Repeat Domains Protect the Amyloid Precursor Protein against Processing.” *Journal of Biological Chemistry*. https://doi.org/10.1074/jbc.M114.619940.

Monti, Giulia, and Olav M Andersen. 2018. “20 Years Anniversary for SORLA/SORL1 (1996-2016).” *Receptors & Clinical Investigation* 4 (May): 1–10. https://doi.org/10.14800/rci.1611.

Muff, Roman, Nicole Bühlmann, Jan A. Fischer, and Walter Born. 1999. “An Amylin Receptor Is Revealed Following Co-Transfection of a Calcitonin Receptor with Receptor Activity Modifying Proteins-1 or -3.” *Endocrinology* 140 (6): 2924–27. https://doi.org/10.1210/endo.140.6.6930.

Mukherjee, Abhisek, Diego Morales-Scheihing, Peter C. Butler, and Claudio Soto. 2015. “Type 2 Diabetes as a Protein Misfolding Disease.” *Trends in Molecular Medicine*. https://doi.org/10.1016/j.molmed.2015.04.005.

Muraro, Mauro J., Gitanjali Dharmadhikari, Dominic Grün, Nathalie Groen, Tim Dielen, Erik Jansen, Leon van Gurp, Marten A. Engelse, Francoise Carlotti, Eelco J.P. de Koning, and Alexander van Oudenaarden. 2016. “A Single-Cell Transcriptome Atlas of the Human Pancreas.” *Cell Systems* 3 (4): 385-394.e3. https://doi.org/10.1016/j.cels.2016.09.002.

Neelankal John, Abraham, Ramesh Ram, and Fang Xu Jiang. 2018. “RNA-Seq Analysis of Islets to Characterise the Dedifferentiation in Type 2 Diabetes Model Mice Db/Db.” *Endocrine Pathology* 29 (3): 207–21. https://doi.org/10.1007/s12022-018-9523-x.

Nielsen, Morten S., Camilla Gustafsen, Peder Madsen, Jens R. Nyengaard, Guido Hermey, Oddmund Bakke, Muriel Mari, Peter Schu, Regina Pohlmann, André Dennes, and Claus M. Petersen. 2007. “Sorting by the Cytoplasmic Domain of the Amyloid Precursor Protein Binding Receptor SorLA.” *Molecular and Cellular Biology* 27 (19): 6842–51. https://doi.org/10.1128/mcb.00815-07.

Nilsson, Stefan K., Stine Christensen, Merete K. Raarup, Robert O. Ryan, Morten S. Nielsen, and Gunilla Olivecrona. 2008. “Endocytosis of Apolipoprotein A-V by Members of the Low Density Lipoprotein Receptor and the Vps10p Domain Receptor Families.” *Journal of Biological Chemistry* 283 (38): 25920–27. https://doi.org/10.1074/jbc.M802721200.

Offe, Katrin, Sara E. Dodson, James T. Shoemaker, Jason J. Fritz, Marla Gearing, Allan I. Levey, and James J. Lah. 2006. “The Lipoprotein Receptor LR11 Regulates Amyloid β Production and Amyloid Precursor Protein Traffic in Endosomal Compartments.” *The Journal of Neuroscience* 26 (5): 1596–1603. https://doi.org/10.1523/JNEUROSCI.4946-05.2006.

Park, Kirily, and C. Bruce Verchere. 2001. “Identification of a Heparin Binding Domain in the N-Terminal Cleavage Site of Pro-Islet Amyloid Polypeptide.” *Journal of Biological Chemistry* 276 (20): 16611–16. https://doi.org/10.1074/jbc.M008423200.

Parks, Brian W., Elizabeth Nam, Elin Org, Emrah Kostem, Frode Norheim, Simon T. Hui, Calvin Pan, Mete Civelek, Christoph D. Rau, Brian J. Bennett, Margarete

Mehrabian, Luke K. Ursell, Aiqing He, Lawrence W. Castellani, Bradley Zinker, Mark Kirby, Thomas A. Drake, Christian A. Drevon, Rob Knight, et al. 2013. “Genetic Control of Obesity and Gut Microbiota Composition in Response to High-Fat, High-Sucrose Diet in Mice.” *Cell Metabolism* 17 (1): 141–52. https://doi.org/10.1016/j.cmet.2012.12.007.

Paulsson, J. F., A. Andersson, P. Westermark, and G. T. Westermark. 2006. “Intracellular Amyloid-like Deposits Contain Unprocessed pro-Islet Amyloid Polypeptide (ProIAPP) in Beta Cells of Transgenic Mice Overexpressing the Gene for Human IAPP and Transplanted Human Islets.” *Diabetologia*. https://doi.org/10.1007/s00125-006-0206-7.

Paulsson, Johan F., and Gunilla T. Westermark. 2005. “Aberrant Processing of Human Proislet Amyloid Polypeptide Results in Increased Amyloid Formation.” *Diabetes*. https://doi.org/10.2337/diabetes.54.7.2117.

Pietilä, Mika, Pranshu Sahgal, Emilia Peuhu, Niklas Z. Jäntti, Ilkka Paatero, Elisa Närvä, Hussein Al-Akhrass, Johanna Lilja, Maria Georgiadou, Olav M. Andersen, Artur Padzik, Harri Sihto, Heikki Joensuu, Matias Blomqvist, Irena Saarinen, Peter J. Boström, Pekka Taimen, and Johanna Ivaska. 2019. “SORLA Regulates Endosomal Trafficking and Oncogenic Fitness of HER2.” *Nature Communications* 10 (1): 2340. https://doi.org/10.1038/s41467-019-10275-0.

Potter, K. J., A. Abedini, P. Marek, A. M. Klimek, S. Butterworth, M. Driscoll, R. Baker, M. R. Nilsson, G. L. Warnock, J. Oberholzer, S. Bertera, M. Trucco, G. S. Korbutt, P. E. Fraser, D. P. Raleigh, and C. B. Verchere. 2010. “Islet Amyloid Deposition Limits the Viability of Human Islet Grafts but Not Porcine Islet Grafts.” *Proceedings of the National Academy of Sciences of the United States of America* 107 (9): 4305–10. https://doi.org/10.1073/pnas.0909024107.

Pottier, C, D Hannequin, S Coutant, A Rovelet-Lecrux, D Wallon, S Rousseau, S Legallic, C Paquet, S Bombois, J Pariente, C Thomas-Anterion, A Michon, B Croisile, F Etcharry-Bouyx, C Berr, J-F Dartigues, P Amouyel, H Dauchel, C Boutoleau-Bretonnière, et al. 2012. “High Frequency of Potentially Pathogenic SORL1 Mutations in Autosomal Dominant Early-Onset Alzheimer Disease.” *Molecular Psychiatry* 17 (9): 875–79. https://doi.org/10.1038/mp.2012.15.

Rajamohamedsait, Hameetha B., and Einar M. Sigurdsson. 2012. “Histological Staining of Amyloid and Pre-Amyloid Peptides and Proteins in Mouse Tissue.” In , 411–24. https://doi.org/10.1007/978-1-61779-551-0_28.

Raleigh, Daniel, Xiaoxue Zhang, Benoît Hastoy, and Anne Clark. 2017. “The β-Cell Assassin: IAPP Cytotoxicity.” *Journal of Molecular Endocrinology* 59 (3): R121–40. https://doi.org/10.1530/JME-17-0105.

Rieck, Sebastian, and Klaus H. Kaestner. 2010. “Expansion of β-Cell Mass in Response to Pregnancy.” *Trends in Endocrinology & Metabolism* 21 (3): 151–58. https://doi.org/10.1016/j.tem.2009.11.001.

Rivera, Jacqueline F., Safia Costes, Tatyana Gurlo, Charles G. Glabe, and Peter C. Butler. 2014. “Autophagy Defends Pancreatic β Cells from Human Islet Amyloid Polypeptide-Induced Toxicity.” *Journal of Clinical Investigation* 124 (8): 3489–3500. https://doi.org/10.1172/JCI71981.

Röcken, Christoph, Reinhold P. Linke, and Wolfgang Saeger. 1992. “Immunohistology of Islet Amyloid Polypeptide in Diabetes Mellitus: Semi-Qantitative Studies in a

Post-Mortem Series." *Virchows Archiv A Pathological Anatomy and Histopathology* 421 (4): 339–44. https://doi.org/10.1007/BF01660981.

Rogaeva, Ekaterina, Yan Meng, Joseph H. Lee, Yongjun Gu, Toshitaka Kawarai, Fanggeng Zou, Taiichi Katayama, Clinton T. Baldwin, Rong Cheng, Hiroshi Hasegawa, Fusheng Chen, Nobuto Shibata, Kathryn L. Lunetta, Raphaelle Pardossi-Piquard, Christopher Bohm, Yosuke Wakutani, L. Adrienne Cupples, Karen T. Cuenco, Robert C. Green, et al. 2007. "The Neuronal Sortilin-Related Receptor SORL1 Is Genetically Associated with Alzheimer Disease." *Nature Genetics* 39 (2): 168–77. https://doi.org/10.1038/ng1943.

Scherzer, Clemens R., Katrin Offe, Marla Gearing, Howard D. Rees, Guofu Fang, Craig J. Heilman, Chica Schaller, Hideaki Bujo, Allan I. Levey, and James J Lah. 2004. "Loss of Apolipoprotein E Receptor LR11 in Alzheimer Disease." *Archives of Neurology* 61 (8): 1200–1205. https://doi.org/10.1001/archneur.61.8.1200.

Schmidt, Vanessa, Nadja Schulz, Xin Yan, Annette Schürmann, Stefan Kempa, Matthias Kern, Matthias Blüher, Matthew N. Poy, Gunilla Olivecrona, and Thomas E. Willnow. 2016. "SORLA Facilitates Insulin Receptor Signaling in Adipocytes and Exacerbates Obesity." *Journal of Clinical Investigation* 126 (7): 2706–20. https://doi.org/10.1172/JCI84708.

Schmidt, Vanessa, Anje Sporbert, Michael Rohe, Tatjana Reimer, Armin Rehm, Olav M. Andersen, and Thomas E. Willnow. 2007. "SorLA/LR11 Regulates Processing of Amyloid Precursor Protein via Interaction with Adaptors GGA and PACS-1." *Journal of Biological Chemistry* 282 (45): 32956–64. https://doi.org/10.1074/jbc.M705073200.

Segerstolpe, Åsa, Athanasia Palasantza, Pernilla Eliasson, Eva Marie Andersson, Anne Christine Andréasson, Xiaoyan Sun, Simone Picelli, Alan Sabirsh, Maryam Clausen, Magnus K. Bjursell, David M. Smith, Maria Kasper, Carina Ämmälä, and Rickard Sandberg. 2016. "Single-Cell Transcriptome Profiling of Human Pancreatic Islets in Health and Type 2 Diabetes." *Cell Metabolism* 24 (4): 593–607. https://doi.org/10.1016/j.cmet.2016.08.020.

Shigihara, Nayumi, Ayako Fukunaka, Akemi Hara, Koji Komiya, Akira Honda, Toyoyoshi Uchida, Hiroko Abe, Yukiko Toyofuku, Motoyuki Tamaki, Takeshi Ogihara, Takeshi Miyatsuka, Henry J. Hiddinga, Setsuya Sakagashira, Masato Koike, Yasuo Uchiyama, Tamotsu Yoshimori, Norman L. Eberhardt, Yoshio Fujitani, and Hirotaka Watada. 2014. "Human IAPP-Induced Pancreatic β Cell Toxicity and Its Regulation by Autophagy." *Journal of Clinical Investigation* 124 (8): 3634–44. https://doi.org/10.1172/JCI69866.

Shih, Alexis Z.L., Yi-Chun Chen, Thilo Speckmann, Esben Søndergaard, Annette Schürmann, C. Bruce Verchere, and Thomas E. Willnow. 2022. "SORLA Mediates Endocytic Uptake of ProIAPP and Protects against Islet Amyloid Deposition." *Molecular Metabolism* 65 (November): 101585. https://doi.org/10.1016/j.molmet.2022.101585.

Singh, Sanghamitra, Saurabh Trikha, Anjali Sarkar, and Aleksandar M. Jeremic. 2016. "Proteasome Regulates Turnover of Toxic Human Amylin in Pancreatic Cells." *Biochemical Journal* 473 (17): 2655–70. https://doi.org/10.1042/BCJ20160026.

Smith, Erin N., Wei Chen, Mika Kähönen, Johannes Kettunen, Terho Lehtimäki, Leena Peltonen, Olli T. Raitakari, Rany M. Salem, Nicholas J. Schork, Marian Shaw,

Sathanur R. Srinivasan, Eric J. Topol, Jorma S. Viikari, Gerald S. Berenson, and Sarah S. Murray. 2010. “Longitudinal Genome-Wide Association of Cardiovascular Disease Risk Factors in the Bogalusa Heart Study.” Edited by Greg Gibson. *PLoS Genetics* 6 (9): e1001094. https://doi.org/10.1371/journal.pgen.1001094.

Verchere, C. Bruce, David A. D’Alessio, Richard D. Palmiter, Gordon C. Weir, Susan Bonner-Weir, Denis G. Baskin, and Steven E. Kahn. 1996. “Islet Amyloid Formation Associated with Hyperglycemia in Transgenic Mice with Pancreatic Beta Cell Expression of Human Islet Amyloid Polypeptide.” *Proceedings of the National Academy of Sciences of the United States of America* 93 (8): 3492–96. https://doi.org/10.1073/pnas.93.8.3492.

Wang, Jing, Jun Xu, Jennifer Finnerty, Machi Furuta, Donald F Steiner, and C Bruce Verchere. 2001. “The Prohormone Convertase Enzyme 2 (PC2) Is Essential for Processing Pro-Islet Amyloid Polypeptide at the NH2-Terminal Cleavage Site.” *Diabetes* 50 (3): 534–39. https://doi.org/10.2337/diabetes.50.3.534.

Wang, Z. L., W. M. Bennet, M. A. Ghatei, P. G.H. Byfield, D. M. Smith, and S. R. Bloom. 1993. “Influence of Islet Amyloid Polypeptide and the 8-37 Fragment of Islet Amyloid Polypeptide on Insulin Release from Perifused Rat Islets.” *Diabetes* 42 (2): 330–35. https://doi.org/10.2337/diab.42.2.330.

Westermark, Gunilla, Michelle Benig Arora, Niles Fox, Raymond Carroll, Shu Jin Chan, Per Westermark, and Donald F. Steiner. 1995. “Amyloid Formation in Response to β Cell Stress Occurs In Vitro, but Not In Vivo, in Islets of Transgenic Mice Expressing Human Islet Amyloid Polypeptide.” *Molecular Medicine* 1 (5): 542–53. https://doi.org/10.1007/BF03401591.

Westermark, P., U. Engstrom, K. H. Johnson, G. T. Westermark, and C. Betsholtz. 1990. “Islet Amyloid Polypeptide: Pinpointing Amino Acid Residues Linked to Amyloid Fibril Formation.” *Proceedings of the National Academy of Sciences of the United States of America* 87 (13): 5036–40. https://doi.org/10.1073/pnas.87.13.5036.

Westermark, Per, Zhan-Chun Li, Gunilla T. Westermark, Arnold Leckström, and Donald F. Steiner. 1996. “Effects of Beta Cell Granule Components on Human Islet Amyloid Polypeptide Fibril Formation.” *FEBS Letters* 379 (3): 203–6. https://doi.org/10.1016/0014-5793(95)01512-4.

Westermark, Per, Christer Wernstedt, Erik Wilander, and Knut Sletten. 1986. “A Novel Peptide in the Calcitonin Gene Related Peptide Family as an Amyloid Fibril Protein in the Endocrine Pancreas.” *Biochemical and Biophysical Research Communications* 140 (3): 827–31. https://doi.org/10.1016/0006-291X(86)90708-4.

Whittle, Andrew J., Meizi Jiang, Vivian Peirce, Joana Relat, Sam Virtue, Hiroyuki Ebinuma, Isamu Fukamachi, Takashi Yamaguchi, Mao Takahashi, Takeyoshi Murano, Ichiro Tatsuno, Masahiro Takeuchi, Chiaki Nakaseko, Wenlong Jin, Zhehu Jin, Mark Campbell, Wolfgang J. Schneider, Antonio Vidal-Puig, and Hideaki Bujo. 2015. “Soluble LR11/SorLA Represses Thermogenesis in Adipose Tissue and Correlates with BMI in Humans.” *Nature Communications* 6 (May): 1–12. https://doi.org/10.1038/ncomms9951.

Wijesekara, Nadeeja, Rosemary Ahrens, Miheer Sabale, Ling Wu, Kathy Ha, Giuseppe Verdile, and Paul E. Fraser. 2017. “Amyloid-β and Islet Amyloid Pathologies Link Alzheimer’s Disease and Type 2 Diabetes in a Transgenic Model.” *The FASEB*

Journal 31 (12): 5409–18. https://doi.org/10.1096/fj.201700431R.

Willnow, Thomas E., and Olav M. Andersen. 2013. “Sorting Receptor SORLA – a Trafficking Path to Avoid Alzheimer Disease.” *Journal of Cell Science* 126 (13): 2751–60. https://doi.org/10.1242/jcs.125393.

Wu, Chun, and Joan-Emma Shea. 2013. “Structural Similarities and Differences between Amyloidogenic and Non-Amyloidogenic Islet Amyloid Polypeptide (IAPP) Sequences and Implications for the Dual Physiological and Pathological Activities of These Peptides.” Edited by Vijay S. Pande. *PLoS Computational Biology* 9 (8): e1003211. https://doi.org/10.1371/journal.pcbi.1003211.

Zraika, S., R. L. Hull, J. Udayasankar, K. Aston-Mourney, S. L. Subramanian, R. Kisilevsky, W. A. Szarek, and S. E. Kahn. 2009. “Oxidative Stress Is Induced by Islet Amyloid Formation and Time-Dependently Mediates Amyloid-Induced Beta Cell Apoptosis.” *Diabetologia* 52 (4): 626–35. https://doi.org/10.1007/s00125-008-1255-x.

Zraika, S., R. L. Hull, C. B. Verchere, A. Clark, K. J. Potter, P. E. Fraser, D. P. Raleigh, and S. E. Kahn. 2010. “Toxic Oligomers and Islet Beta Cell Death: Guilty by Association or Convicted by Circumstantial Evidence?” *Diabetologia* 53 (6): 1046–56. https://doi.org/10.1007/s00125-010-1671-6.

Zraika, Sakeneh, Kathryn Aston-Mourney, Peter Marek, Rebecca L. Hull, Pattie S. Green, Jayalakshmi Udayasankar, Shoba L. Subramanian, Daniel P. Raleigh, and Steven E. Kahn. 2010. “Neprilysin Impedes Islet Amyloid Formation by Inhibition of Fibril Formation Rather Than Peptide Degradation.” *Journal of Biological Chemistry* 285 (24): 18177–83. https://doi.org/10.1074/jbc.M109.082032.

Statutory Declaration

"I, Alexis Zi Le Shih, by personally signing this document in lieu of an oath, hereby affirm that I prepared the submitted dissertation on the topic 'The role of SORLA in islet amyloid polypeptide transport and islet amyloid deposition'/ 'Die Bedeutung von SORLA für den Transport von islet amyloid polypeptide und die Ablagerung von Amyloid in Langerhans-Inseln', independently and without the support of third parties, and that I used no other sources and aids than those stated.

All parts which are based on the publications or presentations of other authors, either in letter or in spirit, are specified as such in accordance with the citing guidelines. The sections on methodology (in particular regarding practical work, laboratory regulations, statistical processing) and results (in particular regarding figures, charts and tables) are exclusively my responsibility.

Furthermore, I declare that I have correctly marked all of the data, the analyses, and the conclusions generated from data obtained in collaboration with other persons, and that I have correctly marked my own contribution and the contributions of other persons (cf. declaration of contribution). I have correctly marked all texts or parts of texts that were generated in collaboration with other persons.

My contributions to any publications to this dissertation correspond to those stated in the below joint declaration made together with the supervisor. All publications created within the scope of the dissertation comply with the guidelines of the ICMJE (International Committee of Medical Journal Editors; http://www.icmje.org) on authorship. In addition, I declare that I shall comply with the regulations of Charité – Universitätsmedizin Berlin on ensuring good scientific practice.

I declare that I have not yet submitted this dissertation in identical or similar form to another Faculty.

The significance of this statutory declaration and the consequences of a false statutory declaration under criminal law (Sections 156, 161 of the German Criminal Code) are known to me."

_____ _____

Date Signature

Declaration of own contribution to the following publication

Alexis Zi Le Shih contributed the following to the below listed publication:

Publication 1:

Alexis Z.L. Shih, Yi-Chun Chen, Thilo Speckmann, Esben Søndergaard, Annette Schürmann, C. Bruce Verchere, and Thomas E. Willnow. 2022. “SORLA Mediates Endocytic Uptake of ProIAPP and Protects against Islet Amyloid Deposition.” Molecular Metabolism 65 (November): 101585. https://doi.org/10.1016/j.molmet.2022.101585.

Contribution:

In this publication, I contributed to the conception of the research question, which is to examine the role of SORLA in islet amyloid formation and regulation of IAPP handling. I generated mouse models used in Figures 2 – 4 and supplementary figures 1 – 3 . In Figures 1, 2, 4, 6, 7 and Supplementary figures 1, I performed immunostaining, confocal microscopy and image analysis. In figures 2, 5 and supplementary figure 2 - 3, I performed experiments, collected and analysed data. In figures 5A, 5B and 8, I created the illustrations with the licensed tool Biorender. In supplementary table 2, I collected samples and analysed gene expression results. I created all figures and tables, drafted the manuscript and addressed reviewers comments.

_____

Signature, date and stamp of first supervising university professor / lecturer

_____

Signature of doctoral candidate

Journal Summary List

Journal Data Filtered By: **Selected JCR Year: 2021** Selected Editions: SCIE;SSCI;AHCI;ESCI **Selected Categories: ENDOCRINOLOGY & METABOLISM**
Selected Category Schema: WOS
Total number: 147 Journals

Rank	Full Journal name	Total Citations	Journal Impact Factor	Eigenfactor Source
1	Nature Reviews Endocrinology	18,734	47.564	0.02824
2	Lancet Diabetes & Endocrinology	17,810	44.867	0.04579
3	Cell Metabolism	61,067	31.373	0.08630
4	ENDOCRINE REVIEWS	18,600	25.261	0.01203
5	Nature Metabolism	4,636	19.865	0.01410
6	DIABETES CARE	89,294	17.152	0.08506
7	METABOLISM-CLINICAL AND EXPERIMENTAL	20,930	13.934	0.01771
8	JOURNAL OF PINEAL RESEARCH	13,422	12.081	0.00692
9	Obesity Reviews	18,669	10.867	0.02021
10	TRENDS IN ENDOCRINOLOGY AND METABOLISM	13,168	10.586	0.01119
11	DIABETOLOGIA	40,193	10.460	0.03863
12	DIABETES	67,750	9.337	0.03524
13	REVIEWS IN ENDOCRINE & METABOLIC DISORDERS	4,204	9.306	0.00430
14	Obesity	25,762	9.298	0.02427
15	Cardiovascular Diabetology	10,971	8.949	0.01495
16	Biology of Sex Differences	2,974	8.811	0.00485
17	Molecular Metabolism	9,081	8.568	0.01808
18	FRONTIERS IN NEUROENDOCRINOLOGY	5,624	8.333	0.00458
19	DIABETES & METABOLISM	4,944	8.254	0.00462
20	DIABETES RESEARCH AND CLINICAL PRACTICE	21,344	8.180	0.02372
21	DIABETES-METABOLISM RESEARCH AND REVIEWS	8,321	8.128	0.00876
22	FREE RADICAL BIOLOGY AND MEDICINE	55,523	8.101	0.02824
23	Current Obesity Reports	3,004	8.023	0.00444
24	ANTIOXIDANTS & REDOX SIGNALING	29,117	7.468	0.01390
25	Diabetes Technology & Therapeutics	6,783	7.337	0.01127
26	JOURNAL OF CEREBRAL BLOOD FLOW AND METABOLISM	24,048	6.960	0.01940
27	EUROPEAN JOURNAL OF ENDOCRINOLOGY	18,397	6.558	0.01631
28	THYROID	17,554	6.506	0.01761
29	BIOFACTORS	5,614	6.438	0.00307
30	DIABETES OBESITY & METABOLISM	15,119	6.408	0.02726

Original Article

MOLECULAR METABOLISM

SORLA mediates endocytic uptake of proIAPP and protects against islet amyloid deposition

Alexis Z.L. Shih [1,2,*], Yi-Chun Chen [3,4,5], Thilo Speckmann [6,7], Esben Søndergaard [8], Annette Schürmann [6,7], C. Bruce Verchere [3,4,5], Thomas E. Willnow [1,2,9,]**

ABSTRACT

Objective: Sorting-related receptor with type A repeats (SORLA) is a neuronal sorting receptor that prevents accumulation of amyloid-beta peptides, the main constituent of senile plaques in Alzheimer disease. Recent transcriptomic studies show that SORLA transcripts are also found in beta cells of pancreatic islets, yet the role of SORLA in islets is unknown. Based on its protective role in reducing the amyloid burden in the brain, we hypothesized that SORLA has a similar function in the pancreas via regulation of amyloid formation from islet amyloid polypeptide (IAPP).

Methods: We generated human IAPP transgenic mice lacking SORLA (hIAPP:SORLA KO) to assess the consequences of receptor deficiency for islet histopathology and function *in vivo*. Using both primary islet cells and cell lines, we further investigated the molecular mechanisms whereby SORLA controls the cellular metabolism and accumulation of IAPP.

Results: Loss of SORLA activity in hIAPP:SORLA KO resulted in a significant increase in islet amyloid deposits and associated islet cell death compared to hIAPP:SORLA WT animals. Aggravated islet amyloid deposition was observed in mice fed a normal chow diet, not requiring high-fat diet feeding typically needed to induce islet amyloidosis in mouse models. *In vitro* studies showed that SORLA binds to and mediates the endocytic uptake of proIAPP, but not mature IAPP, delivering the propeptide to an endolysosomal fate.

Conclusions: SORLA functions as a proIAPP-specific clearance receptor, protecting against islet amyloid deposition and associated cell death caused by IAPP.

Keywords Beta cell; Endocytosis; IAPP; Islet amyloid; SORLA; VPS10P domain receptor

1. INTRODUCTION

Islet amyloid polypeptide (IAPP or amylin) is a peptide hormone secreted together with insulin by beta cells in the pancreatic islets of Langerhans. IAPP is synthesized as a 67 amino acid precursor ($proIAPP_{1-67}$) with two propeptide regions extended at its N- and C-terminus. The majority of $proIAPP_{1-67}$ and its partially processed intermediate $proIAPP_{1-48}$ are further processed and modified in secretory granules to yield the 37 amino acid mature IAPP [1,2]. IAPP contributes to energy homeostasis through mediating satiety, delaying gastric emptying, and modulating insulin secretion [3,4]. Human IAPP (hIAPP) is amyloidogenic and susceptible to aggregation into toxic oligomers and insoluble islet amyloid, a pathological feature of type 2 diabetes [5,6]. Impaired processing, overproduction, or impaired catabolism of IAPP may promote such amyloid deposition in the islet [7,8]. However, the regulation of IAPP production and turnover, which underlies islet amyloid formation, remains incompletely understood.

Similar to type 2 diabetes, accumulation of amyloid plaques is a pathological hallmark in Alzheimer disease (AD) [9]. The amyloidogenic agent in AD is amyloid-beta peptide (Aβ), a proteolytic product of the amyloid precursor protein (APP). Accumulation of Aβ in the brain is controlled by SORLA (sorting protein-related receptor containing LDLR class A repeats), a type I transmembrane receptor and major AD risk gene [10–12]. SORLA reduces overall Aβ burden via two mechanisms. Acting as an intracellular sorting receptor for APP, it moves the precursor from endosomal compartments to the Golgi to prevent proteolytic breakdown to Aβ in endosomes [10,13]. In addition, it sorts newly produced Aβ to lysosomes for catabolism, further reducing Aβ build-up in the brain parenchyma [14,15]. In line with a central role for SORLA in brain amyloidosis, genetic variants in its gene, *SORL1*, have been associated with sporadic [11,12] and familial [16] forms of AD.

[1]Max-Delbrück-Center for Molecular Medicine, Berlin, Germany [2]Charité — Universitätsmedizin Berlin, Corporate Member of Freie Universität Berlin and Humboldt-Universität zu Berlin, Berlin, Germany [3]BC Children's Hospital Research Institute and Centre for Molecular Medicine and Therapeutics, Vancouver, BC, Canada [4]Department of Pathology & Laboratory Medicine, University of British Columbia, Vancouver, BC, Canada [5]Department of Surgery, University of British Columbia, Vancouver, BC, Canada [6]Department of Experimental Diabetology, German Institute of Human Nutrition Potsdam-Rehbruecke (DIfE), Nuthetal, Germany [7]German Center for Diabetes Research (DZD), München-Neuherberg, Germany [8]Steno Diabetes Center Aarhus, Aarhus University Hospital, Aarhus, Denmark [9]Department of Biomedicine, Aarhus University, Aarhus, Denmark

*Corresponding author. Max-Delbrück-Center for Molecular Medicine, Robert-Rössle-Str. 10, D-13125 Berlin, Germany. E-mail: Alexis.Shih@mdc-berlin.de (A.Z.L. Shih).

**Corresponding author. Max-Delbrück-Center for Molecular Medicine, Robert-Rössle-Str. 10, D-13125 Berlin, Germany. E-mail: willnow@mdc-berlin.de (T.E. Willnow).

Received June 7, 2022 • Revision received July 27, 2022 • Accepted August 25, 2022 • Available online 30 August 2022

https://doi.org/10.1016/j.molmet.2022.101585

Abbreviations

Aβ	Amyloid-beta peptide
AD	Alzheimer disease
APP	Amyloid precursor protein
CPE	Carboxypeptidase E
GSIS	Glucose-stimulated insulin secretion
GTT	Glucose tolerance test
HFD	High-fat diet
hIAPP	Human islet amyloid polypeptide
IP	Intraperitoneal
KO	Knockout
ND	Normal diet
PAM	Peptidyl-glycine alpha-amidating monooxygenase
PC	Prohormone convertase
SORLA	Sorting protein-related receptor containing LDLR class A repeats
ThioS	Thioflavin S
VPS10P	Vacuolar protein sorting 10 protein
WT	Wildtype

On top of the relevance of SORLA for amyloidogenic processes in neurons, recent single-cell RNA sequencing analyses of human and mouse islets uncovered SORLA expression in pancreatic beta cells [17–19]. Because SORLA binds to a broad range of ligands [20], we hypothesized that this receptor may play a role in beta cell physiology; specifically, in regulating IAPP handling and islet amyloid formation. In this study, we tested if and how SORLA controls IAPP trafficking and processing, islet amyloid deposition, and glucose homeostasis. We examined the expression and subcellular localization of SORLA in islet beta cells and its interaction with pro- and mature forms of IAPP. Furthermore, we investigated the consequences of receptor deficiency for islet amyloid formation, beta cell function, and overall metabolic characteristics in mice expressing hIAPP, an animal model of islet amyloid deposition.

2. MATERIALS AND METHODS

2.1. Animal studies

Human IAPP transgenic (FVB/N-Tg(Ins2-IAPP)RHFSoel/J) mice were purchased from the Jackson Laboratory (#08232). Global SORLA knockout mice (*Sorl1*$^{-/-}$) on a C57BL/6J background were generated previously [10]. SORLA WT and KO mice expressing *hIAPP* transgene, as well as hIAPP-null littermates, were generated by crossing hIAPP transgenic males with *Sorl1*$^{+/+}$ or *Sorl1*$^{-/-}$ females, respectively. Since islet amyloid deposition is primarily observed in male hIAPP transgenic mice and rarely found in females [21], all experiments were conducted in male mice. Animals were housed in a facility with controlled environment, 12 h light/dark cycle, and fed a normal chow diet (4.5% crude fat) or a HFD (60% crude fat; #E15741-34; Ssniff, Germany). All animal experiments were performed according to protocols approved by the Berlin State Office for Health and Social Affairs (LAGESO, Berlin, Germany).

2.2. Intraperitoneal glucose tolerance test (IPGTT)

Prior to IPGTT, mice were fasted for 16 h (17:00—09:00). The next morning, mice were weighed and fasting blood glucose was measured in blood collected from the tail tip. For ND-fed mice, a glucose dose of 2.0 g/kg body weight was administered, while a lower glucose dose of 0.75 g/kg body weight was administered to HFD-fed mice to ensure that all glucose measurements fall within the detection range of the glucometer throughout the experiment. Blood glucose was measured at regular intervals from the tail tip.

2.3. Glucose-stimulated insulin secretion (GSIS) *in vivo*

Prior to *in vivo* GSIS, mice were fasted for 16 h (17:00—09:00). The next morning, mice were weighed and 100 μl of fasted blood was collected from the submandibular vein into EDTA-treated blood collection tube. For both ND- and HFD-fed mice, a glucose dose of 2.0 g/kg body weight was administered intraperitoneally. Insulin release was measured in blood collected from the other submandibular vein 30 min after glucose stimulation. Plasma was separated by centrifugation at 1500 x g for 10 min at 4 °C, and stored at −80 °C until further measurement by ELISA.

2.4. Islet isolation, dispersion and culture

Animals were sacrificed by cervical dislocation and the pancreas perfused with 2 ml of 900 U/ml collagenase (Sigma Aldrich, USA) in HBSS (Life Technologies, USA). After surgical removal of the pancreas, it was digested in 2 ml of collagenase solution at 37 °C for 13 min, followed by manual shaking for 60—90 s, two rounds of washing, and passing through a 70 μm filter. Islets were hand-picked and cultured in RPMI 1640 (PAN-Biotech, Germany) supplemented with 2 mM L-Glutamine, 100 U/ml penicillin, 100 mg/ml streptomycin, and 10% FBS (Gibco 10270-106). Islets were recovered overnight prior to secretion assays or dispersion. For subcellular localization studies, islets were dispersed into single cells by pipetting in 0.05% trypsin—EDTA (Gibco, USA) solution for 1 min, seeded onto uncoated glass coverslips, and cultured for six days prior to fixation.

2.5. Staining of tissues or cells for confocal microscopy

Mouse pancreata were harvested and fixed in 4% (wt/vol) paraformaldehyde overnight at 4 °C, subjected to a sucrose gradient with stepwise increase from 15% to 30% (wt/vol), and frozen at −80 °C in cryomolds containing OCT compound. Tissue sections (10 μm) were rehydrated in 0.3% Triton X-100 in PBS-T for 15 min, followed by antigen retrieval in 10 mM citrate buffer with 0.05% Tween-20 (pH 6.0) at 95 °C for 10 min. Human pancreas biopsies from three anonymized, healthy individuals were provided as paraffin-embedded sections by Assoc. Prof. Søndergaard (Steno Diabetes Center Aarhus). The human pancreas biopsies were obtained from two women undergoing surgery for endometrial cancer and from one man with resection of pancreas without any signs of malignancy or other disease. For dispersed mouse islet cells, cells were fixed in 4% (wt/vol) paraformaldehyde for 10 min at room temperature, then permeabilized in 0.3% Triton X-100 with 0.1% BSA in PBS-T (pH 7.4) for 10 min at room temperature. Both pancreatic tissues and islet cells were blocked in 3% BSA in PBS-T overnight at 4 °C, followed by sequential incubation in primary and secondary antibodies (Suppl. Table 1) for 2 and 1 h, respectively, at room temperature. Nuclei were visualized via DAPI staining. Images from a single z-plane were acquired using a Zeiss LSM 700 confocal microscope (10X objective for tissue samples; 63X objective for dispersed islet cells).

Amyloid staining: Islet amyloid was assessed based on thioflavin S (Sigma-Aldrich, USA) staining, as previously described [8]. Islet amyloid prevalence was quantified as the percentage of islets containing amyloid. Islet amyloid severity was quantified as percentage of ThioS-positive area over total islet area. Morphological

analyses were performed in CellProfiler (Cambridge, MA, USA). Both islet amyloid prevalence and severity were assessed based on the mean value of 22–30 islets per mouse.

TUNEL staining: Cell death was measured via terminal deoxynucleotidyl transferase dUTP nick end labeling (TUNEL) staining according to manufacturer instructions (Roche Applied Science, Germany). The percentage of TUNEL positive islet cells per mouse was determined as the mean of 22 to 30 islets, with an average of 259 ± 16 cells analyzed per islet.

Proximity ligation assay (PLA): PLA was performed on dispersed islet cells to assess close interaction (<40 nm) between endogenous SORLA and mouse IAPP (Peninsula Laboratories T-4145) or human IAPP (Peninsula Laboratories T-4149) in beta cells. The experiment was performed according to manufacturer's protocol (Sigma-Aldrich, USA). Beta cells and early endosomes were identified through immunostaining for insulin and Rab4, respectively.

2.6. Islet perifusion

The assay was performed using a PERI 4.2 machine (Biorep Technologies, USA). Groups of 30 islets were continuously perifused with KRBH buffer (129 mM NaCl, 4.8 mM KCl, 1.2 mM $MgSO_4$, 1.2 mM KH_2PO_4, 5 mM $NaHCO_3$, 2.5 mM $CaCl_2$, 10 mM HEPES and 0.25% BSA, at pH 7.4) with the indicated glucose concentration at a flow rate of 100 μl/min. Initially, islets were equilibrated in 11 mM glucose KRBH for 60 min (flow-through discarded), followed by sequential incubation (flow-through collected in 96-well plate) with 11 mM glucose (18 min), 1.67 mM glucose (60 min), 16.7 mM glucose (34 min), 1.67 mM glucose (30 min), and 30 mM KCl in 1.67 mM glucose KRBH (10 min). At the end of the assay, islets were retrieved and lysed in TE buffer (10 mM Tris–HCl, 1 mM EDTA and 1% Triton X-100) to measure DNA content (Quant-iT Picogreen DNA kit, Thermo Fisher Scientific, USA). Insulin levels were measured by ELISA and normalized to DNA content.

2.7. Acid ethanol extraction of insulin content in pancreas and islets

Total pancreas was excised, weighed, and placed in 5 ml of ice-cold acid ethanol solution (0.18 M HCl in 70% ethanol). Pancreatic tissues were mechanically homogenized and incubated in acid ethanol at 4 °C overnight. For insulin extraction from islets, 30 islets per pancreas sample were incubated in 30 μl of ice-cold acid ethanol and vortexed for 1 min. The homogenate was incubated on ice for 3 h with additional vortex every 30 min. The supernatants of pancreas and islet homogenates were collected by centrifugation at 2000 rpm for 15 min at 4 °C and stored at −80 °C until determination of insulin content by ELISA. The pancreatic insulin content was normalized to total pancreas weight, while islet insulin content was normalized to protein concentration as determined by bicinchoninic acid assay.

2.8. ELISAs

Insulin was measured using the Ultra Sensitive Mouse Insulin ELISA kit (Crystal Chem, USA). Human $proIAPP_{1-48}$ and mature IAPP were measured via an in-house ELISA as described [22].

2.9. Microscale thermophoresis (MST)

Mouse sequence of $proIAPP_{1-70}$, $proIAPP_{1-51}$ and mature amidated IAPP peptides (NCBI Reference Sequence: NP_034621) were synthesized commercially (Biosyntan, Germany). Peptides were dissolved in PBS and stored at −80 °C prior to binding assays. Recombinant His-tagged SORLA ectodomain (including residue 728-1526) was previously purified [10]. For microscale thermophoresis (MST), SORLA ectodomain was fluorescently labeled using the Protein Labeling Kit RED-NHS (NanoTemper Technologies, Germany). Concentrations of the target molecule (labeled SORLA ectodomain in PBS with 0.05% Tween 20, pH 7.4) was kept constant (3 nM), while the concentration of the non-labeled binding ligand (IAPP peptides) was serially titrated from 7.6 nM to 250 μM. K_d was derived using MO.Affinity Analysis software version 2.3 (NanoTemper Technologies, Germany).

2.10. Cell culture

Neuroblastoma SH-SY5Y cells (ATCC CRL-2266) were cultured in DMEM/F12 media (Gibco, USA) supplemented with 10% FBS, 1% NEAA, 100 U/ml penicillin and 100 mg/ml streptomycin. SH-SY5Y cells stably overexpressing SORLA were previously generated [15] and maintained in the presence of 90 μg/ml zeocin (Invitrogen, USA). Cells were routinely tested for mycoplasma infection.

2.11. IAPP peptide uptake assay

Synthetic mouse (pro)IAPP peptides were the same as described above. Synthetic human $A\beta_{1-40}$ peptides were purchased from Bachem, Germany (#4095737). SH-SY5Y parental cells and SH-SY5Y cells stably overexpressing SORLA were seeded onto uncoated glass coverslips one day prior to the peptide uptake assay. Cells were incubated in serum-free medium for 30 min prior to treatment with 20 μM (pro)IAPP for 30 min. Simultaneous treatment with 100 μM dynasore (Cayman Chemical, USA) was used to examine the role of clathrin-mediated endocytosis. Cells were fixed in 4% (wt/vol) paraformaldehyde and immunofluorescence staining was performed to visualize internalized peptides, SORLA, and subcellular organelles. Lysosomes were labeled by preincubating cells with 500 nM LysoTracker Deep Red (Thermo Fisher Scientific, USA) in normal growth media for 1 h prior to the uptake assay.

2.12. Statistical analysis

Statistical analyses were performed using GraphPad Prism 6.0 (GraphPad Software, USA). Normal distribution of data was tested with the D'Agostino-Pearson normality test. Data with sample size too small for normality test ($n < 8$) were analyzed by unpaired t-test. Comparisons of results between groups were analyzed using Student's t-test, one-way or two-way ANOVA. Data are presented as mean ± SEM.

3. RESULTS

3.1. SORLA is expressed in islet beta cells

First, we validated existing transcriptome data on SORLA expression in islets [17–19] by immunohistology on mouse and human pancreatic sections. In mouse islets, SORLA was mainly expressed in insulin-producing beta cells, but to some extent also in glucagon-producing alpha cells, somatostatin-producing delta cells and pancreatic polypeptide (PPY)-producing PP cells (Figure 1A). Expression of SORLA was lost in islets of mice carrying a targeted global disruption of *Sorl1*, hereinafter referred to as SORLA knockout (KO) (Figure 1B) [10]. In human islets, SORLA was predominantly expressed in beta cells and not found in alpha cells (Figure 1C). Overall, these data confirm SORLA expression in both murine and human beta cells.

3.2. Loss of SORLA increases islet amyloid prevalence and severity *in vivo*

To study the impact of SORLA activity on islet amyloid formation, we crossed SORLA KO mice (on a C57BL/6J background) with a

analyses were performed in CellProfiler (Cambridge, MA, USA). Both islet amyloid prevalence and severity were assessed based on the mean value of 22–30 islets per mouse.

TUNEL staining: Cell death was measured via terminal deoxynucleotidyl transferase dUTP nick end labeling (TUNEL) staining according to manufacturer instructions (Roche Applied Science, Germany). The percentage of TUNEL positive islet cells per mouse was determined as the mean of 22 to 30 islets, with an average of 259 ± 16 cells analyzed per islet.

Proximity ligation assay (PLA): PLA was performed on dispersed islet cells to assess close interaction (<40 nm) between endogenous SORLA and mouse IAPP (Peninsula Laboratories T-4145) or human IAPP (Peninsula Laboratories T-4149) in beta cells. The experiment was performed according to manufacturer's protocol (Sigma-Aldrich, USA). Beta cells and early endosomes were identified through immunostaining for insulin and Rab4, respectively.

2.6. Islet perifusion

The assay was performed using a PERI 4.2 machine (Biorep Technologies, USA). Groups of 30 islets were continuously perifused with KRBH buffer (129 mM NaCl, 4.8 mM KCl, 1.2 mM $MgSO_4$, 1.2 mM KH_2PO_4, 5 mM $NaHCO_3$, 2.5 mM $CaCl_2$, 10 mM HEPES and 0.25% BSA, at pH 7.4) with the indicated glucose concentration at a flow rate of 100 μl/min. Initially, islets were equilibrated in 11 mM glucose KRBH for 60 min (flow-through discarded), followed by sequential incubation (flow-through collected in 96-well plate) with 11 mM glucose (18 min), 1.67 mM glucose (60 min), 16.7 mM glucose (34 min), 1.67 mM glucose (30 min), and 30 mM KCl in 1.67 mM glucose KRBH (10 min). At the end of the assay, islets were retrieved and lysed in TE buffer (10 mM Tris–HCl, 1 mM EDTA and 1% Triton X-100) to measure DNA content (Quant-iT Picogreen DNA kit, Thermo Fisher Scientific, USA). Insulin levels were measured by ELISA and normalized to DNA content.

2.7. Acid ethanol extraction of insulin content in pancreas and islets

Total pancreas was excised, weighed, and placed in 5 ml of ice-cold acid ethanol solution (0.18 M HCl in 70% ethanol). Pancreatic tissues were mechanically homogenized and incubated in acid ethanol at 4 °C overnight. For insulin extraction from islets, 30 islets per pancreas sample were incubated in 30 μl of ice-cold acid ethanol and vortexed for 1 min. The homogenate was incubated on ice for 3 h with additional vortex every 30 min. The supernatants of pancreas and islet homogenates were collected by centrifugation at 2000 rpm for 15 min at 4 °C and stored at −80 °C until determination of insulin content by ELISA. The pancreatic insulin content was normalized to total pancreas weight, while islet insulin content was normalized to protein concentration as determined by bicinchoninic acid assay.

2.8. ELISAs

Insulin was measured using the Ultra Sensitive Mouse Insulin ELISA kit (Crystal Chem, USA). Human $proIAPP_{1-48}$ and mature IAPP were measured via an in-house ELISA as described [22].

2.9. Microscale thermophoresis (MST)

Mouse sequence of $proIAPP_{1-70}$, $proIAPP_{1-51}$ and mature amidated IAPP peptides (NCBI Reference Sequence: NP_034621) were synthesized commercially (Biosyntan, Germany). Peptides were dissolved in PBS and stored at −80 °C prior to binding assays. Recombinant His-tagged SORLA ectodomain (including residue 728-1526) was previously purified [10]. For microscale thermophoresis (MST), SORLA ectodomain was fluorescently labeled using the Protein Labeling Kit RED-NHS (NanoTemper Technologies, Germany). Concentrations of the target molecule (labeled SORLA ectodomain in PBS with 0.05% Tween 20, pH 7.4) was kept constant (3 nM), while the concentration of the non-labeled binding ligand (IAPP peptides) was serially titrated from 7.6 nM to 250 μM. K_d was derived using MO.Affinity Analysis software version 2.3 (NanoTemper Technologies, Germany).

2.10. Cell culture

Neuroblastoma SH-SY5Y cells (ATCC CRL-2266) were cultured in DMEM/F12 media (Gibco, USA) supplemented with 10% FBS, 1% NEAA, 100 U/ml penicillin and 100 mg/ml streptomycin. SH-SY5Y cells stably overexpressing SORLA were previously generated [15] and maintained in the presence of 90 μg/ml zeocin (Invitrogen, USA). Cells were routinely tested for mycoplasma infection.

2.11. IAPP peptide uptake assay

Synthetic mouse (pro)IAPP peptides were the same as described above. Synthetic human $A\beta_{1-40}$ peptides were purchased from Bachem, Germany (#4095737). SH-SY5Y parental cells and SH-SY5Y cells stably overexpressing SORLA were seeded onto uncoated glass coverslips one day prior to the peptide uptake assay. Cells were incubated in serum-free medium for 30 min prior to treatment with 20 μM (pro)IAPP for 30 min. Simultaneous treatment with 100 μM dynasore (Cayman Chemical, USA) was used to examine the role of clathrin-mediated endocytosis. Cells were fixed in 4% (wt/vol) paraformaldehyde and immunofluorescence staining was performed to visualize internalized peptides, SORLA, and subcellular organelles. Lysosomes were labeled by preincubating cells with 500 nM LysoTracker Deep Red (Thermo Fisher Scientific, USA) in normal growth media for 1 h prior to the uptake assay.

2.12. Statistical analysis

Statistical analyses were performed using GraphPad Prism 6.0 (GraphPad Software, USA). Normal distribution of data was tested with the D'Agostino-Pearson normality test. Data with sample size too small for normality test ($n < 8$) were analyzed by unpaired t-test. Comparisons of results between groups were analyzed using Student's t-test, one-way or two-way ANOVA. Data are presented as mean ± SEM.

3. RESULTS

3.1. SORLA is expressed in islet beta cells

First, we validated existing transcriptome data on SORLA expression in islets [17–19] by immunohistology on mouse and human pancreatic sections. In mouse islets, SORLA was mainly expressed in insulin-producing beta cells, but to some extent also in glucagon-producing alpha cells, somatostatin-producing delta cells and pancreatic polypeptide (PPY)-producing PP cells (Figure 1A). Expression of SORLA was lost in islets of mice carrying a targeted global disruption of *Sorl1*, hereinafter referred to as SORLA knockout (KO) (Figure 1B) [10]. In human islets, SORLA was predominantly expressed in beta cells and not found in alpha cells (Figure 1C). Overall, these data confirm SORLA expression in both murine and human beta cells.

3.2. Loss of SORLA increases islet amyloid prevalence and severity *in vivo*

To study the impact of SORLA activity on islet amyloid formation, we crossed SORLA KO mice (on a C57BL/6J background) with a

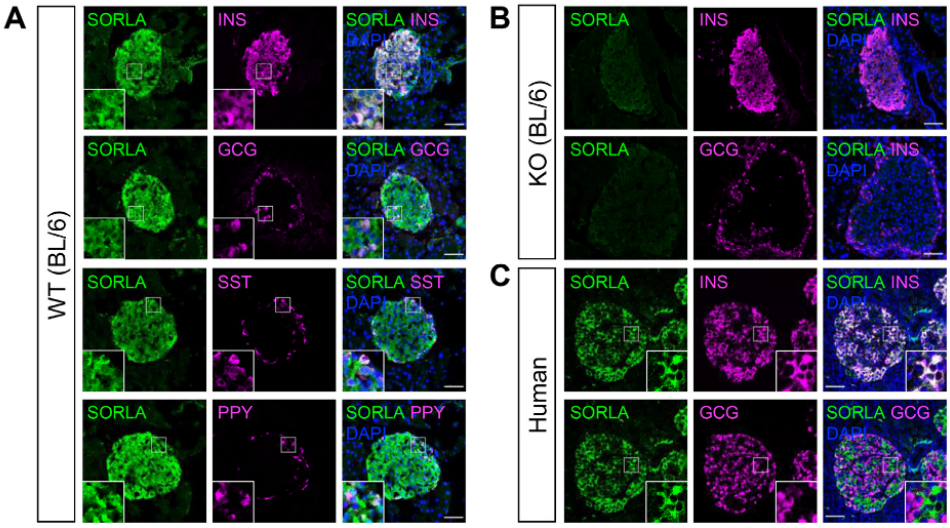

Figure 1: Expression of SORLA in murine and human pancreatic islets. (**A, B**) Immunofluorescence staining of pancreatic sections from (A) WT (BL/6) and (B) SORLA KO (BL/6) mice for SORLA (green), insulin (INS, magenta), glucagon (GCG, magenta), somatostatin (SST, magenta), and pancreatic polypeptide (PPY, magenta). Nuclei were counterstained with DAPI (blue). Prominent expression of SORLA is seen in WT but not SORLA KO islets. (**C**) Immunodetection of SORLA (green) and insulin or glucagon (magenta) on representative sections of human pancreatic biopsies from three non-diabetic patients. Single and merged channel configurations are shown. The insets depict higher magnifications of the areas indicated by white boxes in the overview images. Scale bars, 50 μm.

transgenic line expressing hIAPP under the control of the rat insulin II promoter (on an FVB/N background) [23,24]. Male mice hemizygous for the *hIAPP* transgene and genetically deficient for *Sorl1* (hIAPP:SORLA KO), as well as hIAPP-expressing control animals (hIAPP:SORLA WT) were selected for analysis. We also generated non-transgenic control groups (SORLA WT, SORLA KO) to assess the impact of SORLA deficiency on glucose homeostasis in the absence of the *hIAPP* transgene. In addition to age, dietary stress imposed by high-fat diet (HFD) feeding contributes to islet amyloid formation [25]. Therefore, we performed our studies in mice fed a normal chow diet (ND) or a HFD (60% crude fat) for 6 months, starting at 4 weeks of age. We first examined the effects of SORLA deficiency on islet amyloid deposition by staining pancreatic tissue sections from 7-month old hIAPP:SORLA WT and hIAPP:SORLA KO mice with thioflavin S (ThioS) (Figure 2A). Remarkably, the prevalence of islet amyloid deposition was significantly higher in hIAPP:SORLA KO mice compared to WT mice on ND (WT 17.3 $\pm$ 4.7% vs KO 70.3 $\pm$ 9.7% amyloid containing islets, $p < 0.0001$) (Figure 2B). The protective effect of SORLA against islet amyloid prevalence was maintained under HFD (WT 44.2 $\pm$ 8.0% vs KO 71.8 $\pm$ 7.8% amyloid containing islets, $p = 0.035$) (Figure 2B). Furthermore, the severity of islet amyloid was significantly increased in ND-fed hIAPP:SORLA KO mice as compared to WT mice, which developed almost no islet amyloid (WT 0.56 $\pm$ 0.16% vs KO 6.9 $\pm$ 1.8% ThioS positive area of total islet area, $p = 0.019$) (Figure 2C). However, no significant difference in amyloid severity between hIAPP:SORLA WT and KO mice was seen when animals were fed a HFD (WT 2.9 $\pm$ 0.8% vs KO 7.8 $\pm$ 2.6% ThioS positive area of total islet area, $p = 0.0798$) (Figure 2C). This lack of SORLA protection under HFD may be attributed to an already aggravated amyloid burden in SORLA-deficient mice and blunted response under dietary stress.

Islet amyloid is associated with apoptotic cell death and impaired beta cell function. Accordingly, we performed TUNEL staining to test whether the increased islet amyloid observed in SORLA-deficient mice also correlated with increased cell death (Figure 2D). Compared to hIAPP:SORLA WTs, the percentage of apoptotic cells per islet was significantly higher in the ND-fed hIAPP:SORLA KO mice. Consistent with data on islet amyloid severity, this effect of SORLA-deficiency was not seen in mice fed a HFD (Figure 2E). Amyloid deposition as a possible cause of islet cell death in SORLA mutant mice was substantiated by linear regression analysis, which demonstrated a positive correlation between the severity of islet amyloid and extent of apoptosis (Figure 2F). We attempted to further identify the islet cell type mainly impacted by apoptosis by co-staining for insulin or glucagon. However, as exemplified in the representative images in Figure 2D, TUNEL positive cells mostly lack staining for these hormones, suggesting loss of hormone expression as a consequence of pathology. A lack of insulin expression was also observed in islet areas positive for ThioS amyloid staining (Figure 2A). Because hIAPP:SORLA KO islets showed a trend towards reduced insulin positive islet area (Figure S1B, ND: WT 59.2 $\pm$ 1.2% vs KO 56.3 $\pm$ 1.1%, $p = 0.10$), while glucagon positive islet area was comparable between SORLA genotypes (Figure S1C, ND: WT 11.3 $\pm$ 0.5% vs KO 11.3 $\pm$ 0.9%, $p = 0.97$), we suspect apoptotic cells are likely to be beta cells.

Although SORLA deficiency increased amyloid burden and cell death in ND-fed hIAPP-expressing mice, no significant differences in their overall islet morphology, including total islet area as well as alpha and beta cell areas were observed between genotypes (Figure S1A–C). To determine if compensatory upregulation of cell proliferation may account for the maintenance of islet tissue area in receptor-mutant mice, we examined cell proliferation by staining for proliferation marker Ki67

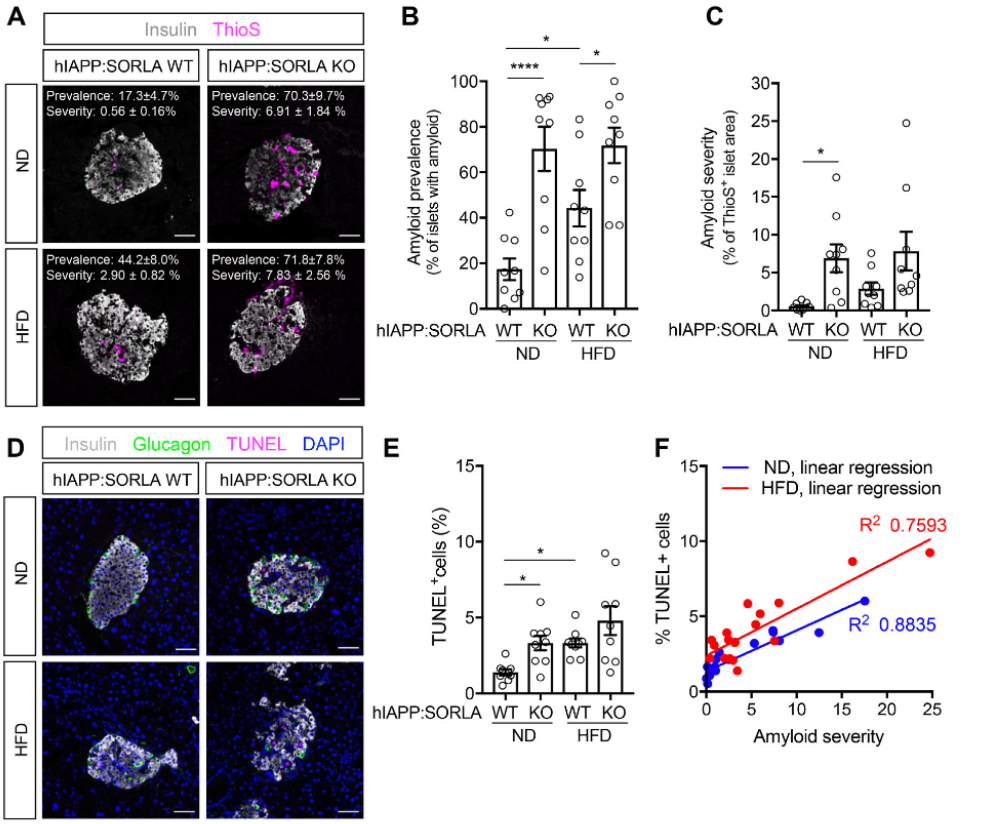

Figure 2: SORLA deficiency promotes islet amyloid deposition and islet cell death in hIAPP-expressing mice. Pancreatic sections from 33- to 35-weeks old mice of the indicated genotypes were examined for (A–C) islet amyloid deposition and (D, E) cell death ($n = 9$ mice per genotype, 20–30 islets per mouse). Animals were fed a normal chow diet (ND) or a high-fat diet (HFD) for 6 months. Scale bars, 50 μm. (**A**) Islet amyloid was assessed by staining with thioflavin S (ThioS, magenta) and immunostaining for insulin (white). Quantifications of (**B**) amyloid prevalence (percentage of islets with amyloid) and (**C**) amyloid severity (percentage of ThioS$^+$ amyloid area per islet area) on replicate pancreatic sections as exemplified in panel (A). (**D**) Apoptotic cell death was assessed by TUNEL staining (magenta). Sections were also immunostained for insulin (white) and glucagon (green). Nuclei were counterstained with DAPI (blue). (**E**) Quantification of the percentage of TUNEL$^+$ cell per islet on replicate pancreatic sections as exemplified in (D). **(F)** Linear regression analyses documented a positive correlation of islet amyloid severity with apoptotic cell death in islets from hIAPP-expressing mice ($n = 18$). Data are shown as mean ± SEM. Statistical significance of differences was determined by two-way ANOVA with post hoc test. $^*p < 0.05$, $^{****}p < 0.0001$.

(Figure S1D). Overall, few proliferative cells were observed in islets with numbers remaining comparable in ND-fed hIAPP:SORLA WT and KO mice (Figure S1E).

Together, these findings indicate that hIAPP:SORLA KO mice at 7 months of age likely represent an early stage of islet amyloid formation towards a trajectory of severe islet pathology.

3.3. Glucose metabolism and beta cell function of hIAPP-expressing SORLA KO mice

In addition to histological assessments of islet amyloid burden, we also monitored the metabolic consequences of SORLA deficiency in both hIAPP-transgenic and non-transgenic mice over time. Since the rat insulin II promoter used to drive beta cell expression of the *hIAPP* transgene was reported to also induce transgene expression in the hypothalamus [26], we examined whether such undesirable expression of *hIAPP* in the brain was present in our mouse models using qPCR. Gene expression analysis demonstrated robust expression of *hIAPP* in islets of hIAPP-transgenic mice. However, no *hIAPP* transcripts were detectable in the hypothalamus or brain cortex of these animals (Suppl. Table 2). This data ensured that metabolic characterizations in our models were not confounded by off-target expression of *hIAPP* in the brain.

At 30 weeks of age, hIAPP:SORLA KO mice on a ND grew slightly heavier than hIAPP:SORLA WT animals (Figure 3A, WT 37.4 ± 1.2 g vs KO 41.8 ± 1.6 g, p = 0.03). However, SORLA deficiency did not impact fasting blood glucose levels, regardless of *hIAPP* transgene expression (Figure 3B). Expression of hIAPP resulted in impaired glucose tolerance when compared with non-transgenic controls (Figure 3C), while SORLA KO animals showed normal glucose tolerance compared to WT controls (Figure 3C). Additionally, we determined

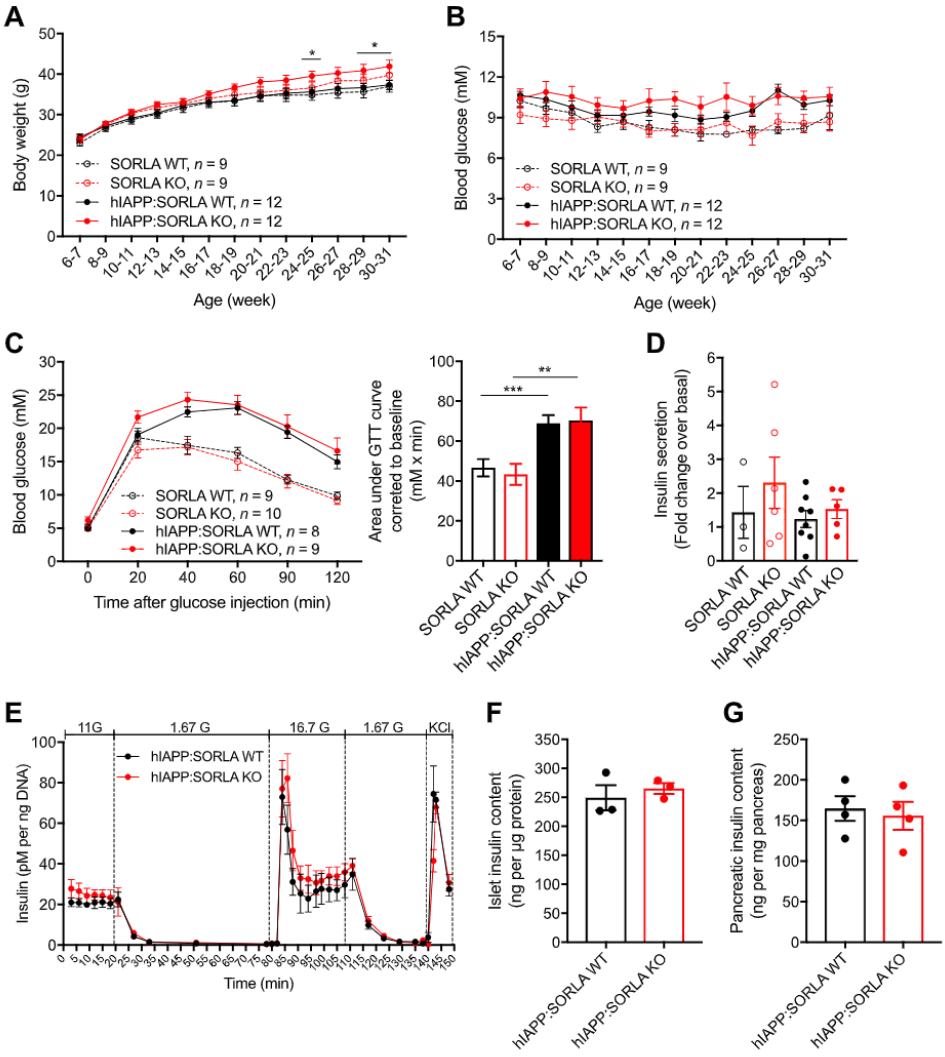

Figure 3: Metabolic characterization and beta cell function of hIAPP-expressing wildtype and SORLA-deficient mice on a normal chow diet. (**A and B**) Bi-weekly (A) body weight and (B) 6 h fasting blood glucose measurements of mice of the indicated genotypes. **(C)** Glucose tolerance test (GTT) performed in 30- to 32-weeks old mice after a 16 h fast via intraperitoneal glucose injection (2 g/kg). Response to glucose clearance was quantified based on area under the curve. **(D)** Glucose-stimulated insulin secretion (GSIS) was assessed in 31- to 33-weeks old mice of the indicated genotypes. A glucose dose of 2 g/kg was administered intraperitoneally after a 16 h fast. Data are represented as fold change in insulin secretion at 30 min post-glucose injection compared to basal levels. **(E)** Dynamic GSIS was tested on perifused islets from 31- to 33-weeks old hIAPP-expressing SORLA WT or KO mice ($n = 3$ mice per genotype, with technical duplicates). **(F and G)** Quantifications of insulin content in (F) isolated islets (n = 3) and (G) whole pancreas (n = 4) of hIAPP-expressing SORLA WT or KO mice. Data are shown as mean ± SEM. Statistical significance of differences (A, C) was determined by unpaired Student's t-test. $^{**}p < 0.01$, $^{***}p < 0.001$.

the effect of SORLA deficiency on beta cell function by measuring glucose-stimulated insulin secretion (GSIS) in mice (Figure 3D) and isolated islets (Figure 3E). The fold change in insulin secretion upon intraperitoneal glucose administration was similar between SORLA genotypes (Figure 3D). Similarly, SORLA deficiency did not significantly impact glucose- or KCl-stimulated insulin secretion in perifusion experiments of islets from hIAPP-expressing mice (Figure 3E). Furthermore, there were no significant differences in insulin content in both isolated islets (Figure 3F) nor pancreas (Figure 3G) between SORLA genotypes.

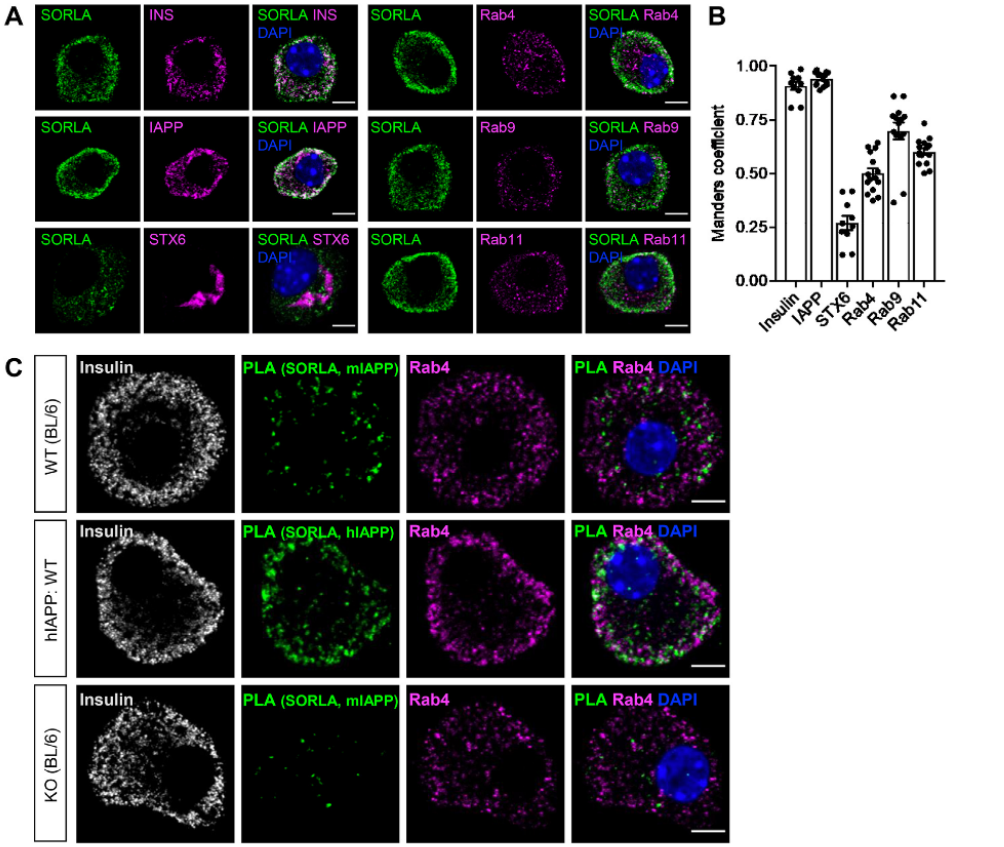

Figure 4: SORLA co-localizes with IAPP to the endocytic compartment of islet beta cells. (A) Dispersed islet cells from WT(BL/6) mice were immunostained for SORLA (green) and the following cell compartment markers (magenta): insulin, INS or IAPP (secretory vesicles), syntaxin-6 (STX6; *trans*-Golgi), Rab4 (early endosomes), Rab9 (late endosomes), or Rab11 (recycling endosomes). Nuclei were counterstained with DAPI. Single and merged channel configurations are shown. Scale bars, 5 μm. **(B)** Degree of co-localization between SORLA and each compartment marker was quantified by Manders' co-localization coefficient ($n = 10-15$ cells). **(C)** Proximity ligation assay detected close proximity of SORLA and mouse or human IAPP (green) in dispersed islet cells from WT(BL/6) or hIAPP:SORLA WT mice. Cells were additionally immunostained for insulin (white), Rab4 (magenta), and nuclei counterstained with DAPI (blue). Single as well as merged channel configurations are shown. Scale bars, 5 μm. Data are shown as mean ± SEM.

To further determine if SORLA promotes the development of diabetes (dependent or independent of hIAPP), we challenged mice with HFD for an extended period of 6 months starting at 4 weeks of age. SORLA-deficient mice also grew heavier on HFD compared to their WT littermates (Figure S2A). Yet, similar to ND-fed mice, SORLA-deficient animals and their WT littermates on HFD had comparable fasting blood glucose levels (Figure S2B). At 30–32 weeks of age, hIAPP:SORLA KO mice trended to show signs of impaired glucose tolerance, but this finding did not reach statistical significance (Figure S2C). We suspect this slightly impaired glucose tolerance to be attributed to their increased body weight, as there were no observable differences in *in vivo* glucose-stimulated insulin secretion when compared to hIAPP:SORLA WT mice (Figure S2D).

Taken together, our *in vivo* data demonstrated that loss of SORLA promotes islet amyloid burden and islet cell loss without overt impact on blood glucose homeostasis. This defect was observed in normal chow-fed mice and did not require any additional dietary stressor. These findings suggest a possible role for SORLA in regulating amyloid development under physiological conditions and early stages of diabetes pathology.

3.4. Loss of SORLA does not alter proIAPP processing

Next, we explored the molecular mechanism whereby SORLA controls IAPP handling and islet amyloid deposition. Since impaired processing of proIAPP has been implicated in islet amyloid formation [1,7,27], we initially tested whether SORLA may function as an intracellular sorting receptor regulating IAPP maturation in islet beta cells, similar to its function in sorting APP in neurons [10,15]. Accordingly, we measured fasting plasma levels of proh$IAPP_{1-48}$ and mature hIAPP in our mouse models by ELISA and calculated the ratio of pro- to mature hIAPP as an

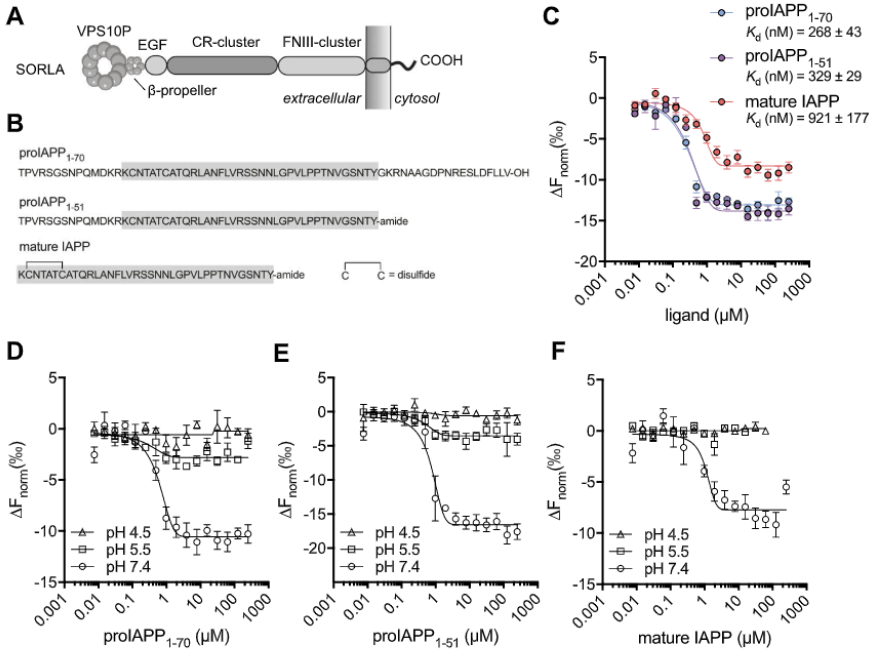

Figure 5: SORLA preferentially binds proIAPP in a pH-dependent manner. (A) Structural domains of SORLA, including vacuolar protein sorting 10 protein (VPS10P) domain, β-propeller, epidermal growth factor (EGF) repeats, fibronectin type III (FNIII) domain, and clusters of complement-type repeats (CR). **(B)** Amino acid sequences of murine proIAPP$_{1-70}$, proIAPP$_{1-51}$, and mature IAPP peptides. **(C)** Binding characteristics between the ectodomain of SORLA and murine IAPP peptides. The His-tagged ectodomain of human SORLA was recombinantly produced in HEK293-EBNA cells and purified using Ni^{2+} affinity chromatography [10]. Binding of different forms of IAPP peptide to the ectodomain of SORLA was determined by microscale thermophoresis (MST) at pH 7.4. The concentration of the fluorescently-labeled SORLA ectodomain was kept constant (3 nM), while non-labeled IAPP was serially titrated from 7.6 nM–250 μM. The change in thermophoresis is expressed as fluorescence intensity normalized to the lowest concentration of labeled IAPP ligand (y-axis = ΔF_{norm}(‰0)). Average K_d was derived from at least three independent experiments. Data are shown as mean ± SEM. **(D–F)** Binding of (D) proIAPP$_{1-70}$, (E) proIAPP$_{1-51}$, and (F) mature IAPP to the SORLA ectodomain was tested by MST at pH 4.5, 5.5, and 7.4 as detailed in (C).

indicator of processing efficiency. Both hIAPP-expressing SORLA WT and KO mice had similar levels of mature hIAPP, prohIAPP$_{1-48}$, and ratio of pro- to mature hIAPP, regardless of ND (Figure S3A–C) or HFD (Figure S3D–F) feeding. To further validate these *in vivo* results, we measured levels of secreted mature hIAPP and prohIAPP$_{1-48}$ from isolated islets in standard glucose culture (11 mM), and following low (1.67 mM) or high glucose (16.7 mM) conditions (Figure S3G). No significant differences in the amounts or ratios of secreted mature hIAPP and prohIAPP$_{1-48}$, (Figure S3H–J), nor in total islet content of mature and prohIAPP$_{1-48}$ (Figure S3K, L), were noted in SORLA genotypes across all conditions. These data suggest that SORLA does not impact proIAPP processing, neither directly nor indirectly.

3.5. SORLA is a receptor for soluble IAPP

Prior studies in various cell types have shown that SORLA mainly localizes to the Golgi, cell surface, and endosomes, in line with its function in sorting cargo between plasma membrane, secretory and endocytic compartments [28]. We tested if SORLA localizes to similar subcellular compartments in beta cells by immunostaining for SORLA and organelle markers in dispersed islet cells from WT (BL/6) mice (Figure 4A). Quantification of double-immunostained cells using Manders' co-localization coefficient showed that SORLA most highly co-localized with secretory granule markers (insulin and IAPP); moderately with early (Rab4), late (Rab9), and recycling endosomes (Rab11); and to a lesser extent with the *trans*-Golgi network (STX6) (Figure 4B). We performed proximity ligation assays (PLA) to substantiate close spatial proximity of SORLA with murine IAPP in any of these cell compartments in primary islet beta cells. In these studies, PLA signals were observed distinctly around the cell periphery and in the vicinity of the early endosome marker Rab4 (Figure 4C, top panels). To ascertain that SORLA interacts similarly with murine and human IAPP, we repeated the same experiment on dispersed islet cells from hIAPP-expressing WT animals (Figure 4C, middle panels), showing comparable PLA patterns for both mouse and human IAPP. As expected, no interactions between SORLA and IAPP were detected in cells deficient in SORLA (Figure 4C, bottom panels). Together, these results suggest a prominent interaction of SORLA with IAPP in early endosomes, potentially by acting as an endocytic receptor for the peptide.

To examine whether SORLA was able to act as a receptor for pro- or mature forms of IAPP, we tested their binding interactions using microscale thermophoresis (MST). In this experiment, we used a His-tagged version of the human SORLA ectodomain (Figure 5A), recombinantly expressed and purified from HEK293-EBNA cells [10]. Ligand binding of the ectodomain was tested using commercially synthesized forms of mouse IAPP, namely N-terminally extended proIAPP

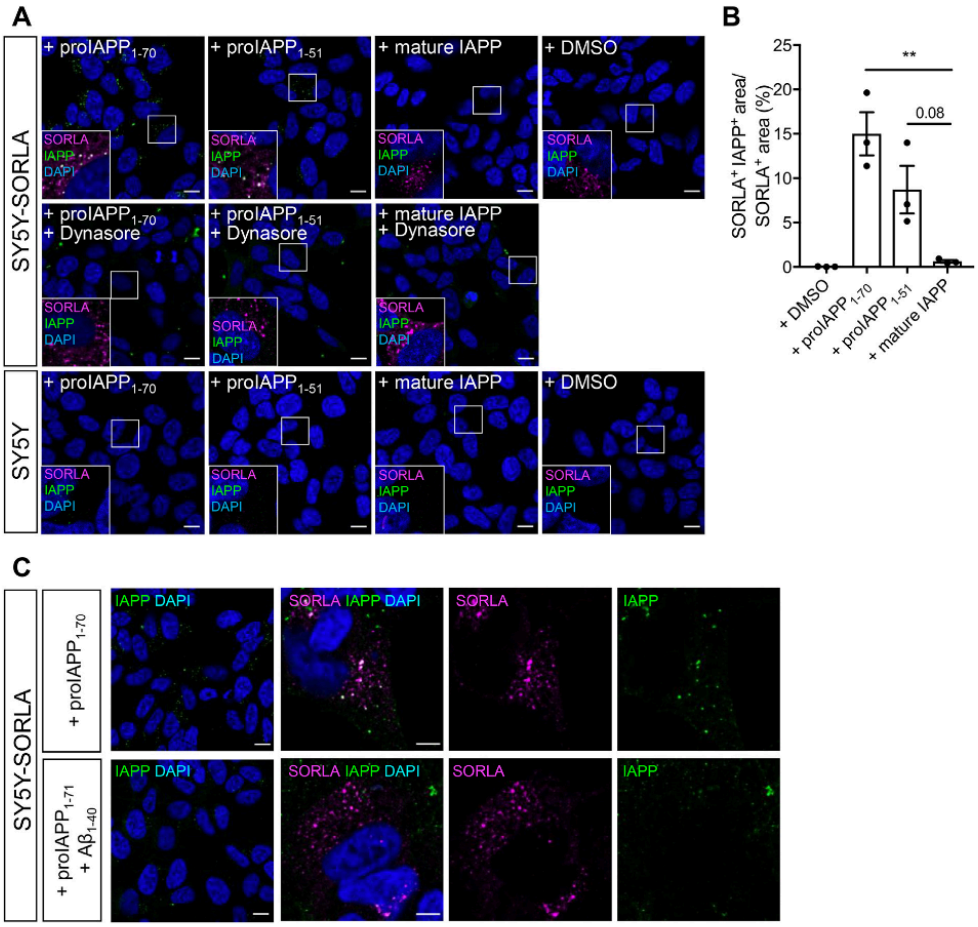

Figure 6: SORLA mediates endocytic uptake of proIAPP, but not mature IAPP. (A) SY5Y cells stably overexpressing SORLA (top, middle panels) and parental SY5Y cells (bottom panel) were incubated with 20 μM of proIAPP$_{1\text{-}70}$, proIAPP$_{1\text{-}51}$, or mature IAPP peptides, or with 0.1% DMSO (solvent control). Where indicated, cells were also treated with 100 μM dynasore to block dynamin-mediated endocytosis. After 30 min, the cells were fixed and immunostained for SORLA (magenta) and IAPP (green). Nuclei were counterstained with DAPI. The insets depict higher magnifications of the areas indicated by white boxes in the overview images. Scale bars, 10 μm. **(B)** The amount of internalized IAPP peptides was quantified based on the percentage of SORLA immunosignals co-localizing with IAPP peptides ($n = 3$ independent experiments, each with 3–4 images per condition). **(C)** Competition of proIAPP$_{1\text{-}70}$ uptake in SY5Y-SORLA cells by A$\beta_{1\text{-}40}$. Cells were treated with 20 μM proIAPP$_{1\text{-}70}$ alone or in the presence of 100 μM A$\beta_{1\text{-}40}$ for 30 min. Presence of SORLA and internalized proIAPP$_{1\text{-}70}$ in cells were then immunolabeled by anti-SORLA (magenta) and anti-IAPP antibodies (green), respectively, and nuclei counterstained with DAPI (blue). Representative images from three independent experiments. Scale bars, 5 μm. Data are shown as mean ± SEM. Statistical significance of differences in (B) was determined by one-way ANOVA with post hoc test. $^{**}p < 0.01$.

(proIAPP$_{1\text{-}70}$), C-terminally extended proIAPP (proIAPP$_{1\text{-}51}$), or mature IAPP peptides (Figure 5B). Mouse IAPP peptides were used in these experiments as they exhibit better solubility and stability *in vitro* as compared to the aggregation-prone human peptides [29]. This strategy enabled us to determine if SORLA interacts with nascent soluble IAPP, preceding misfolding and fibrillation. Binding interactions were detected by comparing multiple measurements over a temperature gradient, with a constant concentration of fluorescently-labeled SORLA ectodomain and a serial titration of unlabeled IAPP peptides. By performing affinity analysis using K_d model of fit, the SORLA ectodomain was shown to interact with all three forms of IAPP (Figure 5C). However, binding was substantially stronger to the unprocessed forms (proIAPP$_{1\text{-}70}$ $K_d \sim 268 \pm 43$ nM; and proIAPP$_{1\text{-}51}$ $K_d \sim 329 \pm 29$ nM) as compared to a relatively weaker interaction with mature IAPP ($K_d \sim 921 \pm 177$ nM). The ability to discharge bound cargo in the acidic milieu of endosomes is a characteristic feature of endocytic

receptors, including SORLA [14]. In line with this observation, binding of IAPP peptides to SORLA was strongest at pH 7.4, weaker at pH 5.5, and absent at pH 4.5 (Figure 5D—F).

3.6. SORLA mediates endocytosis of proIAPP, but not mature IAPP

The above data indicated that SORLA may act as a receptor for monomeric IAPP peptides, possibly delivering them to lysosomal catabolism. To corroborate this hypothesis, we tested the ability of SORLA to mediate endocytic uptake of IAPP *in vitro*. Here, we assessed mouse IAPP peptide uptake in a neuroblastoma SH-SY5Y cell line stably overexpressing SORLA. This cell line is commonly used to study SORLA-mediated sorting functions [10,15]. Moreover, this cell line does not express endogenous IAPP (Figure 6A, DMSO panel), enabling us to examine cellular uptake of unlabeled, synthetic IAPP peptides.

Evaluating cellular uptake of exogenously added IAPP peptides in SY5Y cells expressing SORLA, intracellular accumulation was seen for proIAPP$_{1\text{-}70}$ and proIAPP$_{1\text{-}51}$, but not for mature IAPP (Figure 6A, top panels). Quantifications showed that proIAPP$_{1\text{-}70}$ was the most readily internalized species in the presence of SORLA (Figure 6B). SORLA-dependent uptake of the proIAPP peptides was inhibited by treatment with dynasore, an inhibitor of clathrin-mediated endocytosis (Figure 6A, middle panels). No uptake was seen in parental SY5Y cells lacking SORLA expression (Figure 6A, bottom panels).

Since SORLA is known to bind small peptides, including Aβ, via its VPS10P domain [30], we next tested if proIAPP$_{1\text{-}70}$ also binds to the same region in the receptor's ectodomain. We found that the level of internalized proIAPP$_{1\text{-}70}$ in SORLA-expressing SY5Y cells was significantly reduced in the presence of a 5-fold molar excess of Aβ (Figure 6C), indicating that proIAPP$_{1\text{-}70}$ and Aβ compete for the same binding site in SORLA.

Finally, immunostaining revealed that internalized proIAPP peptides were predominately directed to early endosomes (EEA1, 89.9%) (Figure 7A,B). To identify whether endocytosed peptides were further transported to lysosomes for degradation, or to the TGN for recycling, we co-stained with a lysosomal dye (LysoTracker) or TGN38, respectively. Our results showed that proIAPP peptides co-localize more with lysotracker (51.6%) than with TGN38 (25.2%) (Figure 7A,B), arguing for delivery to lysosomes rather than the TGN recycling of internalized propeptides.

4. DISCUSSION

Overproduction or hypersecretion of IAPP under conditions of increased insulin demand have been proposed as underlying mechanisms of islet amyloid formation. However, excessive formation of the peptide alone is insufficient to promote islet amyloid formation, as evidenced by the lack of islet amyloid found in hIAPP transgenic mice or non-diabetic individuals with hyperinsulinemia [31,32]. Thus, alternative mechanisms are likely involved in maintaining IAPP homeostasis and minimizing its propensity to form amyloid. We have identified a unique cellular pathway that counteracts the initial stages of IAPP aggregation. In our model, SORLA acts as a clearance receptor specific for soluble,

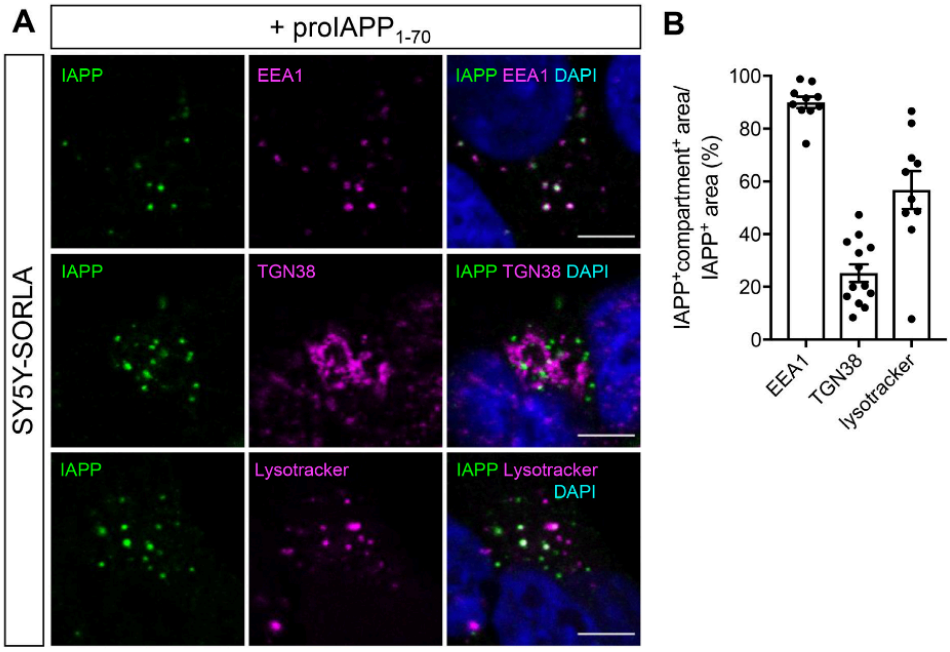

Figure 7: SORLA delivers proIAPP towards endolysosomal compartments. (A) SY5Y-SORLA cells were treated with 20 μM proIAPP$_{1\text{-}70}$ for 30 min as described in Figure 6A. Subsequently, the cells were immunostained for IAPP (green) and compartment makers EEA1 and TGN38 (magenta). Lysosomes were labeled by preincubating cells with Lysotracker Deep Red (magenta) for 1 h prior to uptake assay. Nuclei were counterstained with DAPI (blue). Scale bars, 5 μm. (**B**) Quantifications of object-based colocalization between internalized proIAPP$_{1\text{-}70}$ and each compartment marker ($n = 10—13$ images per marker).

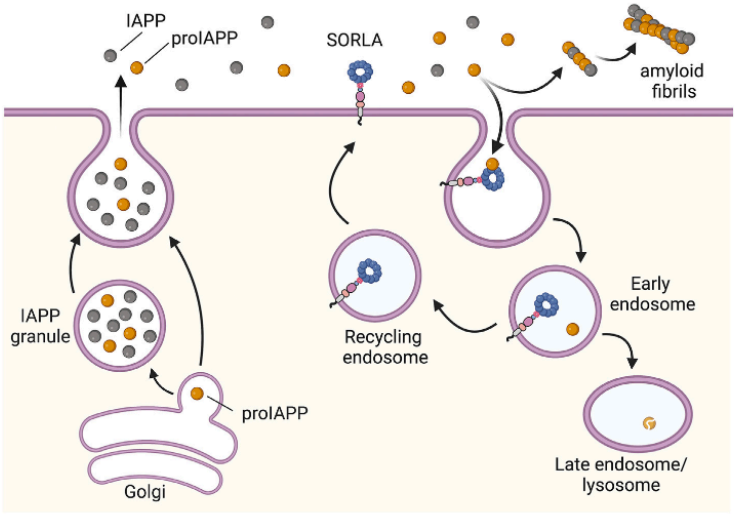

Figure 8: Model for SORLA-mediated endocytosis of proIAPP. SORLA functions as an endocytic receptor for clearance of pro- but not mature IAPP released from islet beta cells. Following pH-dependent release of proIAPP in early endosomes, SORLA recycles back to the cell surface, whereas proIAPP is destined for lysosomal degradation. SORLA-mediated clearance of proIAPP released from cells counteracts pancreatic amyloid fibril formation. Created with BioRender.

monomeric proIAPP released from islet beta cells. Receptor-mediated endocytosis of proIAPP delivers it to lysosomal catabolism, reducing its extracellular buildup and aggregation into fibrils, thereby protecting islets from amyloid-induced cell death (Figure 8).

The cellular pathways for IAPP biosynthesis are complex, involving movement of nascent proIAPP along the biosynthetic route from the endoplasmic reticulum to the Golgi, as well as transport of its partially processed proIAPP intermediate to secretory granules for final processing and maturation. Extensive studies have identified prohormone convertases (PC1/3 and PC2) [33,34], peptidyl-glycine alpha-amidating monooxygenase (PAM) [35] and carboxypeptidase E (CPE) [36] as key regulators of proIAPP processing and post-translational modification. However, the identity of a sorting receptor responsible for transporting IAPP along its biosynthetic pathway remains unknown. CPE has been proposed to carry additional function as a sorting receptor for directing prohormones, including proinsulin, to the regulated secretory granules [37]. However, conflicting results from other studies have challenged the role of CPE as a prohormone sorting receptor [38]. Following a hypothesis-driven approach, we therefore explored a possible role for the VPS10P domain receptor SORLA in IAPP transport. VPS10P domain receptors are a distinct class of sorting receptors that direct intracellular trafficking and processing of proteins along the secretory and endocytic paths of cells [39]. With relevance to islet biology, the VPS10P domain receptor SorCS1 directs replenishment of secretory granules with insulin [40], providing a molecular explanation for its association with type 2 diabetes in humans and mice [41,42]. While our data dispute a similar function for SORLA in intracellular sorting and release of IAPP (Figure S3), they reveal a surprising role for this receptor in the clearance of extracellular soluble proIAPP (Figure 6). SORLA-mediated proIAPP clearance is blocked by dynasore, indicating a clathrin-dependent mechanism of uptake. In addition, internalized proIAPP molecules are preferentially sorted to endolysosomal compartments (Figure 7), suggesting that they are destined for lysosomal catabolism. In support of this assumption, binding of IAPP to SORLA is lost at low pH (Figure 5). pH dependency of binding is a hallmark of endocytosis, enabling receptors to discharge their cargo in acidified endosomes. Because of a low endocytic activity of islet beta cells *in vitro*, we have not been able to directly document SORLA-dependent uptake of proIAPP in this cell type. However, predominant localization of SORLA to early, late, and recycling endosomes in isolated beta cells (Figure 4) suggests a similar endocytic receptor function as in SY5Y cells.

Our observation that SORLA-mediated uptake of soluble, monomeric proIAPP is impaired by Aβ (Figure 6C) indicates that proIAPP binds to the same site as Aβ in a funnel formed by the VSP10P domain, a 700 amino acid module shared by the ectodomains of all VSP10P domain receptors [43]. Importantly, the affinity of SORLA is higher for the pro- compared to the mature form of the peptide ($K_d \sim 300$ vs. 921 nM), explaining its ability to clear pro- but not mature IAPP. This observation is noteworthy, as it addresses an open question concerning the origin of islet amyloid. Loss of the proIAPP receptor SORLA increases islet amyloid deposition in mice (Figure 2). This finding supports earlier hypotheses that proIAPP is likely a critical species in initiating early steps of amyloid deposition [7,44]. There have also been debates on the extracellular or intracellular origin of islet amyloid [45–47]. Our model of SORLA-mediated endocytosis of proIAPP provides new evidence to support islet amyloid formation in the extracellular space as a consequence of aberrant accumulation of secreted IAPP.

As a caveat, we have not directly tested binding of human IAPP peptides to SORLA, as their enhanced propensity for aggregation *in vitro* precluded analysis by microscale thermophoresis. Human IAPP differs from murine IAPP in its amyloidogenicity due to differences in the amino acid sequence at position 20–29 of the mature IAPP peptide [48]. In addition, there are differences in the amino acid sequence of flanking propeptide regions between human and mouse IAPP amino

acid sequences, which may also impact amyloidogenicity and/or protein—protein interactions. Therefore, documenting direct binding between SORLA and human IAPP remains an open question. Still, our findings document comparable close proximity of SORLA with mouse and human IAPP in islet beta cells and shared colocalization patterns in the vicinity of early endosomal compartment (Figure 4C). Furthermore, the obvious impact of SORLA deficiency on islet amyloid formation in transgenic mice expressing human IAPP (Figure 2A) provides encouraging evidence to support a role of SORLA in control of human IAPP metabolism.

Significant amounts of islet amyloid are already present in normal chow-fed hIAPP-expressing mice lacking SORLA, but not in wildtype control. This finding is surprising as previous studies on hIAPP transgenic mice reported no spontaneous islet amyloidosis unless additional diabetogenic traits, such as obesity or insulin resistance, were introduced genetically [49], pharmacologically [23] or through dietary interventions [50]. Our data suggest that SORLA has an important role in maintaining IAPP homeostasis under physiological conditions. This protective effect against islet amyloid is blunted under conditions of dietary stress, possibly because it is masked by hypersecretion of hIAPP following HFD feeding, especially in our transgenic mouse model which overexpresses supraphysiological levels of human IAPP (Figure S3D,E). This saturating effect of overexpression may also explain the lack of changes in circulating plasma proIAPP levels in SORLA-deficient hIAPP transgenic mice. Still, the lack of an overt impact of SORLA deficiency on systemic glucose homeostasis (Figure 3) suggests that the effects on proIAPP uptake and islet amyloid formation are likely attributed to a loss of islet-specific receptor activities.

The severity of islet amyloid deposition correlates with beta cell dysfunction, apoptosis, and hyperglycemia [21,51,52]. *In vitro* studies have demonstrated that synthetic hIAPP-induced amyloid fibrils are toxic to beta cells in cultured islets [53], and that pharmacological inhibition of hIAPP fibril formation improves viability of cultured islets [54]. In the present study of 7-month-old animals, we observed aggravated cell death in islets of hIAPP-expressing SORLA-deficient mice *in vivo*, in line with enhanced islet amyloid in these animals. However, cell death did not progress to overt beta cell dysfunction and impairment in glucose metabolism under the experimental conditions tested here. At present, we cannot conclude whether changes in experimental procedures, such as extending the observational period by an additional 6 months or further increasing the number of biological replicates may uncover an overt islet dysfunction in mutant mice. Still, the observed increase in cell death can be expected to have negative impacts on islet function in SORLA deficient mice at an older age when mice develop prolonged chronic metabolic stress, following further accumulation of amyloid deposits.

In conclusion, our studies have identified a protective role for SORLA against amyloid development not only in the brain, but also in islet beta cells through mediating catabolism of the aggregation-prone peptide ligands. Future studies will corroborate whether this receptor plays a similarly important role in glucose homeostasis and onset of diabetes as it does in neurodegeneration and risk of AD.

FUNDING

Studies were funded in part by a Helmholtz Graduate School fellowship at Max-Delbrück-Center (MDC) to AZLS, and a JDRF postdoctoral fellowship (#3-PDF-2017-373-A-N) to YCC. Further funding was provided by the Canadian Institutes of Health Research Operating grant (PJT-153156) to CBV, and the European Research Council (BeyOND No. 335692), the Alzheimer Forschung Initiative (#18003), and the Novo Nordisk Foundation (NNF18OC0033928) to TEW.

CONTRIBUTION STATEMENT

AZLS conceived and designed the study, performed experiments, collected, analyzed and interpreted data. YCC performed experiments, collected and analyzed data on human IAPP ELISAs. TS and AS contributed to the use of, experimental design, and data interpretation of automated islet perifusion assays. ES provided tissue sections on human pancreatic biopsies. CBV contributed to the design of experiments, interpreted data and provided critical reagents for human IAPP ELISA. TEW contributed to the design of experiments, interpreted data and provided critical reagents. AZLS and TEW wrote the manuscript with editorial input, review and approval for publication from all authors. AZLS and TEW are guarantors of this work.

DATA AVAILABILITY

Data will be made available on request.

ACKNOWLEDGEMENT

We are indebted to C. Kruse and K. Kampf for expert technical assistance and to V. Schmidt-Krüger for help in obtaining animal experimentation licenses. We thank the Advanced Light Microscopy Platform and the Preclinical Research Center of the MDC for technical support and assistance in this work.

CONFLICT OF INTEREST

The authors declare no competing interest related to this manuscript.

APPENDIX A. SUPPLEMENTARY DATA

Supplementary data to this article can be found online at https://doi.org/10.1016/j.molmet.2022.101585.

REFERENCES

[1] Chen, Y.-C., Taylor, A.J., Verchere, C.B., 2018. Islet prohormone processing in health and disease. Diabetes, Obesity and Metabolism 20:64—76. https://doi.org/10.1111/dom.13401.

[2] Marzban, L., Trigo-Gonzalez, G., Verchere, C.B., 2005. Processing of pro-islet amyloid polypeptide in the constitutive and regulated secretory pathways of β cells. Molecular Endocrinology. https://doi.org/10.1210/me.2004-0407.

[3] Lutz, T.A., 2010. The role of amylin in the control of energy homeostasis. American Journal of Physiology - Regulatory, Integrative and Comparative Physiology 298(6). https://doi.org/10.1152/ajpregu.00703.2009.

[4] Gebre-Medhin, S., Olofsson, C., Mulder, H., 2000. Islet amyloid polypeptide in the islets of Langerhans: friend or foe? Diabetologia 43(6):687—695 https://doi.org/10.1007/s001250051364.

[5] Hull, R.L., Westermark, G.T., Westermark, P., Kahn, S.E., 2004. Islet amyloid: a critical entity in the pathogenesis of type 2 diabetes. Journal of Clinical Endocrinology and Metabolism. https://doi.org/10.1210/jc.2004-0405.

[6] Clark, A., Wells, C.A., Buley, I.D., Cruickshank, J.K., Vanhegan, R.I., Matthews, D.R., et al., 1988. Islet amyloid, increased A-cells, reduced B-cells and exocrine fibrosis: quantitative changes in the pancreas in type 2 diabetes. Diabetes Research 9(4):151—159.

[7] Paulsson, J.F., Andersson, A., Westermark, P., Westermark, G.T., 2006. Intracellular amyloid-like deposits contain unprocessed pro-islet amyloid

polypeptide (proIAPP) in beta cells of transgenic mice overexpressing the gene for human IAPP and transplanted human islets. Diabetologia. https://doi.org/10.1007/s00125-006-0206-7.

[8] Courtade, J.A., Wang, E.Y., Yen, P., Dai, D.L., Soukhatcheva, G., Orban, P.C., et al., 2017. Loss of prohormone convertase 2 promotes beta cell dysfunction in a rodent transplant model expressing human pro-islet amyloid polypeptide. Diabetologia. https://doi.org/10.1007/s00125-016-4174-2.

[9] Haass, C., Selkoe, D.J., 2007. Soluble protein oligomers in neurodegeneration: lessons from the Alzheimer's amyloid β-peptide. Nature Reviews Molecular Cell Biology 8(2):101–112. https://doi.org/10.1038/nrm2101.

[10] Andersen, O.M., Reiche, J., Schmidt, V., Gotthardt, M., Spoelgen, R., Behlke, J., et al., 2005. Neuronal sorting protein-related receptor sorLA/LR11 regulates processing of the amyloid precursor protein. Proceedings of the National Academy of Sciences 102(38):13461–13466. https://doi.org/10.1073/pnas.0503689102.

[11] Rogaeva, E., Meng, Y., Lee, J.H., Gu, Y., Kawarai, T., Zou, F., et al., 2007. The neuronal sortilin-related receptor SORL1 is genetically associated with Alzheimer disease. Nature Genetics 39(2):168–177. https://doi.org/10.1038/ng1943.

[12] Lambert, J.C., Ibrahim-Verbaas, C.A., Harold, D., Naj, A.C., Sims, R., Bellenguez, C., et al., 2013. Meta-analysis of 74,046 individuals identifies 11 new susceptibility loci for Alzheimer's disease. Nature Genetics 45(12):1452–1458. https://doi.org/10.1038/ng.2802.

[13] Offe, K., Dodson, S., Shoemaker, J., Fritz, J., Gearing, M., Levey, A., Lah, J., 2006. The lipoprotein receptor LR11 regulates amyloid beta production and amyloid precursor protein traffic in endosomal compartments. Journal of Neuroscience 26(5):1596–1603. https://doi.org/10.1523/JNEUROSCI.4946-05.2006.

[14] Caglayan, S., Takagi-Niidome, S., Liao, F., Carlo, A.S., Schmidt, V., Burgert, T., et al., 2014. Lysosomal sorting of amyloid-β by the SORLA receptor is impaired by a familial Alzheimer's disease mutation. Science Translational Medicine 6(223). https://doi.org/10.1126/scitranslmed.3007747.

[15] Dumanis, S.B., Burgert, T., Caglayan, S., Füchtbauer, A., Füchtbauer, E.M., Schmidt, V., et al., 2015. Distinct functions for anterograde and retrograde sorting of SORLA in amyloidogenic processes in the brain. Journal of Neuroscience 35(37):12703–12713. https://doi.org/10.1523/JNEUROSCI.0427-15.2015.

[16] Pottier, C., Hannequin, D., Coutant, S., Rovelet-Lecrux, A., Wallon, D., Rousseau, S., et al., 2012. High frequency of potentially pathogenic SORL1 mutations in autosomal dominant early-onset Alzheimer disease. Molecular Psychiatry 17(9):875–879. https://doi.org/10.1038/mp.2012.15.

[17] Segerstolpe, Å., Palasantza, A., Eliasson, P., Andersson, E.M., Andréasson, A.C., Sun, X., et al., 2016. Single-cell transcriptome profiling of human pancreatic islets in health and type 2 diabetes. Cell Metabolism 24(4):593–607. https://doi.org/10.1016/j.cmet.2016.08.020.

[18] Neelankal John, A., Ram, R., Jiang, F.X., 2018. RNA-seq analysis of islets to characterise the dedifferentiation in type 2 diabetes model mice db/db. Endocrine Pathology 29(3):207–221. https://doi.org/10.1007/s12022-018-9523-x.

[19] Muraro, M.J., Dharmadhikari, G., Grün, D., Groen, N., Dielen, T., Jansen, E., et al., 2016. A single-cell transcriptome atlas of the human pancreas. Cell Systems 3(4):385–394. https://doi.org/10.1016/j.cels.2016.09.002 e3.

[20] Monti, G., Andersen, O.M., 2018. 20 Years anniversary for SORLA/SORL1 (1996-2016). Receptors & Clinical Investigation 4:1–10. https://doi.org/10.14800/rci.1611.

[21] Verchere, C.B., D'Alessio, D.A., Palmiter, R.D., Weir, G.C., Bonner-Weir, S., Baskin, D.G., et al., 1996. Islet amyloid formation associated with hyperglycemia in transgenic mice with pancreatic beta cell expression of human islet amyloid polypeptide. Proceedings of the National Academy of Sciences of the United States of America 93(8):3492–3496. https://doi.org/10.1073/pnas.93.8.3492.

[22] Courtade, J.A., Klimek-Abercrombie, A.M., Chen, Y.C., Patel, N., Lu, P.Y.T., Speake, C., et al., 2017. Measurementof pro-islet amyloid polypeptide (1-48) in diabetes and islet transplants. Journal of Clinical Endocrinology and Metabolism. https://doi.org/10.1210/jc.2016-2773.

[23] Couce, M., Kane, L.A., O'Brien, T.D., Charlesworth, J., Soeller, W., McNeish, J., et al., 1996. Treatment with growth hormone and dexamethasone in mice transgenic for human islet amyloid polypeptide causes islet amyloidosis and β-cell dysfunction. Diabetes. https://doi.org/10.2337/diab.45.8.1094.

[24] Janson, J., Soeller, W.C., Roche, P.C., Nelson, R.T., Torchia, A.J., Kreutter, D.K., et al., 1996. Spontaneous diabetes mellitus in transgenic mice expressing human islet amyloid polypeptide. Proceedings of the National Academy of Sciences. https://doi.org/10.1073/pnas.93.14.7283.

[25] Höppener, J.W.M., Jacobs, H.M., Wierup, N., Sotthewes, G., Sprong, M., de Vos, P., et al., 2008. Human islet amyloid polypeptide transgenic mice: in vivo and ex vivo models for the role of hIAPP in type 2 diabetes mellitus. Experimental Diabetes Research 697035. https://doi.org/10.1155/2008/697035.

[26] Wicksteed, B., Brissova, M., Yan, W., Opland, D.M., Plank, J.L., Reinert, R.B., et al., 2010. Analysis of ectopic cre transgene expression in the brain. Diabetes 1(18):3090–3098. https://doi.org/10.2337/db10-0624.

[27] Paulsson, J.F., Westermark, G.T., 2005. Aberrant processing of human proislet amyloid polypeptide results in increased amyloid formation. Diabetes. https://doi.org/10.2337/diabetes.54.7.2117.

[28] Schmidt, V., Sporbert, A., Rohe, M., Reimer, T., Rehm, A., Andersen, O.M., et al., 2007. SorLA/LR11 regulates processing of amyloid precursor protein via interaction with adaptors GGA and PACS-1. Journal of Biological Chemistry 282(45):32956–32964. https://doi.org/10.1074/jbc.M705073200.

[29] Wu, C., Shea, J.-E., 2013. Structural similarities and differences between amyloidogenic and non-amyloidogenic islet amyloid polypeptide (IAPP) sequences and implications for the dual physiological and pathological activities of these peptides. PLoS Computational Biology 9(8):e1003211. https://doi.org/10.1371/journal.pcbi.1003211.

[30] Kitago, Y., Nagae, M., Nakata, Z., Yagi-Utsumi, M., Takagi-Niidome, S., Mihara, E., et al., 2015. Structural basis for amyloidogenic peptide recognition by sorLA. Nature Structural & Molecular Biology 22(3):199–206. https://doi.org/10.1038/nsmb.2954.

[31] Clark, A., Saad, M.F., Nezzer, T., Uren, C., Knowler, W.C., Bennett, P.H., et al., 1990. Islet amyloid polypeptide in diabetic and non-diabetic Pima Indians. Diabetologia 33(5):285–289. https://doi.org/10.1007/BF00403322.

[32] Westermark, G., Arora, M.B., Fox, N., Carroll, R., Chan, S.J., Westermark, P., et al., 1995. amyloid formation in response to β cell stress occurs in vitro, but not in vivo, in islets of transgenic mice expressing human islet amyloid polypeptide. Molecular Medicine 1(5):542–553. https://doi.org/10.1007/BF03401591.

[33] Wang, J., Xu, J., Finnerty, J., Furuta, M., Steiner, D.F., Verchere, C.B., 2001. The prohormone convertase enzyme 2 (PC2) is essential for processing pro-islet amyloid polypeptide at the NH2-terminal cleavage site. Diabetes 50(3):534–539. https://doi.org/10.2337/diabetes.50.3.534.

[34] Marzban, L., Trigo-Gonzalez, G., Zhu, X., Rhodes, C.J., Halban, P.A., Steiner, D.F., et al., 2004. Role of β-cell prohormone convertase (PC)1/3 in processing of pro-islet amyloid polypeptide. Diabetes 53(1):141–148. https://doi.org/10.2337/diabetes.53.1.141.

[35] Chen, Y.C., Mains, R.E., Eipper, B.A., Hoffman, B.G., Czyzyk, T.A., Pintar, J.E., et al., 2020. PAM haploinsufficiency does not accelerate the development of diet- and human IAPP-induced diabetes in mice. Diabetologia 63(3):561–576. https://doi.org/10.1007/s00125-019-05060-z.

[36] Marzban, L., Soukhatcheva, G., Verchere, C.B., 2005. Role of carboxypeptidase E in processing of pro-islet amyloid polypeptide in β-cells. Endocrinology 146(4):1808–1817. https://doi.org/10.1210/en.2004-1175.

[37] Cool, D.R., Loh, Y.P., 1998. Carboxypeptidase E is a sorting receptor for prohormones: binding and kinetic studies. Molecular and Cellular Endocrinology 139(1–2):7–13. https://doi.org/10.1016/S0303-7207(98)00081-1.

[38] Irminger, J.C., Verchere, C.B., Meyer, K., Halban, P.A., 1997. Proinsulin targeting to the regulated pathway is not impaired in carboxypeptidase E-deficient Cpe(fat)/Cpe(fat) mice. Journal of Biological Chemistry 272(44):27532–27534. https://doi.org/10.1074/jbc.272.44.27532.

[39] Malik, A.R., Willnow, T.E., 2020. VPS10P domain receptors: sorting out brain health and disease. Trends in Neurosciences, 1–16. https://doi.org/10.1016/j.tins.2020.08.003.

[40] Kebede, M.A., Oler, A.T., Gregg, T., Balloon, A.J., Johnson, A., Mitok, K., et al., 2014. SORCS1 is necessary for normal insulin secretory granule biogenesis in metabolically stressed β cells. Journal of Clinical Investigation 124(10):4240–4256. https://doi.org/10.1172/JCI74072.

[41] Clee, S.M., Yandell, B.S., Schueler, K.M., Rabaglia, M.E., Richards, O.C., Raines, S.M., et al., 2006. Positional cloning of Sorcs1, a type 2 diabetes quantitative trait locus. Nature Genetics 38(6):688–693. https://doi.org/10.1038/ng1796.

[42] Goodarzi, M.O., Lehman, D.M., Taylor, K.D., Guo, X., Cui, J., Quiñones, M.J., et al., 2007. SORCS1: a novel human type 2 diabetes susceptibility gene suggested by the mouse. Diabetes 56(7):1922–1929. https://doi.org/10.2337/db06-1677.

[43] Quistgaard, E.M., Madsen, P., Grøftehauge, M.K., Nissen, P., Petersen, C.M., Thirup, S.S., 2009. Ligands bind to Sortilin in the tunnel of a ten-bladed β-propeller domain. Nature Structural & Molecular Biology 16(1):96–98. https://doi.org/10.1038/nsmb.1543.

[44] Marzban, L., Rhodes, C.J., Steiner, D.F., Haataja, L., Halban, P.A., Verchere, C.B., 2006. Impaired NH2-terminal processing of human proislet amyloid polypeptide by the prohormone convertase PC2 leads to amyloid formation and cell death. Diabetes. https://doi.org/10.2337/db05-1566.

[45] Akter, R., Cao, P., Noor, H., Ridgway, Z., Tu, L.H., Wang, H., et al., 2016. Islet amyloid polypeptide: structure, function, and pathophysiology. Journal of Diabetes Research. https://doi.org/10.1155/2016/2798269.

[46] Aston-Mourney, K., Hull, R.L., Zraika, S., Udayasankar, J., Subramanian, S.L., Kahn, S.E., 2011. Exendin-4 increases islet amyloid deposition but offsets the resultant beta cell toxicity in human islet amyloid polypeptide transgenic mouse islets. Diabetologia 54(7):1756–1765. https://doi.org/10.1007/s00125-011-2143-3.

[47] Gurlo, T., Ryazantsev, S., Huang, C.J., Yeh, M.W., Reber, H.A., Hines, O.J., et al., 2010. Evidence for proteotoxicity in β cells in type 2 diabetes: toxic islet amyloid polypeptide oligomers form intracellularly in the secretory pathway. American Journal Of Pathology 176(2):861–869. https://doi.org/10.2353/ajpath.2010.090532.

[48] Westermark, P., Engstrom, U., Johnson, K.H., Westermark, G.T., Betsholtz, C., 1990. Islet amyloid polypeptide: pinpointing amino acid residues linked to amyloid fibril formation. Proceedings of the National Academy of Sciences of the United States of America 87(13):5036–5040. https://doi.org/10.1073/pnas.87.13.5036.

[49] Höppener, J.W.M., Oosterwijk, C., Nieuwenhuis, M.G., Posthuma, G., Thijssen, J.H.H., Vroom, T.M., et al., 1999. Extensive islet amyloid formation is induced by development of Type II diabetes mellitus and contributes to its progression: pathogenesis of diabetes in a mouse model. Diabetologia 42(4):427–434. https://doi.org/10.1007/s001250051175.

[50] Hull, R.L., Andrikopoulos, S., Verchere, C.B., Vidal, J., Wang, F., Cnop, M., et al., 2003. Increased dietary fat promotes islet amyloid formation and β-cell secretory dysfunction in a transgenic mouse model of islet amyloid. Diabetes 52(2):372–379. https://doi.org/10.2337/diabetes.52.2.372.

[51] MacArthur, D.L.A., De Koning, E.J.P., Verbeek, J.S., Morris, J.F., Clark, A., 1999. Amyloid fibril formation is progressive and correlates with beta-cell secretion in transgenic mouse isolated islets. Diabetologia 42(10):1219–1227. https://doi.org/10.1007/s001250051295.

[52] Jurgens, C.A., Toukatly, M.N., Fligner, C.L., Udayasankar, J., Subramanian, S.L., Zraika, S., et al., 2011. β-Cell loss and β-cell apoptosis in human type 2 diabetes are related to islet amyloid deposition. American Journal Of Pathology. https://doi.org/10.1016/j.ajpath.2011.02.036.

[53] Lorenzo, A., Razzaboni, B., Weir, G.C., Yankner, B.A., 1994. Pancreatic islet cell toxicity of amylin associated with type-2 diabetes mellitus. Nature 368(6473):756–760. https://doi.org/10.1038/368756a0.

[54] Potter, K.J., Scrocchi, L.A., Warnock, G.L., Ao, Z., Younker, M.A., Rosenberg, L., et al., 2009. Amyloid inhibitors enhance survival of cultured human islets. Biochimica et Biophysica Acta (BBA) - General Subjects 1790(6):566–574. https://doi.org/10.1016/j.bbagen.2009.02.013.

Curriculum Vitae

"My curriculum vitae does not appear in the electronic version of my paper for reasons of data protection."

List of Publications

[1] **Shih, A.Z.L**., Chen, Y.-C., Speckmann, T., Søndergaard, E., Schürmann, A., Verchere, C.B., et al., 2022. SORLA mediates endocytic uptake of proIAPP and protects against islet amyloid deposition. Molecular Metabolism: 101585, Doi: 10.1016/j.molmet.2022.101585. IF: 8.57

[2] Ulengin-Talkish, I., Parson, M.A.H., Jenkins, M.L., Roy, J., **Shih, A.Z.L**., St-Denis, N., et al., 2021. Palmitoylation targets the calcineurin phosphatase to the phosphatidylinositol 4-kinase complex at the plasma membrane. Nature Communications 12(1): 6064, Doi: 10.1038/s41467-021-26326-4. IF: 17.69

[3] Lee, C.H., **Shih, A.Z.L**., Woo, Y.C., Fong, C.H.Y., Yuen, M.M.A., Chow, W.S., et al., 2017. Which creatinine-based estimated glomerular filtration rate equation best predicts all-cause mortality in Chinese subjects with type 2 diabetes? Diabetes Research and Clinical Practice 126: 25–9, Doi: 10.1016/j.diabres.2017.01.010. IF: 8.18

[4] Lee, C.H., **Shih, A.Z.L**., Woo, Y.C., Fong, C.H.Y., Leung, O.Y., Janus, E., et al., 2016. Optimal Cut-Offs of Homeostasis Model Assessment of Insulin Resistance (HOMA-IR) to Identify Dysglycemia and Type 2 Diabetes Mellitus: A 15-Year Prospective Study in Chinese. PLOS ONE 11(9): e0163424, Doi: 10.1371/journal.pone.0163424. IF: 3.75

[5] Aharoni-Simon, M., Shumiatcher, R., Yeung, A., **Shih, A.Z.L.**, Dolinsky, V.W., Doucette, C.A., et al., 2016. Bcl-2 Regulates Reactive Oxygen Species Signaling and a Redox-Sensitive Mitochondrial Proton Leak in Mouse Pancreatic β-Cells. Endocrinology 157(6): 2270–81, Doi: 10.1210/en.2015-1964. IF: 5.05

[6] Tennant, B.R., Chen, J., **Shih, A.Z.L.**, Luciani, D.S., Hoffman, B.G., 2015. Myt3 Mediates Laminin-V/Integrin-β1-Induced Islet-Cell Migration via Tgfbi. Molecular Endocrinology 29(9): 1254–68, Doi: 10.1210/ME.2014-1387. IF: 3.63

Acknowledgement

First and foremost, I would like to thank my Ph.D. supervisor Prof. Dr. Thomas Willnow for the opportunity to carry out this project. I am grateful to his trust and support to implement this research project from the very beginning till the end. I would also like to thank my thesis advisory committee members Prof. Dr. Michael Gotthardt and Prof. Dr. Michael Bader for their expert advice and critical review of my thesis progress.

I am grateful to all the past and present members of the Willnow lab for their help, patience and constant supply of treats. In particular, I thank Dr. Vanessa Schmidt-Krüger for obtaining experimental licenses for the animal study, Frau. Christine Kruse for genotyping and cell culture, Frau. Kristin Kampf for assisting experimentation during the manuscript revision, and Frau. Verona Kuhle for resolving all problems that I've faced throughout my time in the lab and Berlin. This project would not have been possible without the help from the animal care takers including Frau. Xenia Richter and Herr. Manfred Ströhmann, Herr. Florian Keim and Herr. Daniel Stepczynski.

Science is the most enjoyable and satisfying when you can share your excitement as well as frustrations with friends. I am fortunate enough to have met some wonderful friends who I can talk to and do fun things together in our free time. Thank you to Rishabh, Nino, Maike, Sasha and Kevin for being part of my PhD journey and making it a happy and memorable adventure.

Lastly, I am indebted to my family for their unwavering support and love. I thank Thilo for being my partner in crime, both in science and in life. Together, we have achieved our goal to collaborate and publish together without a fight. I am forever grateful to his care, patience, encouragement and moral support. I am also blessed to have my loving parents. I thank them for all the sacrifices they have made and support they have provided in enabling me to pursue my interests. Their wisdom and kindness have nurtured me to become a better person and scientist. I therefore dedicate this thesis to my parents, David and Teresa.